LRRK2 phosphorylates HuD to affect the post-transcriptional regulation of Parkinson's disease-linked mRNA targets

Alyssa Pastic

Thesis submitted to the University of Ottawa
in partial fulfillment of the requirements for the
M.Sc. program in
Cellular and Molecular Medicine

Date of Submission: December 2018

Department of Cellular and Molecular Medicine
Faculty of Medicine
University of Ottawa
Ottawa, Ontario
Canada

Abstract

Parkinson's Disease (PD) is a late-onset neurodegenerative disease characterized by progressive motor dysfunction caused by a loss of dopaminergic neurons for which there is no known cure. Among the most common genetic causes of PD are mutations in the leucine-rich repeat kinase 2 gene (*LRRK2*), encoding a multi-domain protein with kinase activity. The LRRK2 G2019S mutation causes hyperactivity of the kinase domain and is the most frequent LRRK2 mutation in patients with familial PD, though its role in causing PD pathology remains unclear. Preliminary data from the lab of our collaborator, Dr. David Park, demonstrated through a genetic screen in *Drosophila melanogaster* that the deletion of *rbp9* encoding an RNA-binding protein prevented pathology induced by PD-relevant mutations in the LRRK2 kinase domain. The neuronal homolog of RBP9 in humans is HuD, a member of the Hu family of RNA-binding proteins that regulates the expression of many transcripts involved in neuronal development, plasticity, and survival. In addition, HuD has been shown to modify the age-at-onset or risk of developing PD. Here, we studied the effect of LRRK2 on the post-transcriptional regulation of mRNAs bound by HuD in the context of PD. Our findings showed that HuD is a substrate for LRRK2 phosphorylation *in vitro*, and that LRRK2 G2019S hyperphosphorylates HuD. We demonstrated that LRRK2 kinase activity is required for the binding of several transcripts by HuD that encode PD-relevant proteins such as α-synuclein and neuronal survival factor BDNF. Our findings in human neuroblastoma cells indicated that LRRK2 regulates the protein levels of HuD mRNA targets α-synuclein and BDNF in a mechanism that can by modified by HuD. Finally, we showed that the combination of HuD knockout with LRRK2 G2019S expression in mice rescues aberrant expression of HuD targets in mice with only the LRRK2 G2019S mutation or the knockout of HuD alone. Together, our findings demonstrate that LRRK2 affects the post-transcriptional regulation of HuD-bound mRNAs, and suggest the use of HuD as a potential therapeutic target in patients with PD caused by the LRRK2 G2019S mutation.

Table of Contents

List of Tables

List of Figures

List of Abbreviations

α: alpha (ie. α-synuclein)

aa: Amino acid

ANOVA: Analysis of variance

ARE: AU-rich element

bp: Base pair

BDNF: Brain-derived neurotrophic factor

cDNA: Complementary DNA

Ctrl: Control

DM: Dorsal midbrain

DMSO: Dimethyl sulfoxide

eIF4A: Eukaryotic initiation factor-4A

ELAVL: Embryonic-lethal abnormal vision-like (*ELAVL* genes 1-4 encode HuR, HuB, HuC and HuD respectively)

ELISA: enzyme-linked immunosorbent assay

FDR: False discovery rate

GAPDH: Glyceraldehyde 3-phosphate dehydrogenase

Gap-43: Growth associated protein 43

GFP: Green fluorescent protein

GO: Gene ontology

GSK: LRRK2 kinase inhibitor GSK2578215A

GST: Glutathione S-transferase

IgG: Immunoglobulin

IP: Immunoprecipitation

kDa: Kilodalton

KO: Knockout

LRRK2: Leucine-rich repeat kinase 2

N2A: Mouse neuroblastoma (neuro2A) cell line

p21: Cyclin-dependant kinase inhibitor 1 ($p21^{Wafl}$)

PCR/RT-PCR/qPCR: Polymerase chain reaction/Reverse transcriptase PCR/Quantitative PCR

PD: Parkinson's disease

RBP: RNA-binding protein

RIP: RNA-Immunoprecipitation

RNase: Ribonuclease

RRM: RNA-recognition motif

SDM: Site-directed mutagenesis

SH-SY5Y: Human neuroblastoma SH-SY5Y cell line

SNc: Substantia nigra pars compacta

SNCA: mRNA encoding α-synuclein

STR: Striatum

TBP: Tata-binding protein

UTR: Untranslated region

VM: Ventral midbrain

WB: Western blot

WT: Wild type

4E-BP1: Eukaryotic translation initiation factor 4E-binding protein 1

Acknowledgements

I would like to sincerely thank my supervisor, Dr. Derrick Gibbings, for taking me on as one of his first master's students 3 years ago. He entrusted me with a difficult project for which there was little preliminary data, and this forced me to grow very quickly as a scientist and as a person. I have learned many lessons about perseverance, determination and self-confidence that I am able to apply to other parts of my life, and for that I am immensely grateful. I would also like to thank the members of my thesis advisory committee, Dr. David Park and Dr. Ryan Russell, and my co-supervisor, Dr. Jocelyn Coté for providing me with many helpful suggestions and guidance throughout my project. To all of the members of the Coté lab and Dr. Bernard Jasmin's lab, thank you for being so generous in providing many of the tools and protocols that we needed to get started with this project.

I owe immense gratitude to all of the members of the Gibbings lab, past and present, that have supported me throughout the last 3 years. James and Annie, our lab would be chaos without you. Alex, Ryan, Charles and My-Tran, thank you for dissecting all of those mice so that I didn't have to. Matteo, Jenna and Maisa, thank you for your wise input on many science-related and personal issues. Lastly, Maneka, Olanta and Danielle, you are incredible women and I am so glad that we got the chance to know each other. Without your support, completion of this thesis would not have been possible. Even though our interests are inevitably taking us on separate paths in different countries, I will always draw on you for inspiration and guidance.

Finally, I am very grateful to have a close support network of special people in my life that supported by decision to go to graduate school. Despite being mostly non-science people, I appreciate you always asking me about my research knowing full well that I would descend into a half-hour long description of my latest experiments. I would especially like to thank my parents for all of the opportunities that I have been given and for trusting me to make my own choices in life. And to my brother, your passion and gift for music has always inspired me to follow my love for science. I am forever proud of you and will never stop bragging about your talent to anyone and everyone that will listen.

Introduction

Clinical features of Parkinson's disease

Parkinson's disease (PD) is one of the most common late-onset neurodegenerative diseases, affecting 1-2% of individuals over 60 years of age and up to 5% of individuals over the age of 80 (Bonifati, 2007; Gasser, 2009; Dae-Lee et al., 2012; Osgerby et al., 2017). PD is a progressive neurodegenerative disorder and shows clinical features such as tremors, slow movement, bradykinesia (slow movement), stiffness and eventual cognitive decline (Jankovic et al., 2007; Dauer and Przedborski, 2003). Current treatment options are limited, as medications and surgical procedures such as deep brain stimulation relieve the symptoms of PD but do not reverse, prevent, or slow down the progression of neurodegeneration (Dae-Lee et al., 2012). In order to develop neuroprotective therapeutic options for PD, it is crucial to broaden our understanding of key molecular mechanisms leading to disease pathogenesis.

Pathologically, PD is characterized by the irreversible loss of dopaminergic neurons from the substantia nigra pars compacta (SNc) (Lo Bianco et al., 2002; Dauer and Przedborski, 2003; Jankovic, 2007). The SNc is located in the midbrain and innervates and supplies dopamine to the striatum, a region of the brain that plays a role in fine motor control (Porritt et al., 2005; Gerfen and Surmeier 2012). The death of dopaminergic neurons in the nigrostriatal pathway causes a critical depletion of dopamine in the striatum and affects motor skills (Dauer and Przedborski, 2003; Gerfen and Surmeier 2012). In addition to the degeneration of dopaminergic neurons, PD is often characterized by the presence of proteinaceous cytoplasmic aggregates called Lewy Bodies in the affected brain regions (Spillantini et al., 1998; Lo Bianco et al., 2002; Dauer and Przedborski, 2003). One of the major components of Lewy bodies is α-synuclein, a pre-synaptic nerve-terminal protein that plays a role in dopamine release (Abeliovich et al., 2000). Mounting evidence suggests that α-synuclein aggregation in Lewy bodies is associated with the degeneration of nigrostriatal dopaminergic neurons (Masliah et al., 2000; Dauer and Przedborski, 2003; Recasens et al., 2014). In fact, several point mutations in the gene encoding α-synuclein (*SNCA*) as well as wild type gene duplications and triplications have been associated with PD, further supporting its role in neuropathology (Kruger et al., 1998; Polymeropolous et al., 1998; Olgiati et al., 2015; Mokretar et al., 2018). It is important to note however that the presence of Lewy bodies is neither necessary nor sufficient

for the clinical expression of PD (Luk et al., 2012; Kalia et al., 2015). Parkinsonian motor phenotypes can exist without Lewy body pathology, while Lewy bodies have been detected in human subjects without PD-associated motor features (Luk et al., 2012; Kalia et al., 2015).

PD closely linked to mutations in the *LRRK2* gene

Though most cases of PD are sporadic in origin, approximately 10% of cases have a genetic link and are referred to as familial Parkinson's disease (Farrer et al., 2005; Zabetian et al., 2005). The most common cause of familial PD are mutations in the leucine-rich repeat kinase 2 gene (*LRRK2*) encoding a 2527-amino acid cytoplasmic protein with multiple protein-protein interaction domains, a GTPase domain and a kinase domain possessing autocatalytic serine/threonine activity (Figure 1) (Paisan-Ruiz et al., 2004; Zimprich et al., 2004; Mata et al., 2006*;* Bonifati, 2007; Greggio, 2012). In contrast to other PD-related genes, the neuropathology and clinical phenotypes of familial PD induced by LRRK2 mutations are largely indistinguishable from sporadic PD, suggesting that therapeutic strategies developed to target LRRK2-mediated familial PD may be applicable on a broader level to sporadic cases (Paisan-Ruiz et al., 2004; Zimprich et al., 2004; Mata et al., 2006).

Numerous studies have proposed roles for LRRK2 in a wide variety of cellular processes including autophagy (Plowey et al., 2007; Alegre-Abarrategui et al., 2009), synaptic endocytosis (Shin et al., 2008; Yun et al., 2013), mitochondrial dysfunction (Ramonet et al., 2011; Papkovskaia et al., 2012; Wang et al., 2012) neuroinflammation and immune system function (Moehle et al., 2012; Russo et al., 2014), and cytoskeletal dynamics and rearrangement for neurite morphogenesis (MacLeod et al., 2006; Jaleel et al., 2007; Parisiadou et al., 2009). The exact role of LRRK2 in many of these pathways remains elusive, as several studies have produced contradictory results especially in the field of autophagy (Wallings et al., 2015). The complexity of LRRK2 activity is additionally demonstrated through its proposed role in the pathology of two inflammatory diseases; Crohn's disease (Barrett et al., 2008; Umeno, 2011; Moehle et al., 2012), and *Mycobacterium leprae* infection also known as leprosy (Zhang et al., 2009, Moehle et al., 2012). LRRK2 is highly expressed in macrophages and monocytes which has

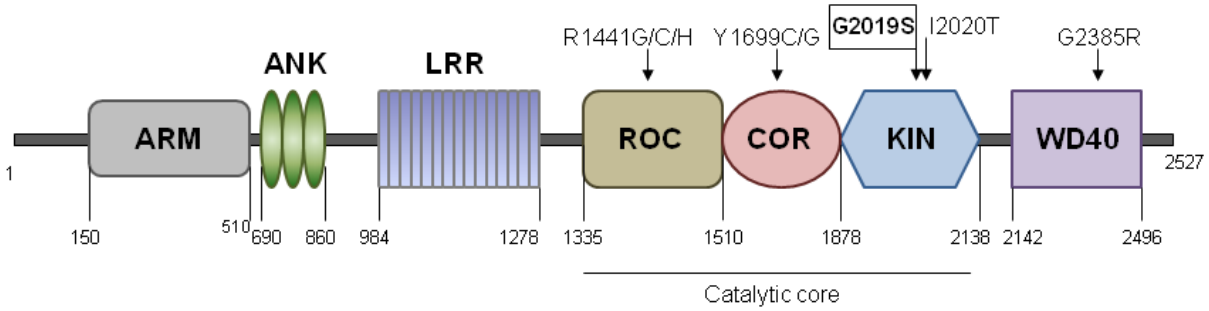

Figure 1: LRRK2 protein domain structure and pathogenic mutations. The catalytic core is made up of the ROC GTPase domain, COR and kinase domain. The G2019S substitution in the kinase domain is recognized as the most common LRRK2 mutation causing Parkinson's disease.

led to the proposed role for LRRK2 in modulating proinflammatory responses in microglia (Dzamko et al., 2012, Moehle et al., 2012). It appears as though each LRRK2-associated disease is caused by a different gene variant, but current studies are working to determine the susceptibility of PD patients to developing Crohn's disease or leprosy, and vice versa (Wallings et al., 2015).

Importance of LRRK2 kinase activity in PD

At least five pathogenic mutations in the *LRRK2* gene have been identified, with the most common mutation leading to Parkinson's disease being the G2019S amino acid substitution in the kinase domain (Figure 1) (West et al., 2005; Mata et al., 2006; Gaig et al., 2007). The G2019S mutation has a clear activating effect, increasing the kinase activity of LRRK2 by approximately 3-fold compared to wild type LRRK2 (West et al., 2005; Smith et al., 2005; Smith et al., 2006; Luzon-Toro et al., 2007; Gloeckner et al., 2009). The LRRK2 G2019S mutation has been described as a gain-of-toxic function mutation and induces progressive neurite shortening and eventual cell death that is not observed when wild type LRRK2 is over-expressed in neuronal cell lines and primary cultures (Smith et al., 2005; MacLeod et al., 2006; Parisiadou et al., 2009). In stark contrast, LRRK2 knockout typically promotes neurite outgrowth in primary cell cultures suggesting a critical role for LRRK2 kinase activity in regulating neuronal differentiation (MacLeod et al., 2006, Parisiadou et al., 2009).

Several research groups have developed and characterized transgenic LRRK2 mice expressing the G2019S mutation. This has proved to be a challenge, as many studies are contradictory as to whether LRRK2 G2019S mice show evidence of PD pathology and whether these mice should be trusted as a model of PD. While Ramonet et al., (2011) showed that LRRK2 G2019S mice exhibit significant dopaminergic neuron loss from the SNc at 19-21 months of age, these findings are contradicted by Li et al., (2010) who did not observe any signs of SNc dopaminergic neuron loss in mice of the same age. Li et al., (2010) also found no abnormalities in the expression levels or aggregation of α-synuclein in the SNc in 12 month old mice, which is a common pathology seen in human PD patients (Spillantini et al., 1998). The majority of studies evaluating the coordination and motor skills of LRRK2 G2019S mice up to 18

months of age report no abnormalities in their performance on a variety of behaviour and locomotor tests (Lin et al., 2009, Li et al., 2010; Ramonet et al., 2011; Longo et al., 2014). Contradicting these findings, a 2012 study by Chen et al. reported that LRRK2 G2019S mice exhibited reduced activity levels (hypokinesia) and impaired motor skills (bradykinesia). The discrepancies between the neuropathology and locomotor behaviour observed in many of these many of these studies can be attributed to the large variation in the methods used to generate transgenic mice. For example, Chen et al., (2012) used mice with 10 copies of the LRRK2 G2019S transgene under the control of CMV enhancer/PDGF-b promoter, which mediated a high level of LRRK2 G2019S expression in SNc dopaminergic neurons. It is therefore possible that the motor phenotypes observed by Chen et al. (2012) are exaggerated in comparison to other transgenic LRRK2 G2019S mouse models with only a few copies of the transgene. All together, these studies suggest that unlike human patients with PD, LRRK2 G2019S is not as detrimental to neuronal survival and motor activity within the lifespan of mice, and that pathology in humans may involve different pathways or factors that are not present in mice (Longo et al., 2014).

In contrast to mouse models of PD, transgenic flies overexpressing PD-associated human LRRK2 (hLRRK2) mutants and corresponding fly LRRK mutants (dLRRK2) show age-dependent dopaminergic neuron loss and dendrite degeneration that is not present in flies over-expressing wild type dLRRK2 (Liu et al., 2007; Imai et al., 2008; Ng et al., 2009). A recent study has shown that these neurological phenotypes in flies expressing hLRRK2 G2019S are accompanied by motor deficits including bradykinesia, akinesia, hypokinesia, and increased tremor (Cording et al., 2017). Similar motor phenotypes were also observed in flies expressing a different human over-active kinase LRRK2 mutant (I2020T), but not in flies expressing a kinase-dead form of LRRK2 or in those expressing the GTPase domain mutation R1441C (Cording et al., 2017, Xiong et al., 2018). These findings suggest a critical role for LRRK2 kinase activity in causing neuropathology and motor phenotypes associated with Parkinson's disease in flies.

Cellular pathways affected by LRRK2

In order to understand the etiology of LRRK2-mediated PD as well as the biological function of LRRK2 in healthy individuals, it is essential to identify LRRK2 kinase substrates and signalling pathways that contribute to neurotoxicity and pathophysiological effects when LRRK2-mediated phosphorylation is misregulated. Identification of these substrates may provide critical insight into developing therapeutics for patients with PD. To date, numerous substrates of LRRK2-mediated phosphorylation have been proposed including certain members of the Rab GTPase family (Steger et al., 2016), Snapin (Yun et al., 2013), Ezrin/Radixin/Moesin (Jaleel et al., 2007; Parisiadou et al., 2009), members of the mitogen-activated protein kinase kinase (MAPKK) family (Gloeckner et al., 2009; Hsu et al., 2010; Chen et al., 2012), eukaryotic initiation factor 4E binding protein 1 (4E-BP1) (Imai et al., 2008; Kumar et al., 2010), ribosomal subunit protein s15 (Martin et al., 2014), and Akt1 (Ohta et al., 2011). These candidate substrates play a broad range of functional roles in cellular homeostasis and survival (Figure 2A) (Greggio et al., 2009; Greggio, 2012; Wallings, 2015). Ezrin, radixin and moesin make up the ERM family of proteins that are involved in maintaining cell membrane structure by anchoring the actin cytoskeleton to the plasma membrane (Jaleel et al., 2007; Parisiadou et al., 2009). Snapin is a regulator of endosomal transport and is essential to autophagy and lysosomal functions in neurons (Yun et al., 2013). The Rab GTPases play roles in intracellular trafficking while MKK3/6 and MKK4/7 of the MAPKK family are involved in cellular stress responses (Hsu et al., 2010; Gloeckner et al., 2009; MacLeod et al., 2013; Steger et al., 2016). Several studies have shown that LRRK2 G2019S increases the phosphorylation of these substrates by approximately 2-4 fold above wild type LRRK2 (Jaleel et al., 2007; Gloeckner et al., 2009; Steger et al., 2016; Lis et al., 2018). Hyperphosphorylation of these substrates by LRRK2 G2019S has been associated with defects in neurite outgrowth and neurotoxicity, but it is poorly understood as to how they contribute to the degeneration of dopaminergic neurons that is specific to the midbrain in PD patients (Figure 2B) (West et al., 2005; Jaleel et al., 2007; Gloeckner et al., 2009; Lin et al., 2010; Parisiadou et al., 2010; Steger et al., 2016; Lis et al., 2018). A recent study has made a potential link between LRRK2 G2019S-mediated hyperphosphorylation of MKK4 and neuronal death in the SNc.

Phosphorylation of MKK4 activates downstream c-Jun N-terminal kinases (c-JNK) which are essential mediators of neuronal cell death (Chen et al., 2012). In the SNc of LRRK2 G2019S mice, over-active MKK4 gave elevated phospho-JNK levels and downstream transcription factors like c-Jun that are responsible for regulating the expression of genes that initiate the apoptotic cascade and caspase production like *Bim* and *FasL* (Chen et al., 2012). Remarkably, elevated levels of Bim and FasL mRNA, and caspases were detected in the SNc of LRRK2 G2019S mice, suggesting that the promotion of apoptosis by LRRK2 G2019S-mediated hyperphosphorylation of MKK4 may be a possible mechanism contributing to SNc dopaminergic neuron degeneration in PD (Chen et al., 2012).

Based on current literature, perhaps the most relevant LRRK2 substrates to PD pathology are eukaryotic initiation factor 4E binding protein 1 (4E-BP1) and ribosomal subunit protein s15. Both substrates have implicated a role for LRRK2 in translational control (Figure 2A) (Imai et al., 2008; Tain et al., 2009; Kumar et al., 2010; Martin et al., 2014). 4E-BP1 inhibits translation initiation by binding and sequestering eIF4E (eukaryotic translation initiation factor), thereby preventing eIF4F complex formation and translation from ensuing (Imai et al., 2008; Tain et al., 2009). Ribosomal protein s15 plays a critical role in assembly of the 40S ribosomal subunit and is central in binding to 16S rRNA (Bubunenko et al., 2006; Martin et al., 2014). Similar to substrates mentioned previously, phosphorylation of 4E-BP1 and s15 is elevated by 2-fold and 1.5-fold respectively in the presence of the LRRK2 G2019S mutant, and has been shown to promote protein synthesis (Figure 2B) (Imai et al., 2008; Martin et al., 2014). Though there appears to be a consensus regarding 4E-BP1 activity being affected by LRRK2, a study by Kumar et al., (2010) suggests that 4E-BP may not be a direct LRRK2 substrate but is instead affected by kinases downstream of LRRK2. Regardless, LRRK2 G2019S-mediated hyperphosphorylation of 4E-BP is suggested to release eIF4E from 4E-BP inhibition, thereby promoting cap-dependent translation (Imai et al., 2008; Tain et al., 2009; Kumar et al., 2010). The large-scale implications of enhanced translation in PD pathology remain unclear, though over-expression of eIF4E has been shown to cause loss of dopaminergic neurons in flies, while over-expression of 4E-BP suppresses dopaminergic neuron degeneration in flies expressing a pathogenic mutation (Imai et al., 2008; Tain et al., 2009). In a study by

Martin et al., (2014), enhanced translation and increased protein synthesis in *Drosophila* expressing the LRRK2 G2019S mutation was abolished by blocking the phosphorylation of s15 through site-directed mutagenesis of the putative phosphorylation site. In accordance with this effect on translation, blocking s15 phosphorylation additionally rescued neurotoxicity in *Drosophila* and human neuronal PD models (Martin et al., 2014).

Lastly, LRRK2 kinase substrate Akt1 is a serine/threonine protein kinase involved in several signalling pathways such as apoptosis (Figure 2A) (Ohta et al., 2011; Chuang et al., 2014). Recent studies have implicated LRRK2 in protecting neurons from apoptotic death through an Akt1-dependent survival pathway (Chuang et al., 2014). In contrast to the increased phosphorylation induced by LRRK2 G2019S mutant of the substrates mentioned above, two separate studies have shown that LRRK2 G2019S fails to phosphorylate Akt1 to the same degree as wild type LRRK2 (Figure 2B), leading to its inactivation (Ohta et al., 2011; Chuang et al., 2014). These sets of data promote speculation that neurons expressing the G2019S mutation exhibit lower resistance to apoptosis and cause cells to be more susceptible to neurodegeneration (Figure 2B) (Ohta et al., 2011; Chuang et al., 2014).

In summary, many candidate LRRK2 kinase substrates and cellular pathways affected by LRRK2 have been associated with neurite outgrowth defects and neurotoxicity in G2019S mutant models. A definitive link between these some of these substrates causing dopaminergic neuron death that is specific to the SNc has yet to be made, but is possible that PD pathology is the cumulative effect of all downstream pathways affected by the LRRK2 G2019S mutant. It is also likely that there are molecular mechanisms and kinase targets contributing to PD pathology that have not been elucidated. Therefore, it is essential to continue exploring the molecular pathways affected by LRRK2 in order to broaden our understanding of PD.

Effects of LRRK2 on the transcriptome

In addition to affecting translational control through phosphorylation of 4E-BP1 and ribosomal protein s15, LRRK2 has been implicated in regulating gene expression at the transcriptional level. Recent

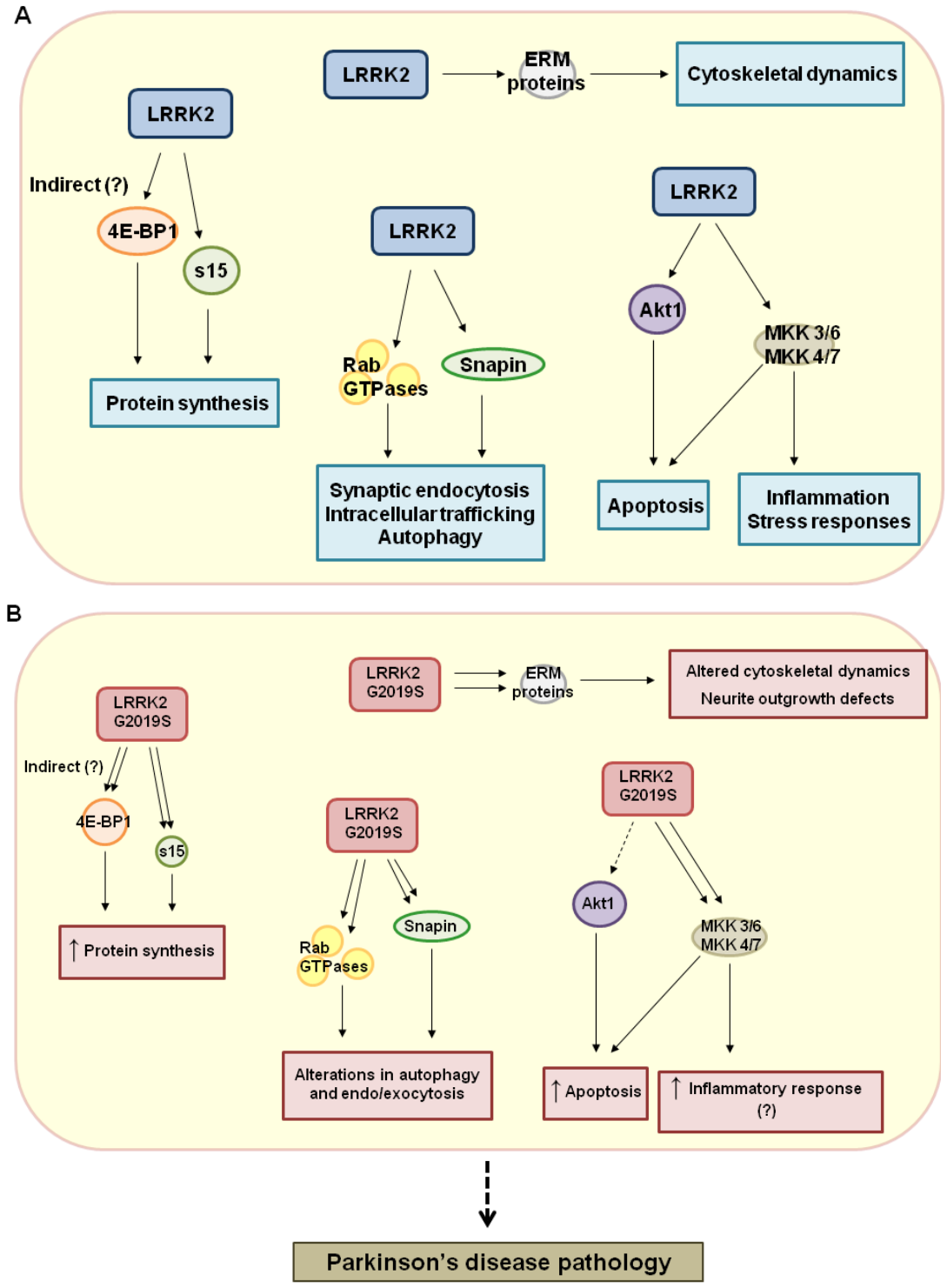

Figure 2: Suggested signalling pathways affected by LRRK2-mediated phosphorylation. (A) Schematic of several known substrates of direct or indirect phosphorylation by LRRK2 and their involvement in cellular pathways. (B) Downstream effects caused by LRRK2 G2019S-mediated hyperphosphorylation (double arrow) or hypophosphorylation (dotted arrow) of substrates. The cumulative effects of the LRRK2 G2019S mutation cause dopaminergic neurodegeneration in Parkinson's disease.

studies assessing the impact of LRRK2 on the transcriptome have uncovered significant misregulation of hundreds of mRNA transcripts in cells and mice expressing the G2019S mutation as well as in LRRK2 knockout conditions (Habig et al., 2008; Schultz et al., 2011; Nikonova et al., 2012; Dorval and Hebert, 2012). Within the extensive list of misregulated transcripts are those encoding proteins involved in cell cycle control, neuronal differentiation, axonal guidance and nervous system development (Habig et al., 2008; Schultz et al., 2011; Nikonova et al., 2012). A study by Nikonova et al., (2012) found that a significant number of transcripts showed an opposite fold-change in LRRK2 knockout mice vs. LRRK2 mutant G2019S mice. This further reinforces the significance of LRRK2 kinase activity in regulating the expression of many transcripts, though the mechanism remains uncertain. In searching for possible cellular pathways in which LRRK2 affects mRNA expression, the most promising mechanism may be through the interaction of LRRK2 with Argonaute 1 and 2 (Ago1 and Ago2). Ago1 and Ago2 are essential components of the microRNA-induced silencing complex (miRISC) that play a central role in gene silencing in the RNA interference pathway (Gehrke et al., 2010; Dorval and Hebert, 2012). However, the effect of LRRK2 on this pathway is poorly understood. A study by Dorval et al., (2014) found that Ago2 function (binding and maturation of miRNAs in miRISC complex) and its sub-cellular distribution is not strongly affected by LRRK2 deficiency, indicating that it is dispensable for Ago2 function.

Novel proposal of relationship between LRRK2 and an RNA-binding protein

The I2020T mutation in LRRK2 is directly adjacent to the G2019S mutation (Figure 1), and has been shown to cause over-activity of the kinase domain to a slightly lesser degree than LRRK2 G2019S (Gloeckner et al., 2009; Greggio and Cookson, 2009). The LRRK2 I2020T mutation has been linked to familial Parkinson's disease, but is not as common as the LRRK2 G2019S mutation in patients with the disease (Mata et al., 2006; Greggio and Cookson, 2009). Nevertheless, the LRRK2 I2020T mutation is a useful tool to gain insight into LRRK2 G2019S disease pathology. A genetic screen in *Drosophila* expressing the human LRRK2 (hLRRK2) pathogenic I2020T mutation was recently performed in the lab

of Dr. David Park, one of our collaborators. This study was conducted using a measurable model of degeneration by the analysis of compound eye phenotypes in flies expressing *hLRRK2-I2020T* under the control of the temperature dependent GAL-UAS system. Controlled expression of *hLRRK2-I2020T* caused retinal degeneration that was marked by structural and pigmental abnormalities (Vederova et al., 2009; Marcogliese et al., 2017). Marcogliese et al., (2017) identified several genes that rescued these phenotypes when their expression was disrupted, indicating that they may have a relation to LRRK2 (Marcogliese et al., 2017). Of particular interest to us was *rbp9*, a gene encoding an RNA-binding protein expressed in the central nervous system of flies (Kim and Baker, 1993). In unpublished data, Marcogliese and colleagues found that the deletion of *rbp9* in flies expressing the pathogenic I2020T mutation suppressed the degenerative phenotype observed in the eye, demonstrating that *rbp9* may be required for LRRK2 I2020T-mediated pathology (Figure 3).

RNA-binding proteins bind to single or double stranded RNA in cells and are key regulators of post-transcriptional control of gene expression, possessing major roles in alternative splicing, polyadenylation, mRNA localization, turnover and translation (Stefl et al., 2004; Keene, 2007; Glisovic et al., 2008; Alipanahi et al., 2014). As mentioned previously, *Lrrk2* knockout and G2019S mutation in mice and cells has been shown to cause significant misregulation of hundreds of transcripts through a mechanism that has yet to be clarified (Habig et al., 2008; Schultz et al., 2011; Nikonova et al., 2012; Dorval and Hebert, 2012). It is therefore possible that LRRK2 exerts control over the transcriptome by affecting the regulation of an RNA-binding protein like RBP9, thereby causing downstream effects on neuronal survival and PD-related phenotypes. This suggests the potential use of an RBP9 protein homolog in humans as a therapeutic target in Parkinson's disease.

RNA-binding protein HuD

Conservation of Drosophila ELAVs and vertebrate Hu proteins

The RBP9 protein belongs to a group of RNA-binding proteins in *Drosophila* called the ELAV family that also includes found-in-neurons (FNE) and the family namesake embryonic-lethal abnormal

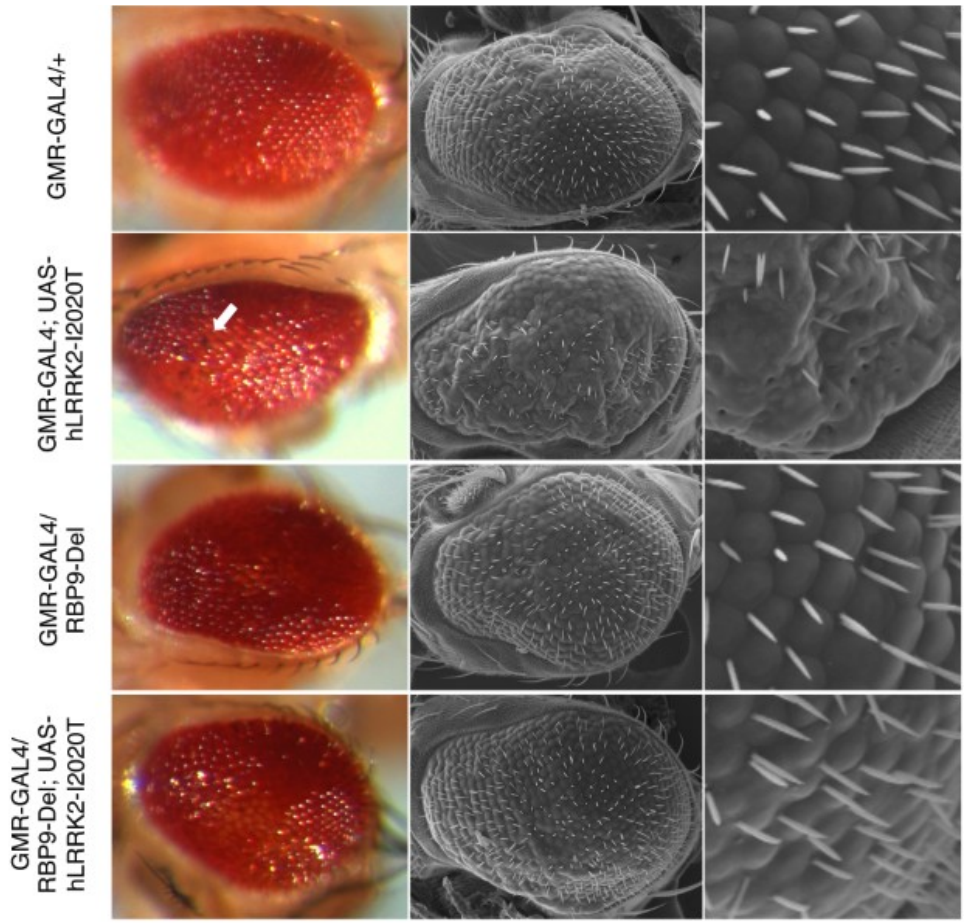

Figure 3: Unpublished data from the lab of D. Park showing scanning electron microscope (SEM) and optical images of fly eye phenotypes. Flies expressing GMR-GAL4/+; UAS-hLRRK2(I2020T) exhibit bristle disorganization, black lesions and other structural abnormalities. GMR-GAL4/RBP9-Del deficiency line does not show any visible abnormalities. GMR-GAL4/RBP9-Del combined with UAS-hLRRK2(I2020T) partially rescues the abnormal eye phenotype of the GMR-GAL4/+; UAS-hLRRK2(I2020T) fly.

vision (ELAV) (Zaharieva et al., 2015). These proteins are co-expressed in a coordinated spatiotemporal pattern the nervous system and have been widely used as neuronal markers (Bräuer et al., 2014; Zaharieva et al., 2015). The mammalian homologs of the *Drosophila* ELAV family are the Hu family of RNA-binding proteins that consists of four highly conserved members; HuB, HuC, HuD and HuR (Figure 4).

It is suggested that ELAV and Hu-protein coding genes are derived from a common ancestor but duplicated independently in vertebrates and arthropods (Samson, 2008; Zakarieva et al., 2015). Since Parkinson's disease pathology manifests in the brain, Hu proteins HuB, HuC and HuD are of particular interest to us, as their expression is primarily restricted to neurons while HuR is expressed ubiquitously (Colombrita et al., 2013; Zakarieva et al., 2015). Unsurprisingly, the neuronal Hu members exhibit a higher degree of amino acid sequence similarity with each other (80-85%) compared to HuR (73-74%) (Okano and Darnell, 1997; Samson, 2008; Bronicki and Jasmin, 2013). The Hu proteins have also maintained considerable amino acid sequence similarity (42-45%) with members of the ELAV family since their divergence from *Drosophila* (Okano and Darnell, 1997). This has suggested the existence of functional redundancy within the Hu/ELAV protein family. A recent study by Zaharieva et al., (2015) showed that FNE, RBP9 and HuR can partially substitute for ELAV function in Drosophila, where knockout of the *elav* gene would otherwise be lethal (Colombrita et al., 2013; Bronicki and Jasmin, 2013).

Cellular localization of Hu proteins

Hu proteins are composed of three highly conserved RNA-recognition motifs (RRMs) that are responsible for recognizing target RNA sequences (Figure 4) (Okano and Darnell, 1997; Colombrita et al., 2013; Zakaraieva et al., 2015). The second and third RRMs are separated by a more variable region called the linker (or hinge) region (Figure 4) (Okano and Darnell, 1997; Kasashima et al., 1999). The linker region contains nuclear localization and export signals (NLS and NES) and has been shown to play a crucial role in cellular localization (Yannoni and White, 1999; Kasashima et al., 1999). It is likely that variability in the linker sequence has lead to evolutionary deviations in the cellular localization in

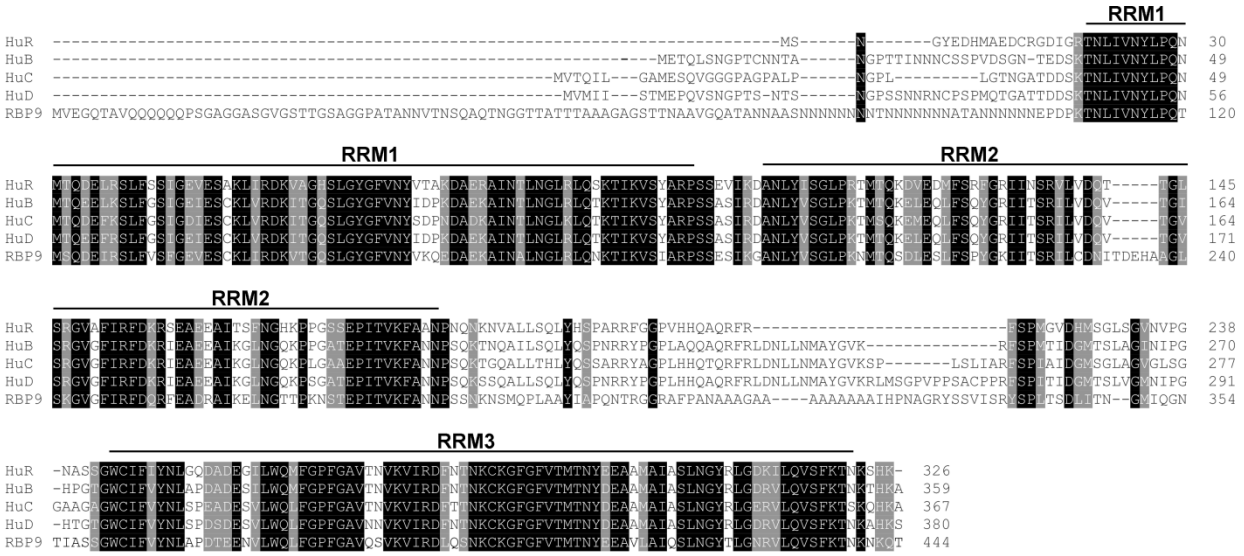

Figure 4: Sequence alignment of the Hu/ELAV proteins. The amino acid sequence of the four human Hu proteins (HuR, HuB, HuC, HuD) is compared with *Drosophila* RBP9 protein. Sequence alignment was performed using the EMBL Clustal Omega online tool (https://www.ebi.ac.uk/Tools/msa/clustalo/). Residues exhibiting 100% conservation are highlighted in black, and conservative substitutions are highlighted in grey. The amino acids making up each RNA recognition motif (RRM) are indicated. The sequence of amino acids between RRM2 and RRM3 is the most variable between Hu/ELAV proteins and is known as the linker or hinge region.

ELAV/Hu proteins, as the *Drosophila* ELAV proteins are largely nuclear, while mammalian Hu proteins predominantly localize in the cytoplasm with the exception of HuR which is found in both the nucleus and cytoplasm (Samson, 2008; Colombrita et al., 2013; Zakarieva et al., 2015). In the cytoplasm, Hu proteins have been associated with regulating mRNA stability, localization and translation (Brennan and Steitz, 2001, Fukao et al., 2009; Lebedeva et al., 2011; Ince-Dunn et al., 2012; Colombrita et al., 2013). While these are the main functions of HuB, HuC, and HuD, the NLS and NES motifs in the hinge region give them the ability to shuttle between the cytoplasm and nucleus (Fan and Steitz, 1998; Kasashima et al., 1999). In the nucleus, they have been implicated in pre-mRNA modification processes such as splicing and polyadenylation (Zhu et al., 2006; Zhu et al., 2008, Zhou et al., 2011). Pre-mRNA processing is the primary function of nuclear-localized *Drosophila* ELAV proteins and mammalian HuR (Samson, 2008; Colombrita et al., 2013; Zakarieva et al., 2015). The nuclear localization of HuR is thought to be mediated by a motif in its linker region aptly named the HuR Nucleoplasmic Shuttling (HNS) sequence (Fan and Steitz, 1998; Kim and Gorospe, 2008). Interestingly, this motif is similar to a sequence in the linker region of *Drosophila* ELAV that has been shown to be essential for nuclear localization (Fan and Steitz, 1998; Yannoni and White, 1999). Nuclear localization of HuR is thought to give it the unique ability of binding to target transcripts while in the nuclear compartment and accompanying them to the cytoplasm, providing transcripts with ongoing protection from degradation (Fan and Steitz, 1998; Brennan and Steitz, 2001).

Hu-binding motifs

The first two RRMs of the Hu proteins are primarily responsible for binding target RNA sequences typically found in the 3' untranslated region (UTR), while the third motif binds poly(A) sequences and stabilizes the protein-RNA complex (Chung et al., 1996; Park et al., 2000; Anderson et al., 2000; Wang and Hall, 2001; Fukao et al., 2009). Many studies have shown that Hu proteins have a strong preference for short 50-150nt sequences known as AU-rich elements (ARE) (Chung et al., 1996; Joseph et al., 1998; Park et al., 2000; Bolognani et al., 2009). Early studies examining Hu binding sites in the 3'UTR of target

transcripts put a strong emphasis specifically on AREs in contributing to the regulation of transcript stability, but this was based on low-throughput experiments and a limited set of target transcripts and sequences (Chung et al., 1996; Joseph et al., 1998; Park et al 2000). Upon the development of high-throughput genome-wide methods like various types of cross-linking and immunoprecipitation (CLIP) assays, reports have emerged showing that as many as half of all transcripts bound by HuD and HuR do not contain an ARE, but instead contain C-rich motifs or U-rich stretches with interspersed guanines or adenosines bound with high affinity by Hu proteins (Table 1) (Bolognani et al., 2009; Mukherjee et al., 2011; Lebedeva et al., 2011; Ince-Dunn et al., 2012). These studies also found that in addition to the 3'UTR, a significant number of Hu binding sites were also located in introns and a few within the 5'UTR (Mukherjee et al., 2011; Lebedeva et al., 2011; Ince-Dunn et al., 2012). It is generally understood that intronic binding of certain transcripts regulates their alternative mRNA splicing while 5'UTR binding acts to promote or repress their translation (Fukao et al., 2009; Mukherjee et al., 2011; Lee et al., 2012).

Molecular and physiological functions of HuD

HuD binds transcripts involved in neurogenesis and differentiation

Of the Hu protein family members, HuD was the first to be cloned and characterized, and is arguably one of the most well-characterized neuronal RBPs (Szabo et al., 1991; Bolognani et al., 2009; Bronicki and Jasmin 2013). It was established early in the field by Kim and Baker (1993) that the amino acid sequence of the RBP9 protein shares its most striking similarity to the sequence of HuD, especially within the RRMs. It is widely recognized as one of the earliest neuronal markers and it post-transcriptionally regulates the expression of many genes that have key roles in neurogenesis, neuronal differentiation and survival (Okano and Darnell, 1997; Aranda-Abreu et al., 1999; Mobarak et al., 2000; Deschênes-Furry et al., 2006; Bronicki and Jasmin, 2013).

An extensive list of transcripts bound by HuD has been characterized by several studies using high-throughput technologies (Bolognani et al., 2009; Scheckel et al., 2016). Many of these transcripts encode proteins that may be pertinent to the pathogenesis of Parkinson's disease such as neurite outgrowth

regulators Gap-43 and tau, brain-derived neurotrophic factor (BDNF) and cell cycle control factor p21^{wafl} (p21) (Mobarak et al., 2000; Anderson et al., 2000; Bolognani et al., 2009; Allen et al., 2013; Vanevski et al., 2015). Gap-43 is primarily expressed in neurons during the initial development of the nervous system or during regeneration of neuronal connections (Mobarak et al., 2000). Overexpression of Gap-43 promotes neurite extension and neuronal plasticity, while down-regulation of Gap-43 induces growth

Table 1: Examples of experimentally-defined 3'UTR motifs bound by HuD in the literature.
Y= C/U; K = G/U; W = A/U

Sequence of HuD binding site	**Identification Method**	**Target transcript**	**Reference**
CUGGUUUUUUAUUUAUGUUUUAAACC	EMSA	*c-fos*	Chung et al., (1996)
AUAUUUAUAUUUUUAUUUUAUUUUUUU; AUACGUAUAUUUUUAUUUUAUUUUUUU; AUAUUUAUAUUUUUAUGCUAUUUUUUU; AUAUUUAUAUCGCUAUUUUAUUUUUUU	Filter binding assay	N/A	Chung et al., (1996)
UCCACUUUCCUCUCUAUUUCUCUCUG	Filter binding assay	*Gap43*	Chung et al., (1997)
UCUUAAUUAUUAUUUGUGUUUUAAUUUA AACACCUCCUCAUG	Filter binding assay	*Cdkn1a*	Joseph et al., (1998)
UU(AUUU)$_3$AUU	EMSA	N/A	Park et al., (2000)
poly(U)	Homopolymer binding assay	N/A	Kasashima et al., (2002)
poly(A)	Homopolymer binding assay	N/A	Fukao et al., (2009)
KUUUGUUUKKUUU; UUUUUUUUUWAAA	Genome-wide *in vivo* immunoprecipitation	N/A	Bolognani et al., (2009)
UUUUUU; UUUUGU; UUGUUU; UGUUUU; AUUUUU; UUUUUG; UUUUUA; UUAUUU; UUUAUU	HITS-CLIP	N/A	Ince-Dunn et al., (2012)

cone collapse and abnormal topographical formation of the brain (Aigner et al., 1995; Anderson et al., 2000). Similar to Gap-43, microtubule-associated protein tau is predominantly expressed in the central nervous system and is involved in neuronal development and axonal growth (Aranda-Abreu et al., 1999).Polymorphisms in the gene encoding tau (*MAPT*) are most often associated with Alzheimer's disease pathology, but certain polymorphisms have also been shown to have a strong association with cognitive impairment and dementia in patients with PD (Goris et al., 2007; Lei et al., 2010). Hyperphosphorylated tau has been found to be incorporated in Lewy bodies in PD patients and co-localizes with phosphorylated α-synuclein to synergistically promote the fibrillization of both proteins (Lei et al., 2010). BDNF plays a role in neuronal survival, network development and synaptic plasticity (Allen et al., 2013). Targeted BDNF knockdown in the dorsal dentate gyrus of mice reduced neuronal differentiation and induced several behaviour impairments, while BDNF knockout has been shown to cause defects in synaptic function (Patterson et al., 1996; Taliaz et al., 2010). Several studies have shown that PD patients exhibit low levels of BDNF in the dopaminergic neurons of the SNc which accompanies the neurodegeneration seen in Parkinson's disease (Howells et al., 2000; Baquet et al., 2005; Costa et al., 2015). Unlike Gap-43, tau and BDNF, p21 is a ubiquitously expressed cell cycle inhibitor and modulates the expression of genes involved in a wide variety of processes surrounding mitosis, DNA replication and repair (Chang et al., 2000). Misregulated p21 expression is most commonly associated with carcinogenesis or senescence, though it has also been shown to modulate neurogenesis in certain regions of the brain (Chang et al., 2000; Pechnick et al., 2007).

HuD regulates mRNA metabolism

HuD has generally been shown to positively regulate the stability of mRNAs encoding Gap-43, p21, Tau and BDNF by binding AREs and other motifs in the 3'UTR (Aranda-Abreu et al., 1999; Mobarak et al., 2000; Wang et al., 2000; Lim and Alkon, 2012; Allen et al., 2013). HuD overexpression in neuronal cell lines and primary cultures has been associated with increased stability of these transcripts and elevated protein expression, as well as accelerated neurite extension and morphological differentiation

(Mobarak et al., 2000; Anderson et al., 2000; Anderson et al., 2001; Fujiwara et al., 2006; Vanevski et al., 2015). On the other hand, downregulation of HuD causes destabilization of target transcripts and defects in neurite outgrowth (Aranda-Abreu et al., 1999; Anderson et al., 2000; Anderson et al., 2001; Allen et al., 2013; Vanevski et al., 2015).

The stability of many transcripts bound by HuD is also regulated by a number of other neuronal RNA-binding proteins that bind AU-rich regions in the 3'UTR. Many of these RBPs such as A+U binding factor 1 (AUF1), Tristetraprolin (TTP), and K homology splicing regulatory protein (KSRP) antagonize the stabilizing role of HuD by promoting mRNA decay (Bronicki and Jasmin, 2013). For example, KSRP binds AREs in *GAP43* mRNA and serves to destabilize and promote its degradation (Bird et al., 2013). Competitive binding assays have shown that KSRP and HuD have similar affinities for the same binding site in *GAP43* transcripts, but that increasing amounts of KSRP can displace HuD from the *GAP43* ARE thereby promoting mRNA decay and limiting axonal outgrowth during development (Bird et al., 2013). This suggests that the ratio of KSRP to HuD in developing neurons may be critical in regulating *GAP43* mRNA levels. Similarly, *CDKN1A* mRNA (encoding p21) is destabilized by RBPs including poly(C) binding protein 4 (PCBP4) and fragile X-related protein 1 (FXR1) (Scoumanne et al., 2010; Majmunder et al., 2016). PCBP4 binds poly(C)-rich regions in the 3'UTR of p21 mRNA while FXR1 binds G-quadriplex (G4) RNA regions that are rich in guanine and form secondary structures (Scoumanne et al., 2010; Majmunder et al., 2016). The regulation of *CDKN1A* transcript stability by these RBPs plays an important role in cell cycle control and senescence in response to DNA damage, but the nature of their possible antagonistic relationship with HuD in neurons for the binding of this transcript is unclear (Scoumanne et al., 2010; Majmunder et al., 2016).

In addition to mRNA stability, HuD and the other Hu proteins regulate alternative polyadenylation, alternative splicing, localization and translation of the transcripts that it binds (Bronicki and Jasmin, 2013). For example, HuD binds mRNA encoding HuR at U-rich motifs in the 3'UTR and serves to regulate its alternative polyadenylation during neuronal development and appears to be crucial in mediating the balance between differentiation and proliferation (Mansfield and Keene, 2011). Generally,

the Hu proteins exert their control over alternative splicing by binding intronic AREs or other high-affinity motifs such as those in Table 1 to promote the inclusion or exclusion of certain exons (Zhu et al., 2006; Zhu et al., 2008; Wang et al., 2010; Zhou et al., 2011; Bronicki and Jasmin, 2013). For example, HuD binds and regulates the alternative splicing of its own mRNA in a pattern that is thought to be imperative in mouse embryonic development (Wang et al., 2010). In the case of neurofibromatosis type 1 mRNA (*NF-1*), HuD binds intronic AREs in the pre-mRNA and blocks exon inclusion by inhibiting the binding of U1/U6 snRNP and auxiliary splicing factors at the 5' and 3' splice site (Zhu et al., 2008). The involvement of HuD in regulating translation was initially proposed by Fukao et al., (2009), who showed that HuD directly binds eukaryotic translation initiation factor eIF4A to enhance cap-dependent translation (Fukao et al., 2009). This interaction along with the poly(A)-binding activity of HuD were shown to be critical for stimulating neurite outgrowth in PC12 cells, offering another mechanism in which HuD can regulate morphological differentiation (Fukao et al., 2009).

Functional significance of HuD in the nervous system

The variety of post-transcriptional mechanisms of regulation exerted by HuD on mRNAs encoding proteins involved in neuronal differentiation and survival provides evidence for HuD as a key regulator of neuronal development (Deschênes-Furry et al., 2006; Bronicki and Jasmin, 2013). As described in the previous section, many studies on neuronal cell lines and primary cultures have highlighted the significance of HuD on neurite extension and neuronal differentiation through overexpression and knock-down experiments (Deschênes-Furry et al., 2006; Bronicki and Jasmin, 2013). This effect appears to be specific to neuronal Hu proteins, as HuB and HuC can also induce morphological differentiation while overexpression of HuR is insufficient to induce neurite extension and differentiation (Wakamatsu and Weston, 1997; Akamatsu et al., 1999; Deschênes-Furry et al., 2006; Katsanou et al., 2009; Mansfield and Keene, 2011). Despite sharing many targets with the neuronal Hu proteins, HuR shows a binding affinity for many targets involved in cell cycle regulation and growth rather than neuronal differentiation and maintenance. Knockout of the gene encoding HuR in mice (*Elavl1*) causes embryonic lethality because of

its severe effects on extra-embryonic placental development and abnormalities in skeletal development (Katsanou et al., 2009).

The manipulation of HuD in mice has given insight into its functional significance in the nervous system. HuD knockout mice show a transient delay in cranial nerve development in early embryonic stages, but show no significant morphological abnormalities of the central nervous system in later stages of development (Akamatsu et al., 2005). Adult HuD knockout mice also show slight motor impairments demonstrated by an abnormal clasping reflex and poor rotarod performance (Akamatsu et al., 2005). Mice with constitutive HuD overexpression exhibited a disruption in fear conditioning and spatial learning, suggesting a role for HuD in neuronal plasticity. Otherwise, these mice showed normal sensory-motor functioning and no morphological deficits in the adult brain (Bolognani et al., 2007). In contrast, loss-of-function of Hu-homolog *elav* in *Drosophila* is embryonic-lethal (Colombrita et al., 2013; Bronicki and Jasmin, 2013). Since there are two other neuronal Hu proteins with similar functions and overlapping expression in mammals, Akamatsu et al., (2005) proposed that they may compensate for the loss of HuD in knockout mice, resulting in only mild effects on nervous system development and motor phenotypes (Akamatsu et al., 2005; Colombrita et al., 2013). This hypothesis is further supported by Okano and Darnell, (1997), who showed that HuD expression in the developing mouse brain and adult brain largely exhibits a high degree of spatio-temporal overlap with HuC (Okano and Darnell, 1997). Similar to HuD knockout mice, the knockout of HuC in mice does not induce any debilitating neurological or motor phenotypes, while double HuC/HuD knockout mice die soon after birth (Akamatsu et al., 2005; Bolognani et al., 2007; Ince-Dunn et al., 2012; Colombrita et al., 2013). This indicates considerable functional overlap and compensatory actions of HuC and HuD while also demonstrating the critical need for neuronal Hu proteins during development.

It is not surprising then that misregulation of HuD in humans is associated with several neuronal pathologies. As previously described, a significant number of HuD target mRNAs are involved in neurite outgrowth, axon guidance, cell cycle progression and neuronal differentiation and survival (Bolognani et al., 2009). Many of these mRNAs have been associated with neurological disorders including Alzheimer's

disease, Huntington's disease, schizophrenia, and Parkinson's disease, and may induce pathology if misregulated by HuD (Bolognani et al., 2009; Bronicki and Jasmin, 2013). In fact, mutations in the gene encoding HuD (*ELAVL4*) and misregulation of protein expression have been implicated to play roles in neuromuscular diseases including spinal muscular atrophy (SMA) and amyotrophic lateral sclerosis (ALS) (Hubers et al., 2010; Akten et al., 2011, Fallini et al., 2012, Bronicki and Jasmin, 2013). Hubers et al., (2010) provided evidence that targeting HuD in the motor neurons may be a viable therapeutic option for patients with SMA. Perhaps then that by studying the relationship between LRRK2 and HuD, we may also be able to suggest its use as a therapeutic target for patients with LRRK2-associated Parkinson's disease. This is supported by the previously described genetic screen in *Drosophila* showing that disruption of Hu-homolog RBP9 expression rescued PD-like pathology in the eye of flies expressing a pathogenic mutation (Figure 3).

The involvement of HuD in PD pathology is mostly speculative at the moment, but is supported by several lines of evidence. First, three separate genetic studies have linked single-nucleotide polymorphisms (SNP) in *ELAVL4* (encoding HuD) with modifying the age-at-onset or risk of Parkinson's disease (Noureddine et al., 2005; Haugarvoll et al., 2007; DeStefano et al., 2008). One SNP in particular was identified in all three studies and is located in the last exon (exon 8) of the *ELAVL4* (Noureddine et al., 2005; Haugarvoll et al., 2007; DeStefano et al., 2008). This SNP results in a substitution of a proline for serine at position 270 in the hinge region of the HuD protein and could affect the secondary structure of the protein and have implications for function (Bolognani and Bird, 2013). Additional evidence supporting the potential role of HuD in PD is the involvement of proteins like tau (whose mRNA is bound by HuD) in PD pathology (Hardy, 2010; Bolognani and Bird, 2013; Schekel et al., 2016). As previously mentioned, tau protein has been found to form insoluble tangles alongside toxic α-synuclein aggregates in patients with PD (Zimprich et al., 2004; Goris et al., 2007; Lei et al., 2010; Moussaud 2014). Since the LRRK2 G2019S mutant has been proposed to facilitate the hyperphosphorylation of tubulin-associated tau in the context of PD pathology, it is possible that HuD-regulation of tau transcript stability and translation exacerbates this effect (Kawakami et al., 2012, Shanley et al., 2015). In addition to tau, a

recent study has proposed that HuR binds the 3'UTR of *SNCA* mRNA encoding α-synuclein, and is involved in its post-transcriptional regulation (Marchese et al., 2017). As previously described, α-synuclein aggregates are one of the key hallmarks of PD pathology that contribute to neurodegeneration (Spillantini et al., 1998). Though there have been no subsequent studies to date to confirming that HuD also binds *SNCA* mRNA, it is enticing to propose a potential role for HuD in regulating its expression in the context of PD (Bolognani and Bird, 2013). Finally, as previously mentioned, several mRNAs bound by HuD such as *BDNF* encode proteins that are associated with apoptosis of dopaminergic neurons, which die preferentially in PD (Bolognani and Bird, 2013). Altogether, this evidence strongly suggests that HuD may have an important role in Parkinson's disease.

Post-translational modifications of HuD

Though HuD plays a critical role in neuronal development and plasticity, few studies to date have examined the molecular mechanisms that control its activity and expression. Given that HuD has been linked to several neuronal disorders if not properly regulated, it is necessary to investigate the molecular events that regulate its function. Post-translational modifications such as phosphorylation and methylation of various residues of HuD have been shown to affect its localization, abundance and function (Pascale et al., 2005; Fujiwara et al., 2006; Hubers et al,. 2010; Lim and Alkon, 2012; Bronicki and Jasmin, 2013; Brauer et al., 2014). CARM1, a methyltransferase that regulates transcription and RNA-processing has been shown to methylate HuD at an amino acid in the linker (hinge) region (Fujiwara et al., 2006; Hubers et al., 2010). This methylation event reduces the interaction between HuD and *CDKN1A* mRNA (encoding p21), thereby reducing transcript stability and decreasing total cellular mRNA levels (Fujiwara et al., 2006; Hubers et al., 2010). Interestingly, other HuD-targeted mRNAs such as *GAP43* and *MAPT* seem unaffected by CARM1-induced methylation of HuD, indicating that certain mechanisms of post-translational regulation are transcript specific (Fujiwara et al., 2006)

The activation of certain isoforms of serine/threonine protein kinase C (PKCα and ε) has been shown to promote the phosphorylation of HuD (Pascale et al., 2005; Lim and Alkon, 2012). Stimulation

of PKC activity enhanced the association of *GAP43* and *BDNF* mRNA with HuD, and also lead to an increase in Gap-43 and BDNF protein expression (Pascale et al., 2005; Lim and Alkon, 2012; Vanevski et al., 2015). Though no evidence has been produced to show that PKC directly phosphorylates HuD, PKC inhibition almost completely blocks the effects described above, indicating a key role for PKC in mediating the phosphorylation and function of HuD (Pascale et al., 2005; Lim and Alkon, 2012).

Post-translational modifications of HuD have not been studied in detail, thus PKC is currently one of the only kinases reported to induce HuD phosphorylation. The majority of studies to date regarding the phosphorylation of Hu proteins have addressed HuR, with more than 20 serine, threonine and tyrosine sites phosphorylated by a variety of proteins including checkpoint kinase 2 (Chk2), p38 mitogen-activated protein kinase (MAPK) and cyclin-dependent kinase 1 (Cdk1) (Abdelmohsen et al., 2007; Kim et al., 2008; Lafarga et al., 2009; Doller et al., 2010; Yu et al., 2011). Most of these sites are located in the first and second RNA-recognition motifs (RRM1/RRM2) or in the linker region, and have been implicated in controlling the nucleoplasmic shuttling of HuR and affecting the ability of HuR to bind its target mRNAs (Doller et al., 2010; Kim et al., 2010; Yu et al., 2011; Brauer et al 2014). Due to the high sequence homology between HuD and HuR, this suggests the potential for HuD as a substrate for phosphorylation by a more expansive list of proteins than PKC.

Objectives of our study

As discussed above, current knowledge surrounding the mechanism in which the LRRK2 G2019S mutation, the most common genetic cause of Parkinson's disease, leads to pathology is largely incomplete. It is imperative that further research be performed to elucidate this mechanism in order to improve therapeutic strategies for patients with the disease. Given that the unpublished work of our collaborator (D. Park) showed that the deletion of the *rbp9* gene in *Drosophila melanogaster* expressing a pathogenic LRRK2 mutation rescued the phenotypic abnormalities otherwise observed in these flies, we hypothesized that *rbp9* may be involved in the pathogenesis of Parkinson's disease. Specifically, we

proposed that LRRK2 acts on the neuronal RBP9 homolog in humans, HuD, to regulate the post-transcriptional expression of the RNAs bound by HuD.

In this study, we explored the relationship between LRRK2 and HuD. First, we evaluated the mechanism in which LRRK2 acts on HuD, and how the manipulation of LRRK2 affected the binding of RNAs by HuD. Next, we used human neuroblastoma cells to assess whether LRRK2 is necessary for the regulation of the total expression of RNAs bound by HuD. Finally, transgenic mice expressing the LRRK2 G2019S mutation were used to evaluate genome-wide effects of the pathogenic mutation on the transcriptome, as well as effects of LRRK2 G2019S on the expression of transcripts bound by HuD. The results of our study offer a compelling insight into a novel mechanism of whereby LRRK2 regulates post-transcriptional gene expression by acting on RNA-binding protein HuD.

Materials and Methods

Cell culture, lysis, transfection and treatments

Mouse neuroblastoma Neuro2A cells and human neuroblastoma SH-SY5Y cells were cultured in DMEM (Wisent) supplemented with 10% fetal bovine serum (FBS), 100U/mL penicillin and 100ug/mL streptomycin. Rat pheochromocytoma PC12 cells were cultured in collagen IV coated dishes in DMEM (Wisent) supplemented with 10% horse serum, 5% FBS, 100U/mL penicillin and 100ug/mL streptomycin. All cell lines were maintained at 37°C with 5% CO_2. Transient DNA transfection was performed 24 hours post-seeding in low-serum (2-5% FBS), antibiotic-free DMEM using lipofectamine 2000 reagent as per manufacturer's instructions (Thermo Fisher Scientific). HuD overexpression assays were performed using the pFRT-DestFLAGHA_HuD plasmid (Addgene #65760); a gift from Thomas Tuschl (Rockefeller University, NY, USA). Transfection control assays were performed in parallel using the pcDNA3-EGFP plasmid (Addgene #13031); a gift from Doug Golenbock. Silencer® Select siRNAs (Thermo Fisher Scientific; Appendix - Table 1) were transfected at a concentration of 10nM using RNAiMax following manufacturer's protocol (Thermo Fisher Scientific). Co-transfection of DNA and siRNA was performed using lipofectamine 2000 and cells were harvested for analyses 60-72h post-transfection. For total protein collection, cells were washed twice in cold PBS, scraped, and incubated in lysis buffer [50mM Tris-HCl (pH 7.4), 75mM NaCl, 0.5mM EDTA, 0.5% Triton-X, 1X protease inhibitor cocktail (Sigma Aldrich), 1X phosphatase inhibitor cocktail (Sigma Aldrich)] at 4°C for 20 min with moderate tumbling. Lysates were centrifuged for 5000 x g for 10 min and supernatants were stored at -20°C until further use. For total RNA collection, 1mL TRIzol reagent (Thermo Fisher Scientific) was added directly to cells following two PBS washes. Cells were allowed to sit at room temperature for 5 min before freezing at -80°C. For experiments involving LRRK2 kinase inhibition, cells were treated with 1μM of DMSO-dissolved LRRK2-selective inhibitor GSK2578215A (Tocris) for 3 hours immediately before cell harvest. Control cells were simultaneously treated with 1μM DMSO.

Mice and tissue homogenization

Mice of desired genotypes for this study were created using heterozygous breeding strategies by crossing C57BL/6 *HuD*$^{+/-}$ mice with C57BL/6 *Lrrk2*$^{+/+}$ or *Lrrk2*$^{G2019S/+}$ mice. *Lrrk2*$^{G2019S/+}$ mice possessed a single copy of the LRRK2 G2019S gene in the endogenous loci. Desired genotypes included: HuD wild type/LRRK2 wild type (*HuD*$^{+/+}$*/Lrrk2*$^{+/+}$), HuD wild type/LRRK2 G2019S (*HuD*$^{+/+}$*/Lrrk2*$^{G2019S/+}$), HuD knockout/LRRK2 wild type (*HuD*$^{-/-}$*/Lrrk2*$^{+/+}$) and HuD knockout/LRRK2 G2019S mice (*HuD*$^{-/-}$*/Lrrk2*$^{G2019S/+}$). All mice used for each application in this study are listed in the Appendix (Table 2). At approximately 4 weeks of age, cortex, ventral midbrain, dorsal midbrain and striatum tissues were harvested by Dr. Charles Campbell, Dr. Alexandre Savard and Olanta Negeri. Ventral midbrain regions contained the substantia nigra and small amounts of surrounding hippocampus while the dorsal midbrain contained the remaining midbrain structures. Tissues were flash frozen immediately after dissection and stored at -80°C. For total protein analysis, a fraction of each brain region was re-suspended in homogenization buffer [50mM Tris-HCl (pH 7.4), 140mM NaCl, 1% SDS, 1% Triton-X and 1X protease inhibitor cocktail (Sigma Aldrich)] in 2.0mL tubes containing stainless steel beads. Tubes were placed in a MagNA lyser for two rounds of rapid oscillation at 7000rpm for 15 sec. Tissues were then incubated with gentle shaking at 4°C for 20 min and centrifuged twice at 10,000 x g for 10 min, placing the supernatant into a new tube between spins. Tissue lysates were stored at -80°C until further use. For total RNA analysis, fractions of brain tissue were resuspended in 1mL TRIzol reagent and frozen at -80°C until RNA isolation was performed. For HuD-RNA immunoprecipitation assays, frozen midbrain tissues were crushed on dry ice using a steel Plattner's Mortar and Pestle (Thomas Scientific) prior to incubation in IP lysis buffer [50mM Tris (pH 7.4), 150mM NaCl, 1% Nonidet P-40, and 1X protease inhibitor cocktail [Sigma Aldrich]) with gentle tumbling for 30min at 4°C. Immunoprecipitation of RNA-protein complexes was performed as outlined in the 'Immunoprecipitation' section.

Western blotting

Protein concentration from cell and tissue lysates was estimated by Bradford Protein Assay following the manufacturer's protocol (Biorad). Samples were prepared for electrophoresis by combining appropriate volumes of each lysate to give 25ug of total protein with Laemmli loading buffer [50mM Tris (pH 6.8), 2% SDS, 10% glycerol, 5% β-mercaptoethanol, 0.1M DTT] and distilled water to equal 25uL. Proteins were denatured by boiling at 99°C for 8-10 min and separated by 10% polyacrylamide gel electrophoresis (SDS-PAGE). Proteins were transferred to polyvinylidene fluoride (PVDF) membranes (Millipore) and membranes were blocked in 5% milk in TBST [10 mM Tris-HCl (pH 8), 150 mM NaCl, 0.05% Tween 20] for 1 hour at room temperature. Membranes were probed with primary antibody overnight at 4°C followed by three washes in TBST for 10 min each. Membranes were then incubated with HRP-labelled secondary antibody at room temperature for 1 hour and washed again for 3x10 min washes in TBST. All antibodies used are listed in the Appendix (Table 3). Proteins were visualized using Luminata Crescendo Western HRP chemiluminescent substrate (Millipore) to the membrane on an Image Quant LAS4010 Biomolecular Imager (GE Healthcare). Quantitative analyses on band intensity levels were performed using the histogram function on Photoshop CS6 software. Mean band intensity was normalized to tubulin or actin levels.

Enzyme-Linked Immunosorbent Assay (ELISA)

SH-SY5Y cells were transfected with the plasmid encoding FLAG-HA-tagged HuD (herein referred to as FLAG-HuD) or the control GFP plasmid, and siRNA targeting LRRK2 or negative control siRNA as previously described (see 'Cell culture, lysis, transfection and treatments'). Media and cell lysates were collected 72 hours post-transfection. Cell lysates were stored at -20°C until protein analysis was performed by western blot to confirm FLAG-HuD transfection and LRRK2 knockdown. Cell culture media was centrifuged at 1500 x g for 10 min and supernatants were immediately used in the Quantikine Human BDNF Immunoassay (R&D Systems) following the manufacturers' instructions. BDNF

concentration in all samples was normalized to an untreated media blank before normalizing test samples to control samples.

Immunoprecipitation

Cells were washed twice with 3mL of phosphate-buffered saline (PBS), and collected in IP lysis buffer [50mM Tris (pH 7.4), 150mM NaCl, 1% Nonidet P-40, 1X protease inhibitor cocktail (Sigma Aldrich)]. For RNA immunoprecipitation, IP lysis buffer also contained 40units/mL of RNaseOUT Recombinant Ribonuclease Inhibitor (Invitrogen). Lysates were incubated at 4°C for 20 min with gentle tumbling followed by centrifugation at 5000 x g for 10 min to pellet cell debris. The supernatant was transferred to a new tube, and pellets were discarded. To pre-clear cell lysates, 10uL of Dynabeads® Protein-G magnetic beads (Thermo Fisher Scientific) per lysate sample were first washed three times in cold IP wash buffer [50mM Tris (pH 7.4), 150mM NaCl and 0.1% Nonidet P-40]. For immunoprecipitation of RNA-protein complexes, wash buffer contained 20units/mL RNaseOUT. Beads were resuspended in 100uL wash buffer and added to each lysate. Lysates with bead mixtures were then incubated at 4°C for 20 min with gentle tumbling, after which supernatants were removed and beads discarded. For immunoprecipitation of the protein-complexes, 2ug of antibody to the protein of interest or 2ug of mouse IgG control antibody (eBioscience) was added to 800ug-900ug of protein from the pre-cleared supernatants and incubated at 4°C for 2 hours with gentle tumbling. In order to sequester the antibody-protein complexes, 20uL of magnetic beads per IP or IgG sample were first washed three times in cold IP wash buffer before being added to each IP and IgG sample. Samples were tumbled gently at 4°C for 1 hour, after which beads were sequestered on a magnetic rack and supernatants were discarded. Beads were gently tumbled in cold IP wash buffer for three washes of 5 min each, with increasing NaCl concentration in buffer for each wash (150mM, 175mM and 200mM). For co-IPs, all beads were resuspended in 20uL IP lysis buffer and 1X Laemmli loading buffer. For RNA-protein immunoprecipitations, 10% of the beads were resuspended in 20uL IP lysis buffer and Laemmli buffer for western blot, while remaining beads were resuspended in TRIzol reagent. Samples for western blot were

boiled at 99°C for 10min and beads were sequestered using a magnetic rack and discarded. Eluted proteins were separated by SDS-PAGE gel electrophoresis and immunoblotting was performed as described previously (see 'Western blotting').

Phosphorylation assay

Pure GST-tagged mouse HuD or GST control proteins were a gift from Dr. Jocelyn Coté. Pure, active, full length wild-type LRRK2, recombinant G2019S LRRK2 (aa. 970-2527) and recombinant D1994A LRRK2 (aa. 970-2527) human proteins were obtained from Thermo Fisher Scientific (catalogue no. A15197, PV4881 and PV 6051 respectively). To identify gel migration and banding pattern of proteins, 500ng of each LRRK2 protein, GST-HuD and GST control were separated by SDS-PAGE and stained with Coomassie Blue G-250 stain. *In vitro* phosphorylation assays were carried out in a 25uL volume by combining 1.5ug of GST-HuD (or GST control) with 60ng of wild-type, G2019S or D1994A LRRK2 in phosphorylation buffer [20mM HEPES (pH 7.5), 10mM $MgCl_2$, 1mM EGTA, 2mM DTT, 1% DMSO and 1X PhosSTOP^{TM} phosphatase inhibitor cocktail (Sigma Aldrich)]. Reactions containing GST-HuD alone, wild-type LRRK2 and G2019S LRRK2 alone were additionally carried out as negative controls. To initiate phosphorylation, 10µM ATP and 10µCi [γ-^{32}P]ATP was added to each tube and reactions were incubated at 30°C for 1hr. A second set of reactions were simultaneously set up as described above but without [γ-^{32}P]ATP to confirm equal use of HuD and LRRK2 protein in each reaction by western blot. Reactions were terminated by the addition of 1XLaemmli loading buffer and were subsequently boiled at 99°C for 5 min. Proteins were separated by western blot as previously described. Membranes were dried and exposed to autoradiography film for 24-72 hours before imaging.

Protein Identification by LC-MS/MS

Samples destined for mass spectrometry were prepared in a sterile work environment and were separated by polyacrylamide gel electrophoresis using 4-20% Mini-PROTEAN TGX Pre-cast Protein Gels (BioRad). Proteins were visualized using the PlusOne Silver Staining Kit following the

manufacturer's protocol (GE Healthcare Life Sciences). Protein bands of interest were excised from gels and stored in 1% acetic acid and sent to the Ottawa Hospital Research Institute Proteomics Core Facility for proteomics analysis. Proteins were digested in-gel using trypsin (Promega) according to the method of Shevchenko et al., (2006). Peptide extracts were concentrated by Vacufuge (Eppendorf). LC-MS/MS was performed using a Dionex Ultimate 3000 RLSC nano HPLC (Thermo Scientific) and Orbitrap Fusion Lumos mass spectrometer (Thermo Scientific). MASCOT software version 2.6 (Matrix Science, UK) was used to infer peptide and protein identities from the mass spectra. The observed spectra were matched against mouse sequences from SwissProt (version 2016-09) and also against an in-house database of common contaminants. The results were exported to Scaffold PTM Viewer (Proteome Software, USA) for further validation and viewing.

Reverse transcription and qPCR

Primer sets for qPCR were designed using the NCBI Primer-BLAST tool with user-guided settings based on the following criteria: 1) product length must be between 120 to 180bp, 2) primers should be between 18-23nt long and have melting temperatures of 58-60°C, 3) primers must have minimal unintended targets and span exon-exon junctions to avoid amplification of genomic DNA. Amplification efficiency of primer sets for each gene of interest was evaluated through standard curve analysis using pooled RNA samples from the cell type and species of interest. NRT (no reverse transcriptase) and NTC (no template control) reactions were also performed with each primer set to asses primer-dimer formation and background genomic DNA amplification. Only the primer sets with efficiencies of 90-110% and >4 Ct values from NTC and NRT controls were used for subsequent RNA expression analysis (Appendix; Table 4).

Total RNA

Total RNA from cells and tissues was extracted from TRIzol reagent following the manufacturer's instructions (Thermo Fisher Scientific) and resuspended in nuclease-free water. RNA was quantified and purity was estimated using the Take3 BioPlate Reader. 250ng of RNA was reverse transcribed in first

strand cDNA synthesis reactions using M-MuLV reverse transcriptase (New England Biolabs) supplemented with Oligo$(dT)_{18}$ and dNTP mix (Thermo Fisher Scientific) following the manufacturer's protocol. cDNA was diluted 1:25 in nuclease-free water and immediately used in quantitative PCR (qPCR). qPCR reactions were carried out using GoTaq ® qPCR master mix (Promega) with primer sets indicated in the Appendix (Table 4). Cycling conditions for all primer sets was as follows: 95°C for 2 min, (95°C for 15 sec, 60°C for 40 sec) x 40 cycles, followed by a melt curve to assess product dissociation. Fold changes in mRNA levels were calculated using the ΔΔCt method. For SH-SY5Y knockdown experiments, mRNA levels were normalized to housekeeping genes GAPDH and TBP (ΔCt). Test conditions were normalized to control conditions for each biological replicate (ΔΔCt), and biological replicates were averaged (n=4). Fold change in each condition was expressed relative to control (1.0). For analysis of total RNA from mouse tissue samples (5-6 mice per genotype), mRNA levels of interest were normalized to actin (ΔCt). ΔCt values were averaged between mice of the same genotype for each mRNA, and were normalized to the average ΔCt in wild type mice to give ΔΔCt.

Immunoprecipitated RNA

RNA from immunoprecipitations was extracted from TRIzol reagent following the manufacturer's instructions (Thermo Fisher Scientific) and resuspended in 25uL of nuclease-free water. During the extraction process, RNA transfer volumes between tubes was consistent in order to compare the quantity of RNA pulled down in each immunoprecipitation. 7uL of RNA was used in first strand cDNA synthesis using iScript Reverse Transcription Supermix (BioRad) according to manufacturer's instructions. cDNA was diluted 1:6 in nuclease-free water and immediately used for qPCR. qPCR reactions were carried out using SsoAdvanced Universal SYBR Green Supermix (BioRad) with primer sets indicated in the Appendix (Table 4). Cycling conditions for all primer sets was as follows: 95°C for 3 min, (95°C for 10 sec, 60°C for 20 sec, 72°C for 20 sec) x 40 cycles, followed by a melt curve to assess dissociation temperatures. Products were run on a 1% agarose gel with 0.3ug/mL EtBr to confirm amplification of one product. Technical replicates that produced undetectable Ct values or multiple/incorrect melt curve peaks were omitted from analysis. mRNA levels in HuD immunoprecipitations were normalized to levels in

control IgG samples and expressed as fold change relative to the IgG. In experiments comparing mRNA enrichment in different conditions, fold changes were normalized to the relative amount of HuD pulled-down in each condition (using band intensity from western blots.) Fold changes in test conditions were normalized to the control condition for each biological replicate.

Site-directed mutagenesis

The FLAG-HuD plasmid was used to create three different mutant plasmids: (i) threonine to alanine at position 144 in the human sequence (T144A) (ii) threonine to alanine and position 169 in the human sequence (T169A) (iii) both mutations (T144A/T169A). Mutations were created with primers indicated in the Appendix (Table 4). Primers were designed to anneal 'back-to-back' on opposing DNA strands in a non-overlap extension site-directed mutagenesis approach described by Hemsley et al., (1989). The forward primer of each set contained the mismatch(es) needed to create the desired site-directed mutation on the 5' end, while the reverse primer was exactly complementary to the wild type sequence and did not overlap with the forward primer. In the case of (iii), mutant plasmid (i) was used in a subsequent round of site-directed mutagenesis PCR with primers for mutation (ii). PCR reactions contained 25ng DNA template, 0.25μM forward and reverse primers, 0.25mM dNTPs and were catalyzed by 0.02U/uL Q5 High-fidelity DNA polymerase (New England Biolabs). Negative control reactions were carried out with the above components except for the primers. Cycling conditions were as follows: 98°C for 3 min, (98°C for 7 sec, 72°C for 7.5 min) x 27 cycles, 72°C for 10min. PCR reactions gave a linear product that was phosphorylated at the 5' end using T4 polynucleotide kinase following manufacturer's instructions (New England Biolabs), followed by ligation using T4 DNA ligase (New England Biolabs) at 16°C overnight. Template DNA in PCR reactions was digested using DPN1 following the manufacturer's instructions (New England Biolabs). 5% of PCR reaction volumes were run on 1% agarose gel with 0.3ug/mL EtBr to confirm product formation and template DNA digestion. DH5α cells were transformed with 5-10% of PCR reaction products from mutagenesis and negative control reactions. DNA was purified from colonies using a plasmid midi-prep kit (Qiagen) as per manufacturer's guidelines and sent for DNA sequencing at

the StemCore DNA Sequencing Facility to confirm mutagenesis (Ottawa Hospital Research Institute). Constructs that were successfully mutated were used in subsequent experiments.

Statistical Analysis

Two-tailed student's t-tests (type 3 - unequal variance) were performed using Microsoft Excel 2007 to identify statistical significance between two independent groups of data. For data with more than two independent groups, a one-way ANOVA (analysis of variance) test was performed. In cases where statistical significance was identified with ANOVA, a Tukey post-hoc test was performed to determine which specific groups differed from each other. ANOVA and post-hoc tests were computed in Prism 3.0. Statistical significance was represented with the following notation: *$p<0.05$; **$p<0.01$, ***$p<0.001$, etc.

Results

Antibody validation and protein expression

Prior to performing any protein-based experiments, specificity of our HuD and LRRK2 antibodies was verified by siRNA knockdown of these proteins in human neuroblastoma SH-SY5Y and mouse neuroblastoma Neuro2A (N2A) cells. Assessment of N2A cell lysates by western blot using the HuD antibody showed a double banding pattern at ~40-42kDa in control cells (Figure 5A). Cells treated with siRNA against HuD showed a 65% decrease in the intensity of both bands upon quantification, confirming the specificity of this antibody. LRRK2 was assessed in SH-SY5Y lysates and showed a strong band just above 245kDa whose intensity was reduced by almost 90% in cells treated with an siRNA against LRRK2 (Figure 5B). A second, weak band was seen at ~180kDa but was not as affected by LRRK2 siRNA, suggesting that it is non-specific (Figure 5B). Endogenous LRRK2 expression was very low in N2A cells, and HuD expression was almost undetectable in SH-SY5Y cells. We compared endogenous expression of these proteins with lysates from wild type and LRRK2 knockout mouse embryonic fibroblasts (MEFs), which also served as a negative control for expression of the neuron-specific protein HuD. Endogenous LRRK2 in N2A cell lysates was comparable to LRRK2 KO MEFs, while HuD was not detected in lysates of SH-SY5Y (Figure 5C). We additionally evaluated protein levels in rat pheochromocytoma PC12 cells and found abundant HuD expression but undetectable levels of LRRK2 (Figure 5C). To achieve co-expression of HuD and LRRK2 in one cell line, we attempted to transfect N2A and PC12 cells with a plasmid encoding wild type LRRK2 and SH-SY5Y cells with a plasmid encoding FLAG-HA-tagged HuD (herein referred to as FLAG-HuD). LRRK2 plasmid transfection was unsuccessful, likely due to the large size of the LRRK2 insert (7584nt) and the resulting plasmid size of ~14kb. Efficient transfection of FLAG-HuD was achieved in SH-SY5Y cells as shown by western blot, giving a double banded pattern at ~44-46kDa when assessed with both HuD and FLAG antibodies indicating that both bands are specific to the protein encoded by our plasmid (Figure 5D). SH-SY5Y cells overexpressing FLAG-HuD were chosen as the model cell line for the majority of our experiments.

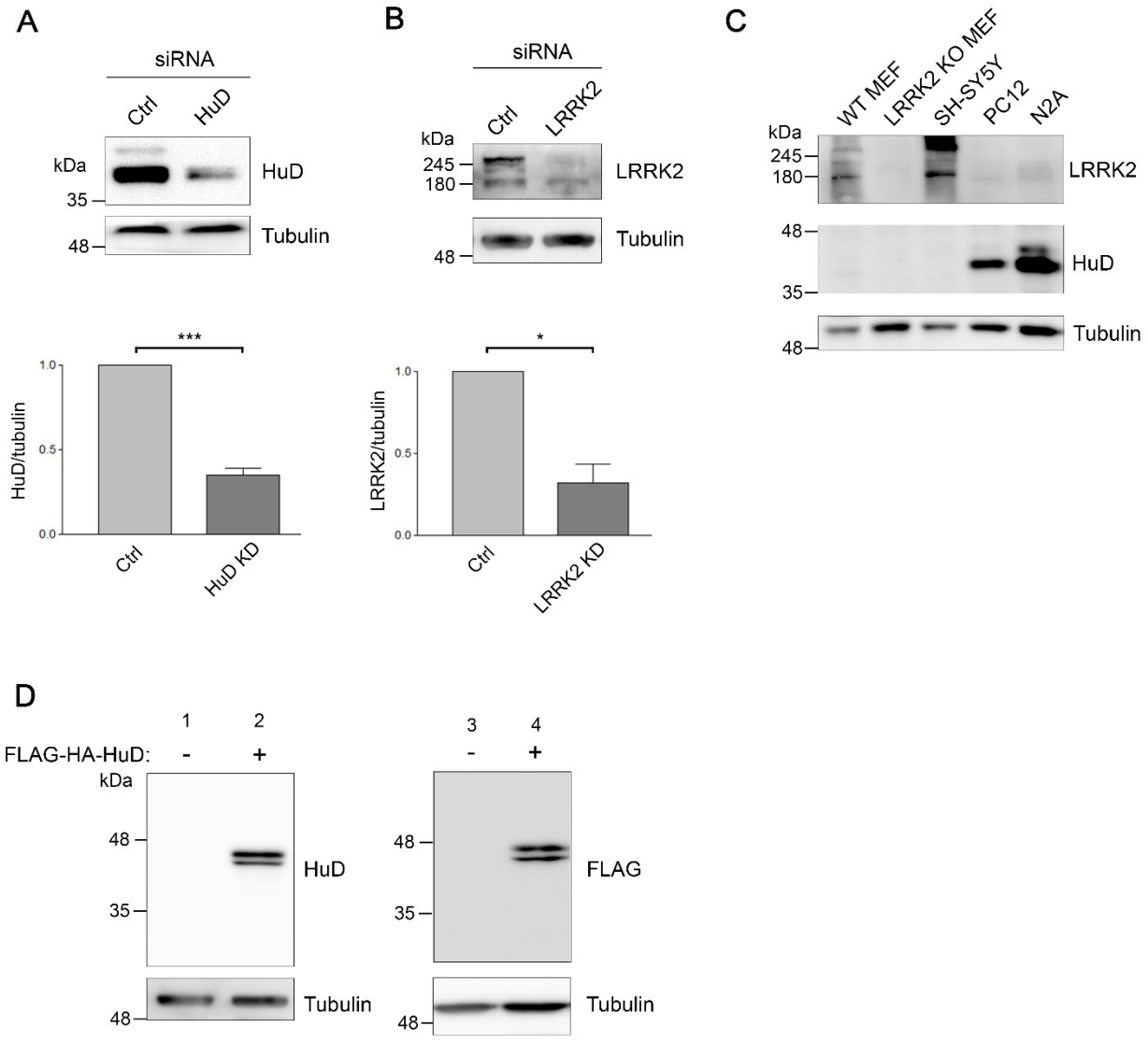

Figure 5: LRRK2 and HuD expression is variable in neuroblastoma cell lines. (A) Neuro2A cells were transfected with control siRNA or siRNA targeting HuD, and (B) SH-SY5Y cells were transfected with control siRNA or siRNA targeting LRRK2. Cells were harvested 72h after transfection and protein levels were analyzed by western blot. Bands were quantified and normalized to tubulin. Data are means +/- SEM; [(A) n=4; (B) n=3]. Asterisks indicate statistical significance as determined by Student's T-test (two-tailed with unequal variance), *p<0.05, ***p<0.001. (C) Endogenous expression of HuD and LRRK2 proteins was evaluated by western blot in wild type (WT) and LRRK2 knockout (KO) mouse embryonic fibroblasts (MEF), human neuroblastoma SH-SY5Y cells, rat pheochromocytoma PC12 cells and mouse neuroblastoma Neuro2A (N2A) cell lysates. (D) Lysates from wild type SH-SY5Y cells (lanes 1 and 3) and cells expressing FLAG-HuD (lanes 2 and 4) were subjected to western blot analysis using antibodies specific to HuD (lanes 1 and 2) or FLAG (lanes 3 and 4). Lysates 1 and 2 were run on separate gels than lysates 3 and 4.

LRRK2 does not associate with HuD in SH-SY5Y cells

To gain an insight into the relationship between LRRK2 and HuD, we performed FLAG-HuD immunoprecipitation assays in SH-SY5Y cells and assessed the lysates for the presence of LRRK2 to determine whether they interact. To verify successful co-precipitation of HuD-binding partners, immunoprecipitates were assessed by western blot for known HuD-associated protein eIF4A (elongation initiation factor 4A). A band corresponding to the molecular weight of eIF4A (~47kDa) was observed in the cell lysate (input) and FLAG-HuD immunoprecipitate but not in the IgG control (Figure 6A). Efficient FLAG-HuD pull-down was confirmed in FLAG-immunoprecipitate at ~44-46kDa and corresponded to the banding pattern seen in the cell lysate (slightly obscured by left-over signal from eIF4A at 47kDa) (Figure 6A). Co-immunoprecipitations using both a HuD and a FLAG antibody were assessed by western blot for the presence of LRRK2 (Figure 6B). A strong banding pattern corresponding to LRRK2 was observed in cell lysates, but we did not observe an equivalent signal in immunoprecipitates regardless of whether FLAG-HuD was pulled-down using the HuD or FLAG antibody (Figure 6B). Though this suggests that HuD and LRRK2 do not associate, it is possible that an interaction may be compromised by the FLAG-tag or HA-tag. It is also possible that a transient interaction exists such as a phosphorylation, but is not robust enough to be captured by co-immunoprecipitation.

LRRK2 phosphorylates HuD *in vitro*

Though we found that LRRK2 and HuD do not participate in a direct, long-lasting interaction by co-immunoprecipitation, we hypothesized that HuD may be a candidate for phosphorylation by LRRK2. To test our hypothesis, we performed *in vitro* kinase assays by incubating wild type LRRK2 (WT), over-active LRRK2 kinase mutant G2019S, or kinase-dead LRRK2 mutant D1994A with purified GST-HuD substrate. Prior to performing these assays, pure proteins were evaluated by Coomassie blue staining to identify their banding pattern and migration on a gel. Three bands corresponding to purified GST-HuD were observed between 48-63kDa, while GST control protein was seen at 25kDa in a single band (Figure 7A). LRRK2 WT full-length protein migrated just above 245kDa while recombinant LRRK2 G2019S and

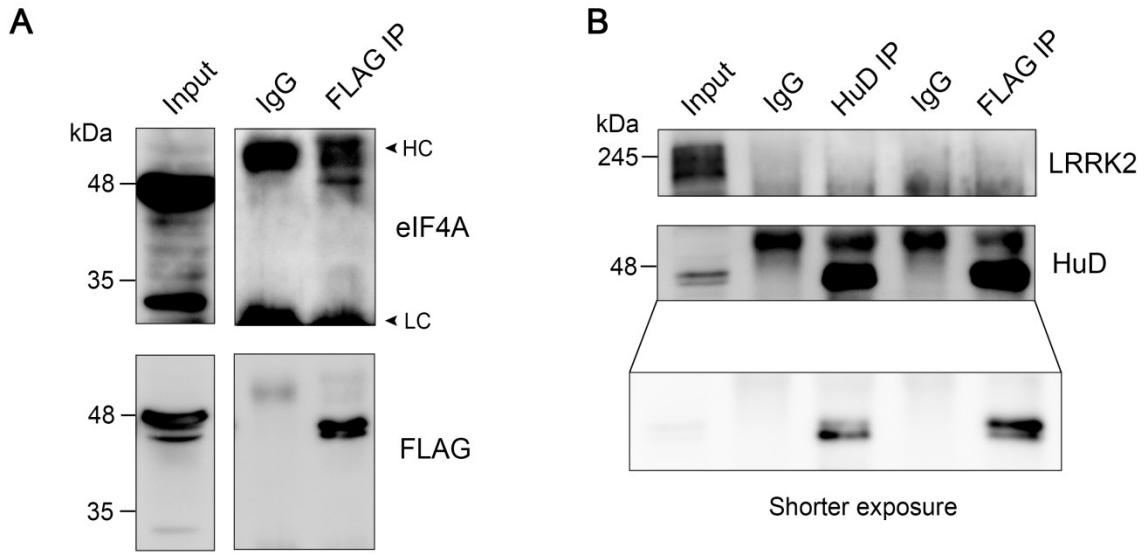

Figure 6: LRRK2 does not co-immunoprecipitate with HuD in SH-SY5Y cells. (A) SH-SY5Y cells expressing FLAG-HuD were subjected to immunoprecipitation with a FLAG antibody and IgG isotype control antibody. Total cell lysate (input) and immunoprecipitates were analyzed by western blot using an antibody against known HuD-binding partner eIF4A to confirm co-precipitation methods, following by the FLAG antibody to verify FLAG-HuD pulldown. Migration of antibody immunoglobulin heavy chain (*HC*) and light chain (*LC*) is indicated. (B) Cell lysates were subjected to immunoprecipitation with a FLAG antibody, HuD antibody, or IgG isotype control antibody. Total lysate (input) and immunoprecipitates were analyzed by western blot using antibodies against HuD and LRRK2.

LRRK2 D1994A proteins (truncated at N-terminus; aa. 970-2527) migrated slightly below 245kDa (Figure 7A; [a]). All three LRRK2 proteins showed a second, faint band between 63-75kDa that likely represents a truncated form of the protein (Figure 7A; [b]).

When GST-HuD was incubated with LRRK2 WT and G2019S, we observed a strong phosphorylation signal corresponding to the molecular weight and Coomassie banding pattern of GST-HuD (Figure 7B; arrowheads). No evidence of phosphorylation was seen when GST-HuD was incubated with kinase-dead LRRK2 D1994A mutant. In assays combining GST-HuD substrate with LRRK2 G2019S, we observed a 3.0-fold increase in band intensity compared to assays containing WT LRRK2 (Figure 7D). All assays were performed in parallel without radioactive ATP and evaluated by western blot to confirm equal use of LRRK2 and GST-HuD (Figure 7C).

In control assays containing active LRRK2 kinase and GST-ctrl, faint background bands were observed with LRRK2 WT and LRRK2 G2019S that were not present when GST was combined with kinase-dead LRRK2 D1994A (Figure 7B; [a-c]). The same banding pattern was evident in LRRK2 WT and G2019S assays carried out with no substrate, suggesting that they represent weak LRRK2 autophosphorylation rather than GST phosphorylation. In fact, background bands at 245kDa correspond to the molecular weight and banding pattern of full-length LRRK2 by Coomassie (Figure 7A&B; [a]), while bands the between 63-75kDa correspond to the size of the truncated proteins identified previously (Figure 7A&B; [b]). Additional, non-specific signals between 48-63kDa were seen in assays with active LRRK2 (regardless of substrate presence), but do not correspond to the masses LRRK2 or HuD by Coomassie (Figure 7B; [c]). Ultimately, our observations not only suggest that HuD is a substrate for LRRK2 phosphorylation, but they also indicate that HuD is hyperphosphorylated by G2019S.

HuD binds mRNAs associated with neuronal function and Parkinson's disease in SH-SY5Y cells

Since we discovered that HuD is phosphorylated by LRRK2, we hypothesized that LRRK2 kinase activity may have an impact on the function of HuD in mRNA binding. Prior to investigating this hypothesis, we first assessed the enrichment of several candidate mRNAs in HuD-RNA

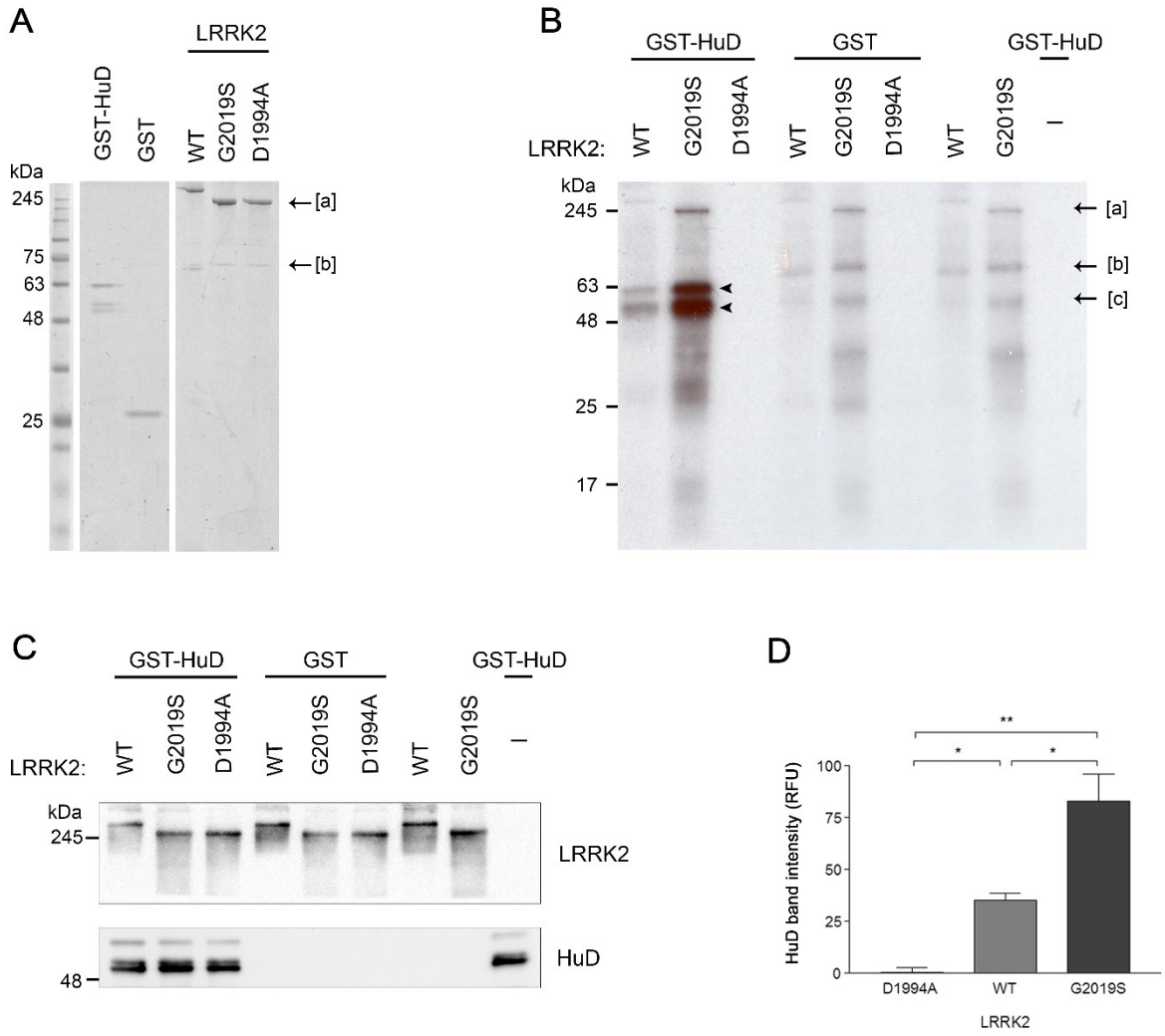

Figure 7: LRRK2 phosphorylates HuD *in vitro.* (A) 500ng of pure GST-HuD, GST control, wild type LRRK2 (WT), over-active kinase mutant LRRK2 G2019S, and kinase-dead mutant LRRK2 D1994A proteins were separated by SDS-PAGE and visualized by Coomassie staining. Full-length LRRK2 WT and recombinant LRRK2 G2019S and D1994A are indicated by [a], while truncated forms of each LRRK2 protein are indicated by [b]. (B) Pure LRRK2 WT, LRRK2 G2019S and LRRK2 D1994A were incubated with GST- HuD or GST control and [γ-32P]ATP. Additional assays were run with LRRK2 WT, LRRK2 G2019S and GST-HuD alone as negative controls. Incorporation of [γ-32P]ATP into protein subtrates was visualized by autoradiography of PVDF membranes. HuD phosphorylation in is indicated by arrowheads. LRRK2 autophosphorylation of full-length and truncated proteins is indicated by [a] and [b], and background phosphorylation is indicated by [c]. (C) Membranes used for autoradiography in (A) were subjected to immunoblotting using antibodies specific for HuD and LRRK2. (D) HuD phosphorylation by LRRK2 WT, G2019S and D1994A was quantified from autoradiographs using Photoshop CS6 software. Data are means +/- SEM; (n=3). Statistical significance of the data set was determined by one-way analysis of variance test (ANOVA) = **p<0.01. Tukey post-hoc tests were used to determine statistical significance of each condition compared to each other, indicated by asterisks; *p<0.05, **p<0.01.

immunoprecipitation assays to identify a sub-set of transcripts to pursue in subsequent experiments. We chose to evaluate several mRNAs known to be bound by HuD including those encoding neurite-development protein Gap-43, cell cycle control factor $p21^{Waf1}$ and BDNF (Brain-Derived Neurotrophic Factor) (Bolognani et al., 2009; Vanevski et al., 2015; Marchese et al., 2017). We also chose to evaluate the HuD-RNA IP enrichment of transcripts encoding PD-relevant proteins tau and α-synuclein; the former mRNA binds HuD while the latter binds HuR, a highly conserved Hu protein family member (Aranda-Abreu et al., 1999; Marchese et al., 2017). Finally, we assessed the binding of mRNA encoding LRRK2 to HuD. Though LRRK2 has not been described as an mRNA target of HuD in existing literature, it contains numerous Hu-binding motifs in its 3'UTR as predicted by the RBPmap motifs database (http://rbpmap.technion.ac.il/), using representative query motifs from Table 1. Potential HuD-binding motifs in the 3'UTR sequence of the human and mouse transcripts encoding LRRK2 are listed in Appendix Table 5. The 3'UTR of human and mouse transcripts encoding α-synuclein was also assessed for HuD-binding motifs using this method and showed many AU- and U-rich regions predicted to be sites for HuD binding (Appendix Table 5). HuD-RNA immunoprecipitation assays performed in SH-SY5Y cells (using FLAG-HuD) showed a striking enrichment in transcripts encoding LRRK2, p21, BDNF and α-synuclein by at least 5000 fold in HuD-RNA IP samples compared to control IgG samples, (expressed as a function of log10 in Figure 8B). *GAP43* mRNA showed a trend towards enrichment in HuD-RNA IPs, but was not statistically significant. In addition, mRNA encoding tau was not enriched in HuD-RNA IPs. As a negative control, the enrichment of *GAPDH* mRNA was assessed in HuD-RNA IPs as it has not been cited to bind HuD in existing literature. As expected, there was no significant difference in *GAPDH* mRNA between HuD-RNA IP and control IgG samples (Figure 8B).

LRRK2 knockdown causes a reduction in mRNA binding by HuD

In order to evaluate whether LRRK2 affects the ability of HuD to bind mRNA, SH-SY5Y cells expressing FLAG-HuD were treated with a control siRNA or siRNA targeting LRRK2 for 60 hours prior to performing RNA-immunoprecipitation assays on lysates. Analysis of total protein in cell lysates by

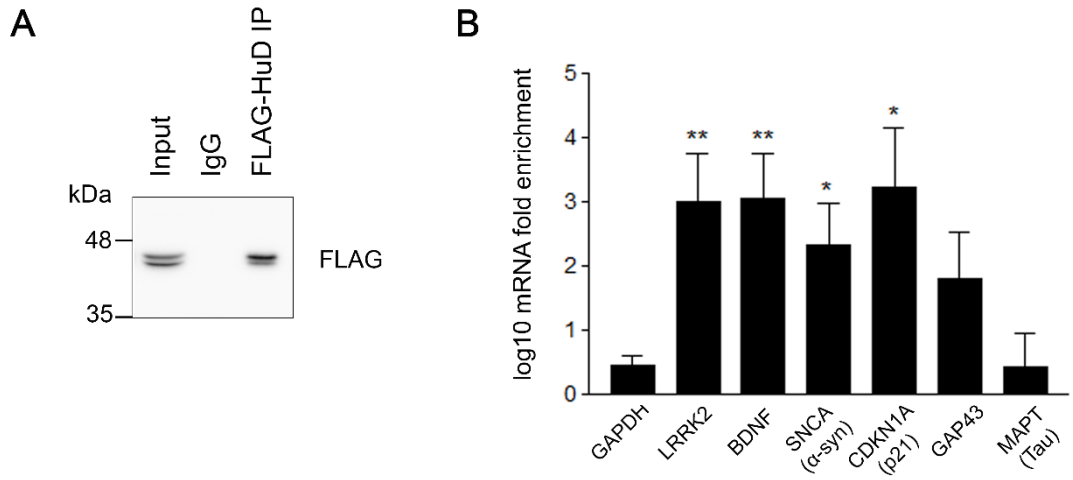

Figure 8: HuD binds mRNAs associated with neuronal function in SH-SY5Y cells. (A) SH-SY5Y cells expressing FLAG-HuD were subjected to immunoprecipitation (IP) in RNase-free conditions using a FLAG antibody or a control IgG antibody. (B) Equal volumes of immunoprecipitated RNA from HuD IPs and IgG IPs was used in RT-qPCR with primers specific for a selected set of mRNAs. Amplification of mRNA in HuD IPs is expressed as fold enrichment relative to amplification in IgG IPs on a log10 scale. Data are means +/- SEM; (n=4). Asterisks indicate statistical significance as determined by Student's T-test (two-tailed with unequal variance), *$p<0.05$, **$p<0.01$.

western blot showed proficient knockdown of LRRK2 by siRNA and equal expression of FLAG-HuD in both control and LRRK2 knockdown conditions (Figure 9A). Western blot of IPs showed efficient pull-down of FLAG-HuD (Figure 9B). Equal volumes of RNA pulled down with HuD in control and LRRK2 knockdown conditions were used in subsequent RT-qPCR reactions, and the enrichment of mRNAs from HuD-IPs in cells treated with LRRK2 siRNA were expressed relative to control siRNA conditions. We chose to evaluate mRNAs that showed a significant positive fold change in our previous HuD-RNA pulldowns in Figure 8 (mRNAs encoding LRRK2, BDNF α-synuclein and p21). We observed a significant reduction in HuD-binding of mRNAs encoding LRRK2, BDNF and α-synuclein by 85%, 90% and 80% respectively in LRRK2 knockdown conditions (Figure 9C). Enrichment of mRNA encoding p21 was reduced by 20% in HuD IPs in LRRK2 knockdown conditions, but data were not statistically significant (Figure 9C). This suggests that LRRK2 is required for the binding of certain transcripts by HuD, while binding of other transcripts may be dependent on additional factors.

We hypothesized that the reduction in mRNA binding by HuD observed as a result of LRRK2 loss is caused by the lack of LRRK2-mediated phosphorylation of HuD. To investigate this, SH-SY5Y cells expressing FLAG-HuD were treated with a selective LRRK2 kinase inhibitor GSK2578215A (GSK) for 3 hours prior to performing HuD-RNA immunoprecipitation assays in cell lysates. GSK is a 2-arylmethyloxy-5-substitutent-N-arylbenzamide compound that shows potent and highly selectivity for LRRK2 across the kinome as demonstrated by Reith et al., (2012) and Qin et al., (2017). Preliminary experiments were also performed using a second LRRK2 kinase inhibitor, 2,4-diaminopyrimidinyl compound HG-10-102-01, but we found that this compound gave inconsistent results and was not as effective as GSK. These observations are supported by West et al. (2015) who reported that HG-10-102-01 shows suboptimal pharmacokinetics and stability.

The efficiency of LRRK2 kinase inhibition by GSK was validated by examining the reduction of LRRK2 autophosphorylation at residue Ser935 by immunoblot. Autophosphorylation of this site has been validated by several studies as a key biomarker of LRRK2 kinase activity in cells, mice and in human

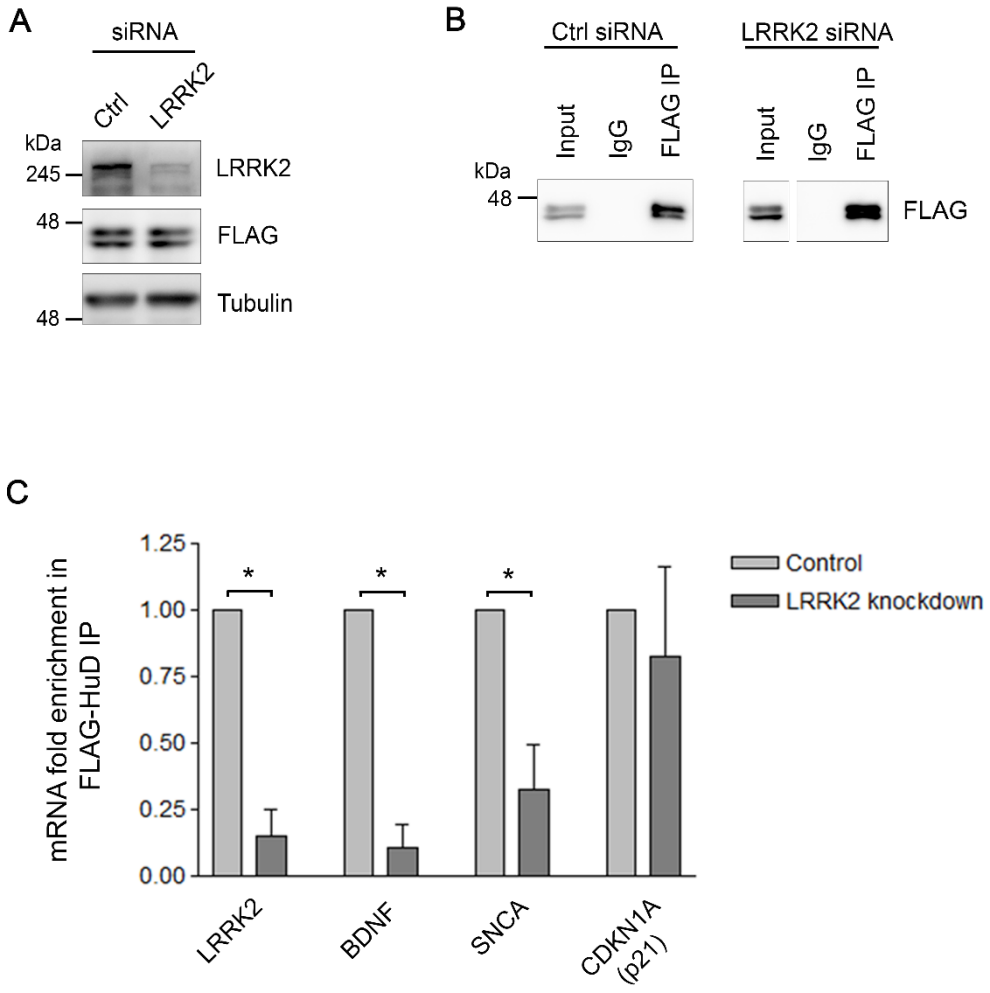

Figure 9: LRRK2 knockdown reduces HuD-mRNA binding. Human neuroblastoma SH-SY5Y cells expressing FLAG-HuD were treated with control siRNA or siRNA targeting LRRK2. Cells were lysed after 60 hours under RNase-free conditions and lysates were subjected to RNA-immunoprecipitation (IP) using a FLAG antibody or a control IgG antibody. (A) FLAG-HuD and LRRK2 expression in total cell lysates was assessed by western blot shows using antibodies specific for LRRK2 and FLAG. (B) Total cell lysate (input) and 10% of immunoprecipitated RNA-protein complexes were assessed by western blot using a FLAG antibody to confirm equal FLAG-HuD pulldown. (IgG and IP samples on LRRK2 knockdown blot were run on the same blot as the input sample but in the opposite order; samples were flipped horizontally to match loading order in control siRNA blot.) (C) Equal volumes of RNA extracted from HuD-RNA IPs and IgG-RNA IPs in each condition was analyzed by RT-qPCR using primers specific for mRNA sequences encoding LRRK2, BDNF, α-synuclein and p21. Fold enrichment of mRNA in IP samples was normalized to relative amount of FLAG-HuD pulled-down in the IPs using band intensity in western blots from (B). Enrichment of mRNA in FLAG-HuD IPs from cells transfected with LRRK2 siRNA is expressed relative to mRNA enrichment in control cells. Data are means +/- SEM; ($n \geq 3$). Asterisks indicate statistical significance as determined by Student's T-test (two-tailed with unequal variance), *$p<0.05$.

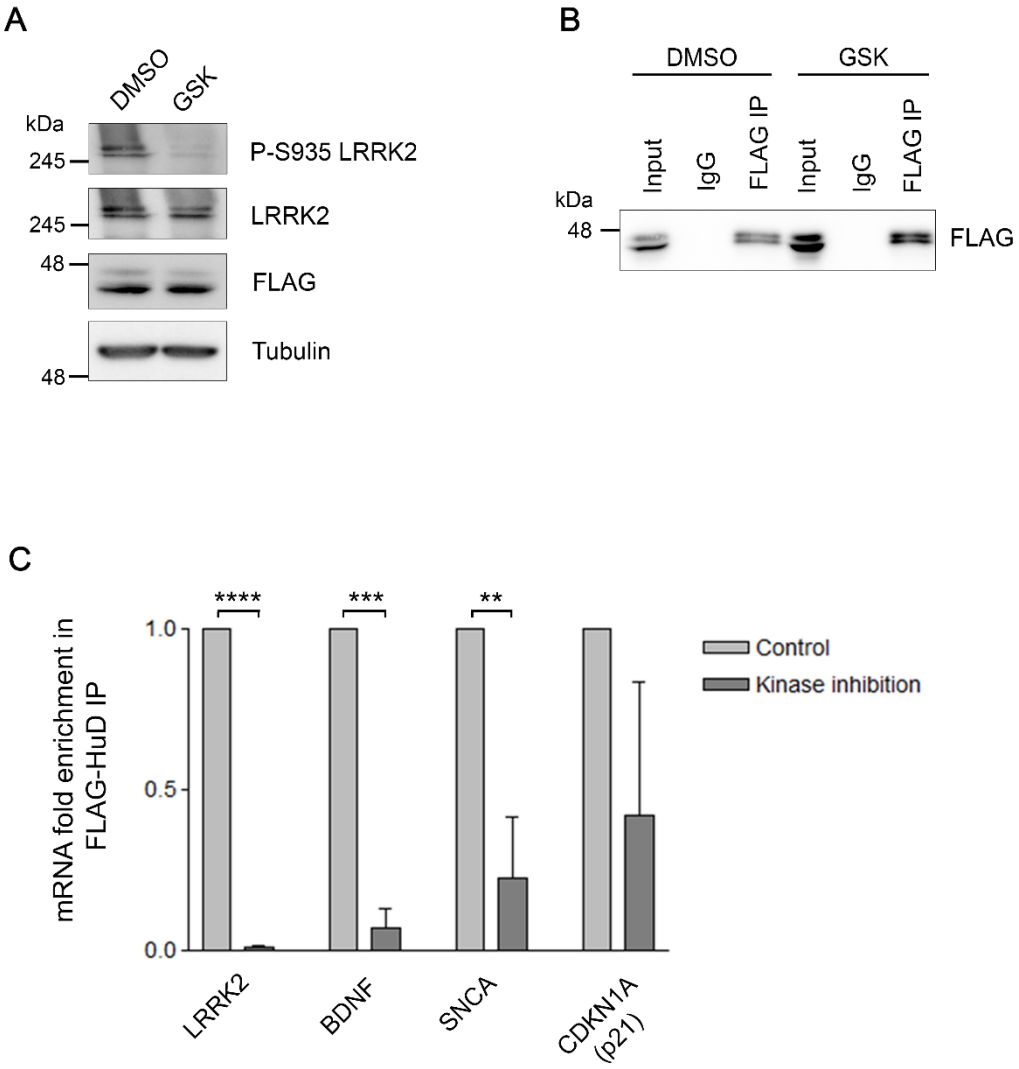

Figure 10: HuD-mRNA binding is inhibited upon loss of LRRK2 kinase activity. Human neuroblastoma SH-SY5Y cells expressing FLAG-HuD were treated with LRRK2 kinase inhibitor GSK2578215A (GSK) or DMSO (control condition) for 3 hours prior to cell lysis. Cells were lysed 48 hours after initial plasmid transfection in RNase-free and phosphatase-free conditions and subjected to RNA-immunoprecipitation (IP) using a FLAG antibody or control IgG antibody. (A) Total cell lysates were analyzed by western blot for LRRK2 autophosphorylation at S935 and for total LRRK2 protein. Expression of FLAG-HuD was verified using a FLAG antibody. (B) FLAG-HuD levels in total cell lysate (input) and 10% of immunoprecipitated RNA-protein complexes were assessed by western blot using a FLAG antibody. (C) Equal volumes of RNA extracted from FLAG-HuD IPs and IgG IPs were used in RT-qPCR with primers specific for mRNAs encoding LRRK2, BDNF, α-synuclein and p21. Enrichment of mRNA in FLAG-HuD IPs from cells treated with the LRRK2 kinase inhibitor is expressed relative to mRNA levels from DMSO control treated cells. Data are means +/- SEM; ($n \geq 3$). Asterisks indicate statistical significance as determined by Student's T-test (two-tailed with unequal variance), **$p<0.01$, ****$p<0.0001$.

patients treated with LRRK2 inhibitors (Dzamko et al., 2012, Chia et al., 2014, Perera et al., 2014). In our studies, western blot of GSK-treated cells showed a striking loss autophosphorylation of LRRK2 at S935 confirming the activity of this inhibitor as previously reported (Figure 10A). Immunoprecipitation of FLAG-HuD using the FLAG antibody showed efficient pull-down in both control and LRRK2 kinase conditions (Figure 10B). Normalization of RNA from HuD IPs was performed as described in the previous section. Similar to LRRK2 knockdown conditions, we observed a significant reduction in HuD-binding of transcripts encoding LRRK2, BDNF and α-synuclein by 99%, 90% and 80% respectively in LRRK kinase inhibition conditions (Figure 10C). Though the binding of mRNA encoding p21 appeared to follow a similar trend as the other mRNAs and was reduced by 50% in LRRK2 kinase inhibition conditions, data exhibited large variation and was not statistically significant (Figure 10C). Together, these findings indicate that LRRK2 kinase activity is necessary for the ability of HuD to bind certain mRNAs.

Increased binding of *Bdnf* mRNA in LRRK2 G2019S mice

Since we discovered that LRRK2 phosphorylates HuD and that the loss of LRRK2 kinase activity reduces the binding of HuD to mRNAs including those encoding LRRK2, BDNF and α-synuclein, we proposed that the over-active kinase mutant G2019S would have the opposite effect on mRNA binding to HuD. To investigate this, we performed HuD-RNA immunoprecipitation assays in the dorsal midbrain regions of 4 week old LRRK2 wild type mice (*Lrrk2*$^{+/+}$) and LRRK2 G2019S knock-in mice (*Lrrk2*$^{G2019S/+}$). Western blot showed efficient immunoprecipitation of HuD from both *Lrrk2*$^{+/+}$ and *Lrrk2*$^{G2019S/+}$ mice (Figure 11A). RT-qPCR was performed on equal volumes of immunoprecipitated RNA from HuD-IP and control IgG samples from four LRRK2 WT mice and three LRRK2 G2019S mice. We chose to evaluate the binding of *Bdnf* mRNA and *Snca* mRNA (encoding α-synuclein) to HuD, as their binding was among the mRNAs most prominently affected in previous *in vitro* experiments in SH-SY5Y cells. *GAPDH* was used as a negative control for mRNA binding to HuD, and showed no enrichment in HuD-RNA IPs compared to IgG-IPs in *Lrrk2*$^{+/+}$ mice and *Lrrk2*$^{G2019S/+}$ mice (Figure 11B). A significant

increase of more than 5000-fold in the binding of *Bdnf* mRNA to HuD was observed in *Lrrk2*$^{G2019S/+}$ mice compared to *Lrrk2*$^{+/+}$ mice (Figure 11B). A similar trend was observed in the binding of *Snca* mRNA to HuD in *Lrrk2*$^{G2019S/+}$ mice, but data was variable between mice of the same genotype and did not give statistical significance (Figure 11B). Together, our findings suggest that the over-active LRRK2 kinase mutant (LRRK2 G2019S) modifies the ability of HuD to bind *Bdnf* mRNA in the dorsal midbrain.

LRRK2 phosphorylates residues in RRM2 and linker region

As our findings have shown thus far, LRRK2 phosphorylates HuD *in vitro* and its kinase activity appears to be crucial in regulating HuD-mRNA binding. In order to gain insight into the mechanism of this effect, it is necessary to determine which HuD residue(s) are phosphorylated by LRRK2. As previously mentioned, the first two RNA-recognition motifs (RRMs) of HuD are necessary for mRNA binding while the third RRM binds the poly(A) tail to stabilize the mRNA-protein complex (Chung et al., 1996; Ma et al., 1997, Anderson et al., 2000, Park et al., 2000, Beckel-Mitchener et al., 2000, Bolognani et al., 2009). The linker region between the second and third RRM has been implicated in Hu-protein mediated alternative splicing, and also contains nuclear localization and export sequences and is required for cytoplasmic shuttling of HuD (Kasashima et al., 2001; Zhu et al., 2008; Zhou et al., 2011).

To identify candidate HuD sites for phosphorylation by LRRK2, we performed mass spectrometry and proteomics analysis on non-radioactive *in vitro* kinase assays combining GST-HuD substrate with mutant LRRK2 G2019S. As a negative control, we used GST-HuD substrate alone, as well as reactions combining GST-HuD with kinase-dead mutant D1994A. Several unique phosphorylation events were detected in assays with LRRK2 G2019S, including four threonine residues in the first two RRMs (T63, T147, T149, T174), one serine between RRM1 and RRM2 (S133), and three serines and one tyrosine in the linker region (S222, S223, S233 and Y259) (Figure 12A). Control assays and LRRK2 G2019S assays both showed phosphorylation of residue S69, suggesting that it is not specific to LRRK2. Phosphorylation intensity of each residue detected is listed in Table 2, and is expressed as a fraction of phosphorylated peptides out of the total number of peptides detected. Peptide coverage was between 65-68% for all

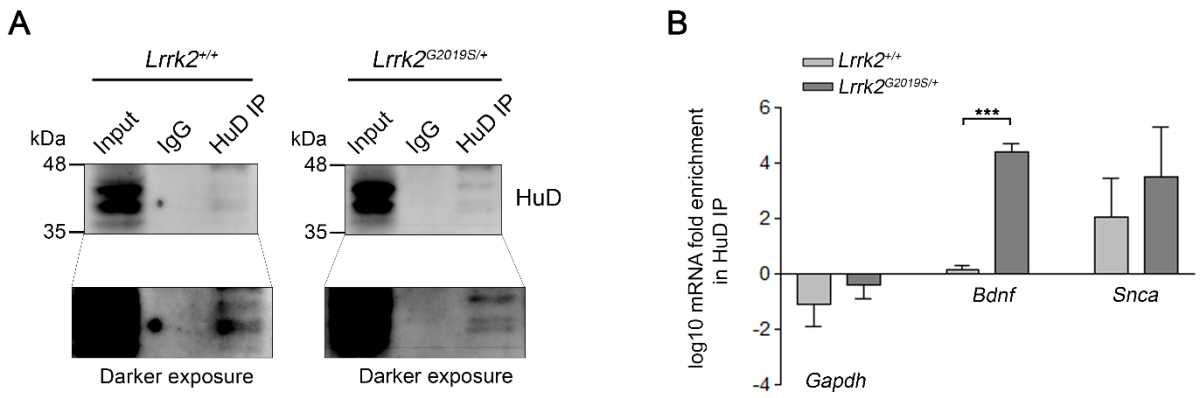

Figure 11: *Bdnf* mRNA is enriched in HuD-RNA IPs from LRRK2 G2019S mice. Dorsal midbrain tissues were isolated from 4 week old LRRK2 wild type mice (*Lrrk2*$^{+/+}$) and LRRK2 G2019S mice (*Lrrk2*$^{G2019S/+}$). Brain tissue lysates were subjected to RNA-immunoprecipitation (IP) using a HuD or IgG isotype control antibody in RNase-free conditions. (A) Western blot of tissue lysates (input) and 10% of immunoprecipitated RNA-protein complexes confirmed HuD pull-down in *Lrrk2*$^{+/+}$ and *Lrrk2*$^{G2019S/+}$ mice. Blots were exposed for a greater amount of time (shown in the darker exposure) to quantify the amount of HuD immunoprecipitated from each brain lysate. (B) Equal volumes of RNA extracted from HuD IPs and IgG IPs from each brain lysate were analyzed by RT-qPCR using primers specific for mRNAs encoding GAPDH, BDNF and α-synuclein. Amplification of targets in HuD IP samples was normalized to amplification in IgG samples. Data are means (*Lrrk2*$^{+/+}$ n=4; *Lrrk2*$^{G2019S/+}$ n=3) +/- SEM, and are expressed on a log10 scale. Asterisks indicate statistical significance as determined by Student's T-test (two-tailed assuming unequal variance), ***p<0.001.

assays. Of all sites detected, only T149, T174 and S233 exhibited a statistically significant difference in intensity between LRRK2 G2019S samples and control samples (HuD alone or LRRK2 D1994A) (Table 2). The highest phosphorylation intensity was exhibited by T149 in RRM2, giving a value approximately 2-fold higher than T174 in RRM2 and S233 in the linker region (Table 2). Due to the close sequence homology between proteins in the Hu family, we were interested in whether these sites are also conserved in HuB, HuC and HuR as well as in *Drosophila* homologs ELAV and RBP9. (Recall that a genetic screen in *Drosophila* expressing a pathogenic LRRK2 mutation showed that the deletion of the *rbp9* gene in these flies rescued pathology). Hu/ELAV sequence alignment showed that HuD phosphorylation site T149 in mice is conserved in RBP9, ELAV and in all mouse and human Hu proteins with the exception of HuC, where a serine residue is found instead of threonine and may therefore still be a candidate for phosphorylation (Figure 12B). Conservation of this site suggests that its potential phosphorylation by LRRK2 plays a common functional role in other mammalian Hu proteins and *Drosophila* homologs. Sites T174 in RRM2 and S233 in the linker region are conserved in all mouse and human Hu proteins but not in either of the *Drosophila* homologs (Figure 12B&C). These phosphorylation events could therefore be involved in regulatory functions unique to mammalian Hu proteins.

Table 2: Intensity values of HuD sites phosphorylated by LRRK2 *in vitro*. Phosphorylation intensity is expressed as the number of phosphorylation events/total # peptides detected (PTM spectrum counts). Data was compiled using Scaffold PTM software. Sites in bold exhibited statistically significant phosphorylation events ($p<0.05$), and were pursued in subsequent experiments.

	PTM spectrum counts			
HuD residue (mouse)	**No LRRK2**	**LRRK2 D1994A**	**LRRK2 G2019S**	**P-value**
T63	-	-	0.022	0.21
S69	0.321	0.056	0.181	0.48
S133	-	-	0.050	0.21
T147	-	-	0.015	0.21
T149	**-**	**-**	**0.062**	**0.04***
T174	**-**	**-**	**0.030**	**0.05***
S222	-	-	0.026	0.21
S223	-	-	0.040	0.09
S233	**-**	**-**	**0.034**	**0.02***
Y259	-	-	0.037	0.07

T149 phosphorylation detected *in vivo*

Next, we attempted to confirm LRRK2-mediated phosphorylation of candidate HuD sites *in vivo* by mass spectrometry and proteomics analysis of immunoprecipitated HuD from mouse cortex tissues. Phosphorylated HuD residues in LRRK2 wild type mice (*Lrrk2*$^{+/+}$) and mice expressing the LRRK2 G2019S mutation (*Lrrk2*$^{G2019S/+}$) were compared to those detected in LRRK2 knockout mice (*Lrrk2*$^{-/-}$). It should be noted that our population size was limited; only two mice of the LRRK WT and LRRK G2019S genotypes and one LRRK2 KO mouse was available for these experiments. Of the sites previously detected from *in vitro* assays, only T147, T149 and S223 were detected *in vivo* (Table 3). Sites T149 and S223 were phosphorylated in all mice, while T147 was detected in LRRK2 WT and KO mice, but not in LRRK2 G2019S mice (Table 3). Phosphorylation intensity of sites in LRRK2 WT and G2019S mice was within 1-2 fold of that observed in LRRK2 KO mice, suggesting that phosphorylation of these sites is not LRRK2-specific, and that there are other kinases capable of phosphorylating these HuD residues.

Table 3: Intensity values of HuD sites phosphorylated *in vivo*. Phosphorylation intensity is expressed as the number of phosphorylation events/total # peptides detected (PTM spectrum counts). Data was compiled using Scaffold PTM software. Sites in bold exhibited statistically significant phosphorylation events ($p<0.05$), and were pursued in subsequent experiments. (Note n=1 for *Lrrk2*$^{-/-}$ and n=2 for *Lrrk2*$^{+/+}$ and *Lrrk2*$^{G2019S/+}$).

	PTM spectrum counts		
HuD residue	***Lrrk2-/-***	***Lrrk2+/+***	***Lrrk2 G2019S/+***
T147	0.50	0.25	-
T149	0.33	0.17	0.13
S223	0.20	0.17	0.13

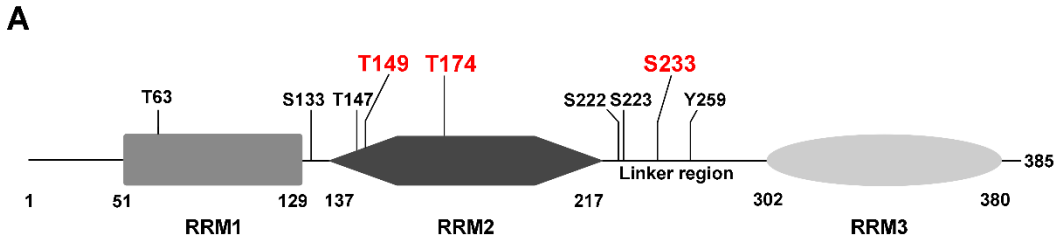

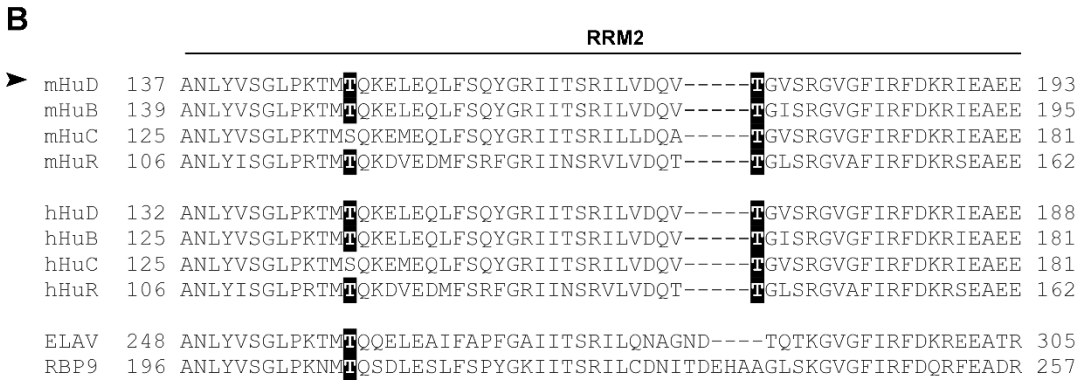

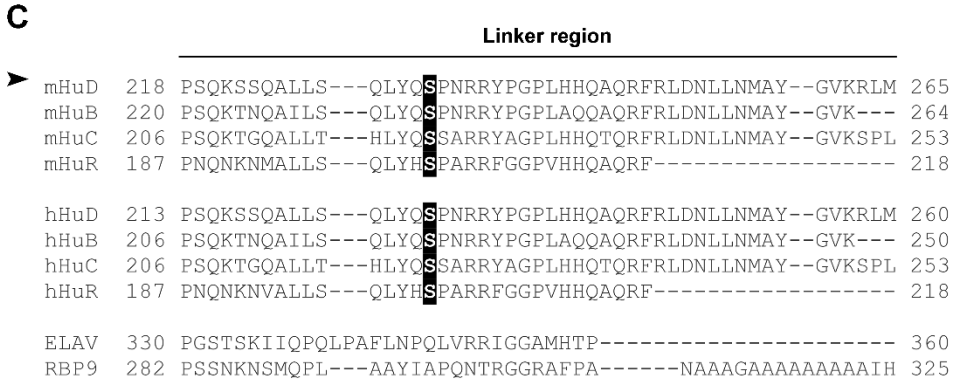

Figure 12: HuD phosphorylation sites are conserved with other Hu proteins and homologs. (A) Diagram depicting the domain architecture of the mouse HuD protein with sites phosphorylated by LRRK2 indicated in RNA-recognition motifs (RRMs) and the linker region. Sites in red exhibited significant phosphorylation intensities in *in vitro* phosphorylation assays upon the incubation of GST-HuD with mutant LRRK2 G2019S, and were chosen for subsequent analysis in protein sequence alignment. The mouse HuD (B) RRM2 sequence and (C) linker sequence was aligned with the amino acid sequences of the other mouse (*m*) and human (*h*) Hu proteins, and *Drosophila melanogaster* homologs ELAV and RBP9 proteins. Sequence alignment was performed using the EMBL Clustal Omega online tool (https://www.ebi.ac.uk/Tools/msa/clustalo/). Primary isoforms of Hu proteins and *Drosophila* proteins were used for alignment. The mouse HuD sequence is denoted by an arrowhead. Significant phosphorylation sites from (A) that are conserved with mouse HuD in are highlighted.

As we were not able to detect LRRK2-specific phosphorylation of HuD *in vivo* by mass spectrometry, we made an alternative attempt to visualize the phosphorylation of threonine residues of HuD by western blot of N2A cell lysates. Lysates from wild type cells were assessed using a general phosphothreonine (P-Thr) antibody (see Appendix Table 3) which showed faint bands by western blot in the cell lysate (input) and dark bands corresponding to the heavy and light antibody chains (*HC* and *LC*) in IgG and IP samples (Appendix; Figure 1). However, no obvious bands corresponded to the molecular weight of HuD in IP or cell lysate samples, suggesting that the antibody is not able to detect phosphorylated HuD residues, or that protein de-phosphorylation is occurring prior to western blotting. We additionally performed immunoprecipitation assays using the P-Thr antibody in an attempt to pull-down phosphorylated proteins. Cell lysates and immunoprecipitates were evaluated by western blot for the presence of HuD, which gave a strong band corresponding to its molecular weight in the input, but not in the control IgG or P-Thr-immunoprecipitate (Appendix; Figure 1). This again suggests that the P-Thr antibody is not specific for phosphorylated residues on HuD or that the phosphorylated residues are not accessible to the antibody.

Non-functional mutations in HuD cause loss of mRNA binding

Due to the pivotal role that RRM2 plays in RNA binding, we chose to assess the importance of phosphorylation sites in this domain identified previously through *in vitro* assays. As previously mentioned, sites T149 and T174 exhibited the highest and most significant phosphorylation intensities compared to other sites identified in RRM2. Remarkably, the RRM2 amino acid sequence in mice is 100% conserved in humans. Sites T149 and T174 become T144 and T169 in humans respectively, and will subsequently referred to as such. Based on current models of HuD crystal structure, T144 appears to be located in an α-helix and T169 is found in a loop connecting two β-sheets (Wang et al, 2001). It is possible that phosphorylation of these residues is important in maintaining the surface charge or biochemical structure of RRM2 and in turn the precision of its contacts with AU-rich mRNA targets. We

therefore hypothesized that loss of LRRK2-mediated phosphorylation of these residues would affect the ability of HuD to bind mRNA.

To evaluate our hypothesis, we used the human FLAG-HuD plasmid to create non-conservative mutations of threonine to alanine at sites T144 and T169 using site-directed mutagenesis. Single HuD mutants T144A and T169A were created as well as a double HuD mutant with both T144A and T169A. Plasmid expression was validated by western blot and was not inhibited by either mutation (Figure 13A). HuD-mRNA binding was evaluated by RNA-immunoprecipitation in SH-SY5Y cells transiently transfected with each plasmid. Western blot of precipitates showed adequate pull-down of wild type FLAG-HuD and all mutants in a banding pattern that corresponded to input samples (Figure 13B). The binding of mRNAs encoding LRRK2, α-synuclein, BDNF, p21 and Gap-43 was evaluated by RT-qPCR. While HuD-binding of *GAP43* mRNA remained fairly consistent regardless of HuD mutation, at least one of the mutations significantly inhibited the binding of mRNAs encoding LRRK2, α-synuclein, BDNF and p21 by HuD (Figure 13C). Single mutant T144A caused a consistent, 65% reduction in binding of mRNAs encoding LRRK2, α-synuclein and p21 compared to wild type HuD, while mutant T169A caused a 50-60% reduction in the binding of these mRNAs (Figure 13C). Double mutant T144A/T169A appeared to have a stronger effect on the binding of *LRRK2* mRNA by HuD than either of the single mutations; decreasing binding by 75%. The double mutant caused a similar reduction in binding of mRNAs encoding p21 and α-synuclein compared to the single mutant T169A. Interestingly, binding of *BDNF* mRNA was not significantly inhibited by either single mutation, but was reduced by 60% by the double mutation (Figure 13C). Taken together, this suggests that both T144 and T169 in HuD are important for the binding of transcripts encoding LRRK2, α-synuclein, BDNF and p21 by HuD. Our findings imply that preventing phosphorylation of these threonine sites by non-conservative mutation to alanine prevents proper binding of these mRNAs. This proposal correlates with our previous observations in LRRK2 knockdown and kinase inhibition conditions, where we also saw a significant reduction in HuD-binding of transcripts encoding LRRK2, BDNF and α-synuclein.

Preliminary analysis of LRRK2, p21 and α-synuclein protein levels was performed in cells expressing each of the HuD mutants to determine whether the non-conservative mutations influence protein expression. With the exception of LRRK2 expression in HuD T169A mutants, we observed a slight increase in protein levels in cells expressing the single mutations (Figure 13D). That said, it should be noted that these findings are the result of two replicates, and were not statistically significant (Figure 13E). Additional replicates should be performed to confirm this effect.

LRRK2 loss gives elevated protein levels of mRNAs bound by HuD

Previous research groups have shown that HuD is required for the stability and expression of target transcripts including Gap-43 and BDNF (Mobarak et al., 2000; Vanevski et al., 2015). Since our findings thus far have illustrated that LRRK2 kinase activity affects the ability of HuD to bind several mRNAs including those encoding α-synuclein, BDNF and LRRK2, we speculated that this would have consequences on their total cellular levels. To investigate this, we assessed the total mRNA and protein levels of α-synuclein, BDNF, p21 and Gap-43 in response to the manipulation of LRRK2 and HuD expression in SH-SY5Y cells. In addition to these HuD-mRNA targets, we also evaluated the expression of HuR; a HuD homolog and mRNA target of HuD that has been implicated to play a role in inflammatory diseases (Katsanou et al., 2005; Suzuki et al., 2006, Chen et al., 2017, Shang and Zhao, 2017). To create conditions in which HuD and LRRK2 expression was present or partially absent, SH-SY5Y cells expressing FLAG-HuD or GFP (+HuD and -HuD conditions respectively) were treated with control siRNA or siRNA against LRRK2 (referred to as +LRRK2 and -LRRK2 conditions respectively). LRRK2 knockdown was confirmed in by western blot (Figure 14A) and RT-qPCR (Figure 14B). Equal transfection and expression of FLAG-HuD in control and LRRK2 knockdown conditions was verified by western blot (Figure 14A).

Western blot was used to evaluate the protein levels of α-synuclein, p21, Gap-43 and HuR in each of our conditions, while levels of the secreted protein BDNF were evaluated by ELISA using cell culture media from each condition. We observed a significant increase in α-synuclein expression in LRRK2

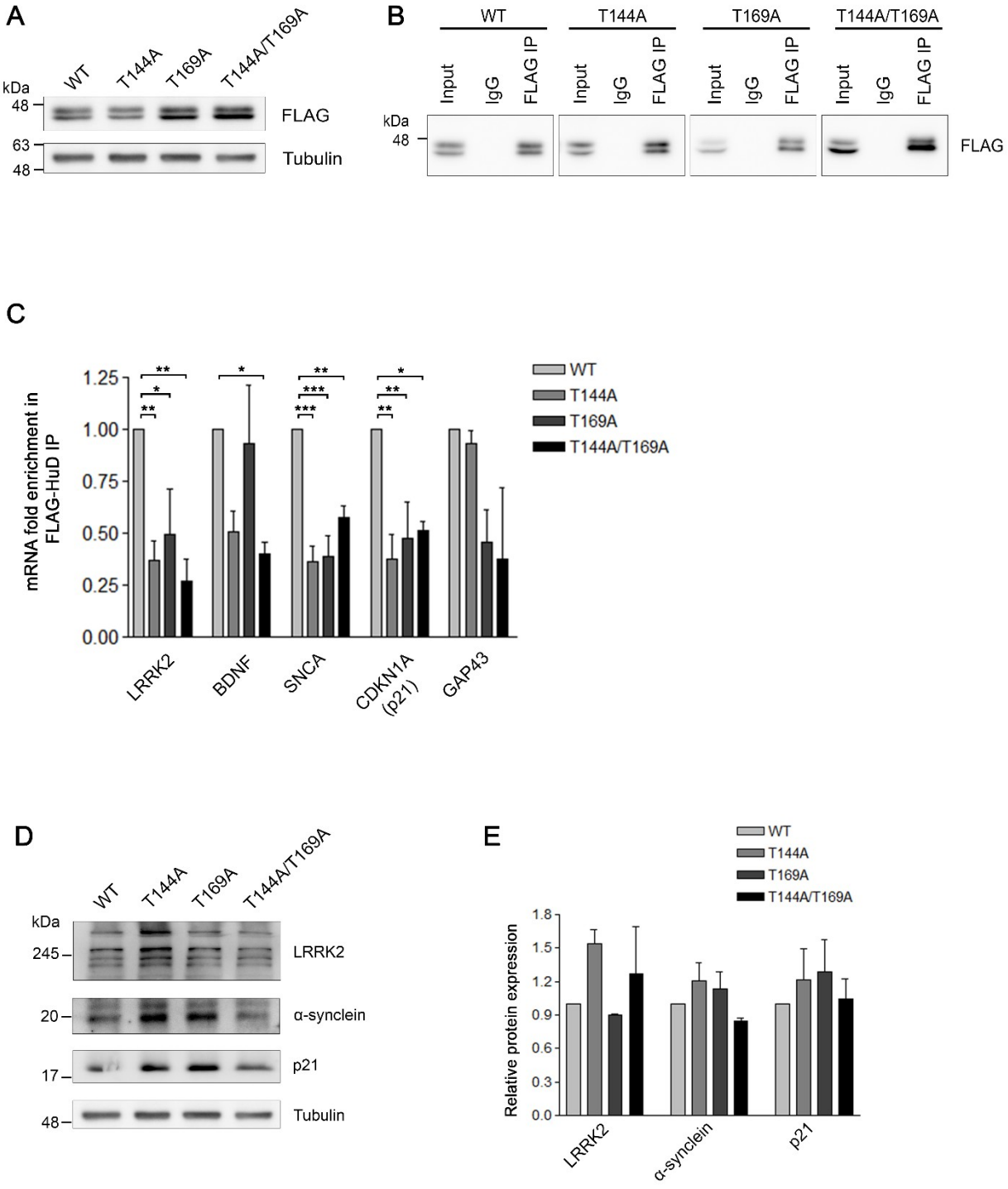
A
WT
T144A
T169A
T144A/T169A
kDa
48
63
48
FLAG
Tubulin
B
WT
T144A
T169A
T144A/T169A
Input
IgG
FLAG IP
kDa
48
FLAG
C
mRNA fold enrichment in FLAG-HuD IP
1.25
1.00
0.75
0.50
0.25
0.00
WT
T144A
T169A
T144A/T169A
LRRK2
BDNF
SNCA
CDKN1A (p21)
GAP43
D
WT
T144A
T169A
T144A/T169A
kDa
245
20
17
48
LRRK2
α-synclein
p21
Tubulin
E
WT
T144A
T169A
T144A/T169A
Relative protein expression
1.8
1.5
1.2
0.9
0.6
0.3
0.0
LRRK2
α-synclein
p21

Figure 13: Non-conservative mutation of HuD residues T144 and T169 to alanine causes reduced mRNA binding by HuD. Human neuroblastoma SH-SY5Y cells were transfected with plasmids encoding FLAG-HuD that contained single mutations T144A or T169A, or double mutation T144A/T169A. Lysates were subjected to RNA-immunoprecipitation (IP) using a FLAG antibody or a control IgG antibody. (A) Plasmid expression in total cell lysates was assessed by western blot using an antibody specific FLAG. (B) Total cell lysate (input) and 10% of immunoprecipitated RNA-protein complexes were assessed by western blot using a FLAG antibody. (C) Equal volumes of RNA extracted from IPs and IgG controls were analyzed by RT-qPCR using primers specific for mRNAs encoding LRRK2, BDNF, α-synuclein, p21 and Gap-43. Enrichment of mRNA in FLAG-HuD IPs from cells expressing HuD-T144A, HuD-T169A and HuD-T144A/T169A is expressed relative to enrichment in cells expressing wild type HuD. Data are means (n=3) +/- SEM. Statistical significance was determined by one-way analysis of variance (ANOVA). Asterisks indicate statistical significance between individual conditions as determined by Tukey's post-hoc tests; *$p<0.05$, **$p<0.01$, ***$p<0.001$. (D) Western blot of cell lysates from (A) were analyzed for expression of LRRK2, α-synuclein and p21. (E) Protein expression in (D) was quantified and expressed relative to wild type FLAG-HuD conditions. Data are means (n=2) +/- SEM. Statistical significance was determined by one-way analysis of variance (ANOVA) and Tukey's post-hoc tests.

knockdown conditions (+HuD/-LRRK2) that was rescued when HuD was also absent (-HuD/-LRRK2) (Figure 14C). Similar to α-synuclein, a significant increase in BDNF was observed as a result of LRRK2 knockdown (+HuD/-LRRK2) (Figure 14E). BDNF protein levels showed a slight rescue back to control levels (+HuD/+LRRK2) when HuD was also absent (-HuD/-LRRK2). Although statistically insignificant, a similar trend in HuR and p21 expression was observed where protein levels increased in response to LRRK2 knockdown, and were rescued when both HuD and LRRK2 were absent (Figure 14C). Gap-43 showed no significant changes in response to LRRK2 and HuD manipulation (Figure 14D).

Interestingly, protein levels of α-synuclein, p21, HuR, Gap-43 and BDNF did not change significantly between FLAG-HuD overexpression (+HuD/+LRRK2) and HuD absence (-HuD/+LRRK2) (Figure 14C-E). These observations they suggest that HuD does not induce changes in protein expression on its own but can modify LRRK2-induced changes in expression. These findings also indicate that while the expression of certain HuD-bound mRNAs appears to be regulated by LRRK2, the expression of others such as Gap-43 are less affected by LRRK2 and may be regulated through alternative mechanisms.

Although we observed a significant increase in protein levels of α-synuclein, BDNF and a trend towards increased HuR and p21 protein levels upon LRRK2 knockdown (+HuD/-LRRK2), their expression at the mRNA level did not follow the same trend. In fact, no significant change in the mRNAs encoding α-synuclein, BDNF, p21, Gap-43 or HuR observed in response to the manipulation of LRRK2 or HuD expression (Figure 14F). This suggests that LRRK2 mediates the translation or post-translational regulation of mRNAs bound by HuD and does not have an effect on the levels of the mRNA themselves.

Using knock-in LRRK2 G2019S and HuD knockout mice to evaluate protein levels

The LRRK2 G2019S over-active kinase mutation is one of the most common pathogenic mutations found in both familial and sporadic cases of Parkinson's disease (Gaig et al., 2007, Bouhouche 2017). Parkinson's disease pathology largely manifests as dopaminergic neuron loss in the region of the midbrain known as the substantia nigra pars compacta (SNc) which innervates and supplies dopamine to the striatum (Huot et al., 2007; Gerfer and Surmeier, 2011; McCarthy et al., 2011*)*. The striatum plays a role

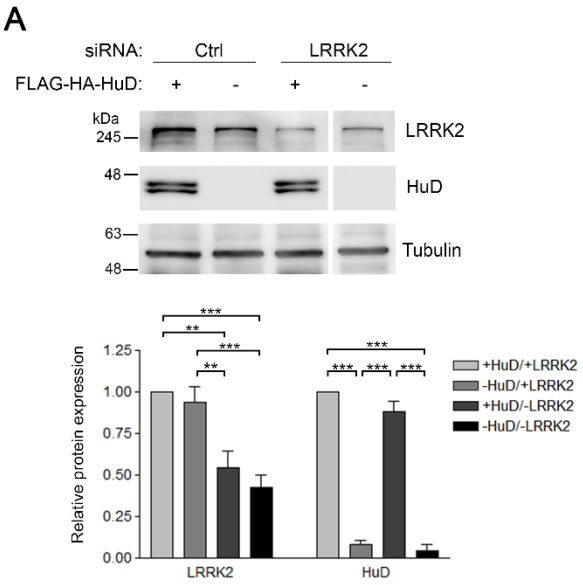
A
siRNA:
Ctrl
LRRK2
FLAG-HA-HuD:
+
-
+
-
kDa
245
LRRK2
48
HuD
63
48
Tubulin
Relative protein expression
1.25
1.00
0.75
0.50
0.25
0.00
LRRK2
HuD
+HuD/+LRRK2
-HuD/+LRRK2
+HuD/-LRRK2
-HuD/-LRRK2

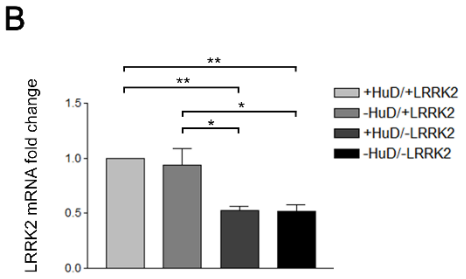
B
LRRK2 mRNA fold change
1.5
1.0
0.5
0.0
+HuD/+LRRK2
-HuD/+LRRK2
+HuD/-LRRK2
-HuD/-LRRK2

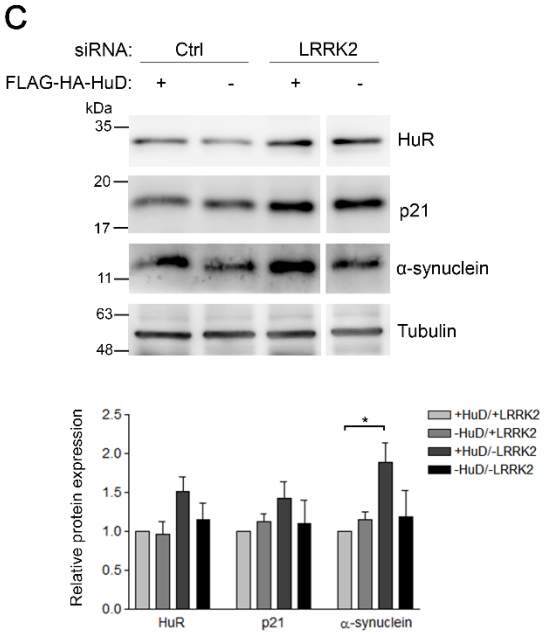
C
siRNA:
Ctrl
LRRK2
FLAG-HA-HuD:
+
-
+
-
kDa
35
HuR
20
17
p21
11
α-synuclein
63
48
Tubulin
Relative protein expression
2.5
2.0
1.5
1.0
0.5
0.0
HuR
p21
α-synuclein
+HuD/+LRRK2
-HuD/+LRRK2
+HuD/-LRRK2
-HuD/-LRRK2

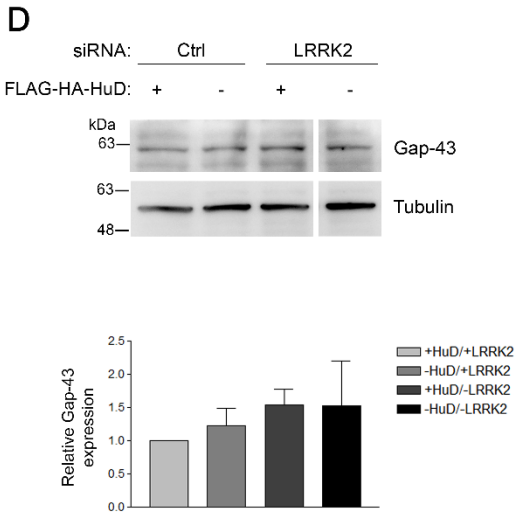
D
siRNA:
Ctrl
LRRK2
FLAG-HA-HuD:
+
-
+
-
kDa
63
Gap-43
63
48
Tubulin
Relative Gap-43 expression
2.5
2.0
1.5
1.0
0.5
0.0
+HuD/+LRRK2
-HuD/+LRRK2
+HuD/-LRRK2
-HuD/-LRRK2

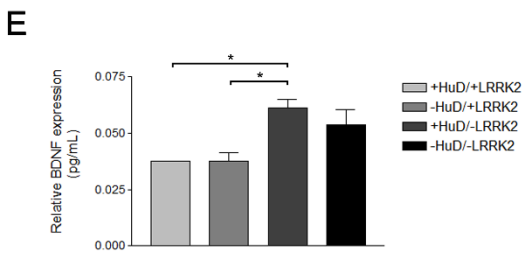
E
Relative BDNF expression (pg/mL)
0.075
0.050
0.025
0.000
+HuD/+LRRK2
-HuD/+LRRK2
+HuD/-LRRK2
-HuD/-LRRK2

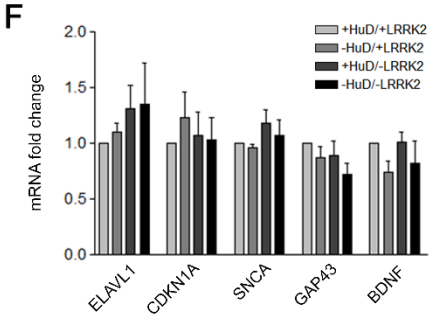
F
mRNA fold change
2.0
1.5
1.0
0.5
0.0
ELAVL1
CDKN1A
SNCA
GAP43
BDNF
+HuD/+LRRK2
-HuD/+LRRK2
+HuD/-LRRK2
-HuD/-LRRK2

Figure 14: LRRK2 knockdown affects protein expression of mRNAs bound by HuD. Human neuroblastoma SH-SY5Y cells were transfected with the plasmid encoding FLAG-HuD or a GFP plasmid, and either control siRNA or siRNA targeting LRRK2. Cells expressing both HuD and LRRK2 were designated as the 'control' condition (+HuD/+LRRK2). Representative blots show one biological replicate per condition (additional biological replicates on blots between +HuD/-LRRK2 and -HuD/-LRRK2 lanes were removed for redundancy). (A) Cell lysates were analyzed by western blot for FLAG-HuD expression and LRRK2 knockdown using appropriate antibodies. (B) LRRK2 knockdown was additionally verified by RT-qPCR. (C) Lysates were assessed for expression of HuR, p21 and α-synuclein using their respective antibodies. (D) Gap-43 protein expression was assessed by western blot and quantified. (E) BDNF protein levels were evaluated by ELISA using cell culture media from cells in each of the above conditions. (F) Total levels of transcripts encoding HuR, p21, α-synuclein, Gap-43 and BDNF were evaluated by RT-qPCR and normalized to *GAPDH* and *TBP* housekeeping genes. For quantification of protein and mRNA in (A-F), levels in test conditions (conditions lacking HuD and/or LRRK2) were normalized to levels in control conditions individually in each set of biological replicates (n=4). Biological replicates were averaged and are shown +/- SEM. Statistical significance of all data sets was determined by one-way analysis of variance (ANOVA). Asterisks indicate statistical significance between individual conditions calculated by Tukey's post-hoc tests; *$p<0.05$, **$p<0.01$, ***$p<0.001$.

in fine motor control and has been shown to be critically affected by the death of dopaminergic neurons in the SNc in Parkinson's disease patients (Kish et al. 1988, Porritt et al, 2005, Gerfer and Surmeier, 2011). Since we discovered that LRRK2 mutant G2019S hyperphosphorylates HuD and causes increased *Bdnf* mRNA binding to HuD in mice, we were interested in how this affects the total expression of mRNAs bound by HuD. We were also interested in whether LRRK2 G2019S-mediated hyperphosphorylation of HuD affects total cellular levels of HuD. To test this, we evaluated total protein levels in the midbrain and striatum regions of 4 week old HuD wild type/LRRK2 wild type ($HuD^{+/+}/Lrrk2^{+/+}$), HuD knockout/LRRK2 wild type ($HuD^{-/-}/Lrrk2^{+/+}$), HuD wild type/LRRK2 G2019S ($HuD^{+/+}/Lrrk2^{G2019S/+}$) and HuD knockout/LRRK2 G2019S mice ($HuD^{-/-}/Lrrk2^{G2019S/+}$). To differentiate between the SNc and other midbrain structures, we divided the midbrain into a ventral region (containing the SNc), and a dorsal region upon dissection.

HuD expression is elevated in LRRK2 G2019S mice

The specificity of our HuD antibody *in vivo* was confirmed by western blot using brain tissue lysates from wild type and HuD knockout mice, and in liver lysates from wild type mice. When blotted for HuD, wild type brain lysates showed three bands between 37-50kDa, two of which were absent in HuD KO mice and corresponded to the molecular weight of HuD (Figure 15A). The third, faint band was observed in both HuD WT and HuD KO mice brain lysates, but was absent in WT liver lysates where HuD and other neuronal-specific Hu proteins (HuB and HuC) are not expressed (Figure 15A). This is likely a non-specific band or cross-reactivity of the antibody with HuB or HuC in the brain lysates. For this reason, only the middle and bottom bands were evaluated for HuD expression in dorsal midbrain (DM), ventral midbrain (VM) and striatum (STR) lysates.

Western blot of lysates from each brain region first confirmed a lack of HuD expression in all $HuD^{-/-}$ mice. In comparing HuD expression in the DM between LRRK2 WT mice ($HuD^{+/+}/Lrrk2^{+/+}$) and LRRK2 G2019S mice ($HuD^{+/+}/Lrrk2^{G2019S/+}$), we observed a large variation in expression within mice of the same genotype (Figure 15B). As a result, quantification of western blots gave no significant difference in HuD

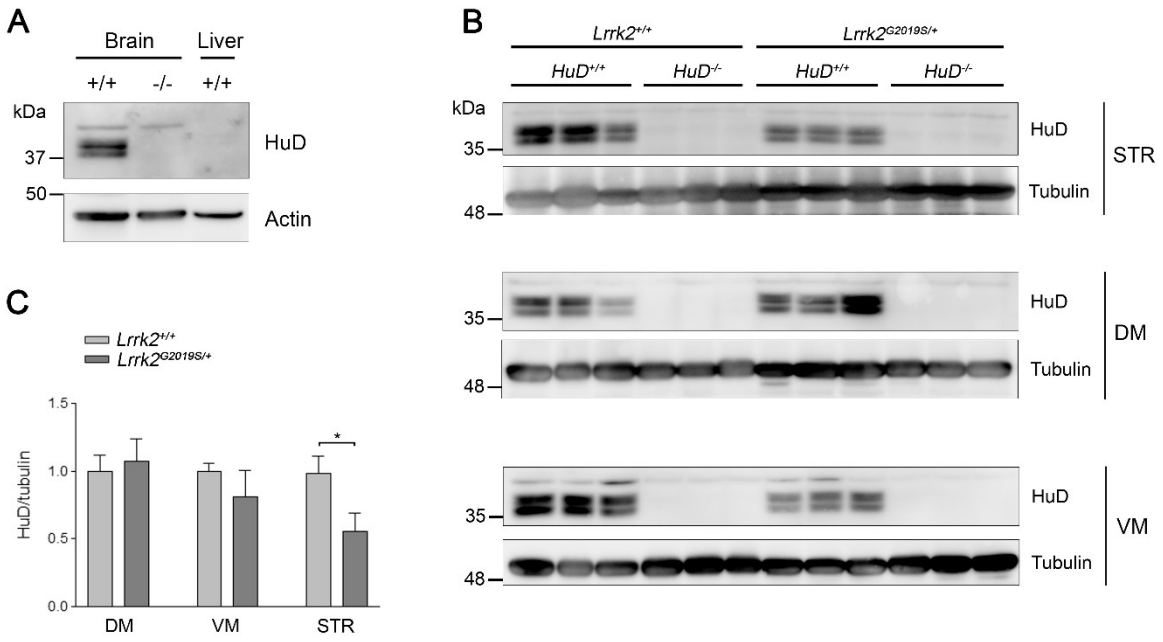

Figure 15: HuD expression is affected by LRRK2 G2019S in the striatum. (A) Specificity of the HuD antibody was verified by western blot using brain lysates from wild type HuD (+/+) and HuD knockout (-/-) mice and liver lysates from wild type mice. (B) Dorsal midbrain (DM), ventral midbrain (VM) and striatum (STR) tissues were isolated from 4 week old wild type mice ($HuD^{+/+}/Lrrk2^{+/+}$), HuD knockout mice ($HuD^{-/-}/Lrrk2^{+/+}$), LRRK2 G2019S mice ($HuD^{+/+}/Lrrk2^{G2019S/+}$), and HuD knockout/LRRK2 G2019S mice ($HuD^{-/-}/Lrrk2^{G2019S/+}$). Lysates were assessed by western blot using the HuD antibody. Representative blots show 3 mice per genotype. (C) HuD expression in wild type LRRK2 and LRRK2 G2019S mice in (B) plus 2-3 additional mice per genotype (not shown) was quantified using tubulin as a loading control. Expression was averaged between mice of the same genotype and is shown relative to wild type mice ($Lrrk2^{+/+}$). Data are means (n=5-6) +/- SEM. Asterisks indicate statistical significance as determined by Student's T-test (two-tailed assuming unequal variance); *$p<0.05$.

expression between *HuD*$^{+/+}$*/Lrrk2*$^{+/+}$ and *HuD*$^{+/+}$*/Lrrk2*$^{G2019S/+}$ mice (Figure 15B). In contrast, we observed a 50% reduction in HuD levels in the striatum of *HuD*$^{+/+}$*/Lrrk2*$^{G2019S/+}$ mice compared to *HuD*$^{+/+}$*/Lrrk2*$^{+/+}$ mice, suggesting that LRRK2 affects HuD protein expression (Figure 15B&C). Similarly, the representative western blot of lysates from the VM showed a visible decrease in HuD expression in *HuD*$^{+/+}$*/Lrrk2*$^{G2019S/+}$ mice compared to *HuD*$^{+/+}$*/Lrrk2*$^{+/+}$ mice (Figure 15B). However, when entire population was quantified (5-6 mice per genotype), the difference in expression was not statistically significant (Figure 15B&C).

HuD modifies expression of BDNF, α-synuclein and LRRK2 protein in mice

Previous experiments in SH-SY5Y cells showed that LRRK2 knockdown caused an increase the in protein expression of mRNAs bound by HuD including BDNF and α-synuclein. Protein levels were rescued with both HuD and LRRK2 loss, indicating that HuD is required for LRRK2-induced effects. We were interested in whether a similar relationship exists between HuD and LRRK2 G2019S. To test this, we evaluated the total protein levels of BDNF, α-synuclein, LRRK2, Gap-43 and HuR in the dorsal midbrain (DM), ventral midbrain (VM) and striatum (STR) tissues of 4 week old mice used in the HuD expression experiments in the previous section. Expression of p21 was also assessed, but was not detected in any of the brain regions. Since p21 is a negative regulator of the cell cycle and is typically expressed in response to cell stress such as tumour suppression, it is likely that our mice exhibited low levels of p21 as they should not have been under such stress (Gartel et al., 1999; Chang et al., 2000; Abbas et al., 2009).

In the dorsal midbrain, a significant elevation in BDNF was evident by western blot in *HuD*$^{-/-}$*/Lrrk2*$^{+/+}$ mice compared to all other mice (Figure 16A). Quantification showed that in fact BDNF is elevated by 4-fold in *HuD*$^{-/-}$*/Lrrk2*$^{+/+}$ mice over control mice (*HuD*$^{+/+}$*/Lrrk2*$^{+/+)}$ (Figure 16B). BDNF expression did not change significantly between control mice and *Lrrk2*$^{G2019S/-}$ mice (regardless of HuD genotype). This suggests that BDNF expression is dependent on HuD, but since protein levels returned to control levels in *HuD*$^{-/-}$*/Lrrk2*$^{G2019S/+}$ mice, it also suggests that BDNF expression can be modified by LRRK2 G2019S. Effects of HuD and LRRK2 on BDNF expression were less prominent in the ventral

midbrain (VM). There was a slight increase of approximately 1.5-fold in all *HuD*$^{-/-}$ mice compared to *HuD*$^{+/+}$ mice, but this difference was insignificant (Figure 16A&B). Unfortunately, BDNF expression in the striatum was at background levels, confounding our ability to make any conclusions (Appendix; Figure 2).

Western blot of α-synuclein expression in the VM showed a striking elevation in *HuD*$^{-/-}$*/Lrrk2*$^{+/+}$ mice in comparison to control mice (Figure 16C). Quantification showed that α-synuclein is in fact elevated by 2.5-fold in *HuD*$^{-/-}$*/LrrkK2*$^{+/+}$ mice compared to control mice. This effect was not as apparent in *Lrrk2*$^{G2019S/+}$ mice (regardless of HuD genotype), where expression was closer to control levels (Figure 16D). This suggests that α-synuclein expression in the VM is dependent on HuD in wild type LRRK2 conditions, but can be rescued back to control levels in the presence of LRRK2 G2019S. Expression of α-synuclein in the DM showed visible variation within mice of the same genotype by western blot (Figure 16C). Upon quantification, we observed a slight increase in α-synuclein in *HuD*$^{-/-}$*/Lrrk2*$^{+/+}$ mice compared to control mice (*HuD*$^{+/+}$*/Lrrk2*$^{+/+)}$, but no other significant changes in other mice (Figure 16D). Finally, in the striatum, we observed a significant increase in α-synuclein in *Lrrk2*$^{G2019S/+}$ mice (regardless of HuD genotype) compared to control mice (Figure 16C&D). This trend is different from those observed in the DM and VM, suggesting that the effect of HuD and LRRK2 on α-synuclein expression varies across brain regions.

We observed an elevation of LRRK2 in the DM of *HuD*$^{-/-}$ mice compared to *HuD*$^{+/+}$ mice (Figure 16E). A comparable elevation of LRRK2 is evident in the striatum, though only in *HuD*$^{-/-}$*/Lrrk2*$^{+/+}$ mice and not in *HuD*$^{-/-}$*/Lrrk2*$^{G2019S/+}$ mice (Figure 16E). Quantification showed that LRRK2 expression increased by a similar magnitude of 2-fold in both tissues with respect to control mice (Figure 16F). The elevation of LRRK2 in the DM of all *HuD*$^{-/-}$ mice suggests that HuD is necessary for the regulation of LRRK2 expression in this region. The fact that elevated LRRK2 levels in the striatum of *HuD*$^{-/-}$*/Lrrk2*$^{+/+}$ mice return to control levels in *HuD*$^{-/-}$*/Lrrk2*$^{G2019S/+}$ mice suggests that a slightly different mechanism of regulation exists in this region that requires LRRK2 G2019S; perhaps involving the over-activity of the

kinase domain. Expression of LRRK2 in the VM was difficult to detect by western blot and confounded our ability to make any observations or conclusions (Appendix; Figure 2).

We additionally assessed the expression of Gap-43 and HuR in the DM and VM lysates of the same mice described above. In the VM, Gap-43 expression showed a trend similar to that of BDNF and α-synuclein, where expression was elevated by 1.5-fold in *HuD*$^{-/-}$*/Lrrk2*$^{+/+}$ mice compared to control mice (*HuD*$^{+/+}$*/Lrrk2*$^{+/+}$) (Figure 17A&B). Gap-43 levels in *HuD*$^{-/-}$*/Lrrk2*$^{+/+}$ mice were rescued in *HuD*$^{-/-}$*/Lrrk2*$^{G2019S/+}$ mice, suggesting that LRRK2 G2019S can modify the effects of HuD knockout on Gap-43. Gap-43 expression did not appear to be affected by HuD knockout or LRRK2 G2019S in the DM (Figure 17A&B). Upon assessment of HuR expression in the VM, no significant differences were observed between mice (Figure 17A&C). In the DM, we observed a significant elevation of HuR by 2-fold in *HuD*$^{-/-}$*/Lrrk2*$^{+/+}$ mice in comparison to control mice (Figure 17A&C). HuR levels in *HuD*$^{-/-}$*/Lrrk2*$^{+/+}$ and *HuD*$^{-/-}$*/Lrrk2*$^{G2019S/+}$ mice were also elevated slightly below 2-fold compared to control mice, but data were not statistically significant.

In summary, we found that HuD knockout in wild type LRRK2 mice caused a significant elevation in the protein expression of mRNAs bound by HuD including BDNF, α-synuclein, LRRK2, Gap-43 and HuR in at least one of the three brain regions analyzed. The most prominent effects were observed in BDNF, α-synuclein and LRRK2. In most cases, levels of these proteins in *HuD*$^{-/-}$*/Lrrk2*$^{G2019S/+}$ mice returned to those observed in control mice. This indicates that the expression of mRNAs bound by HuD is dependent on HuD, but that their expression can be also modified by LRRK2 G2019S.

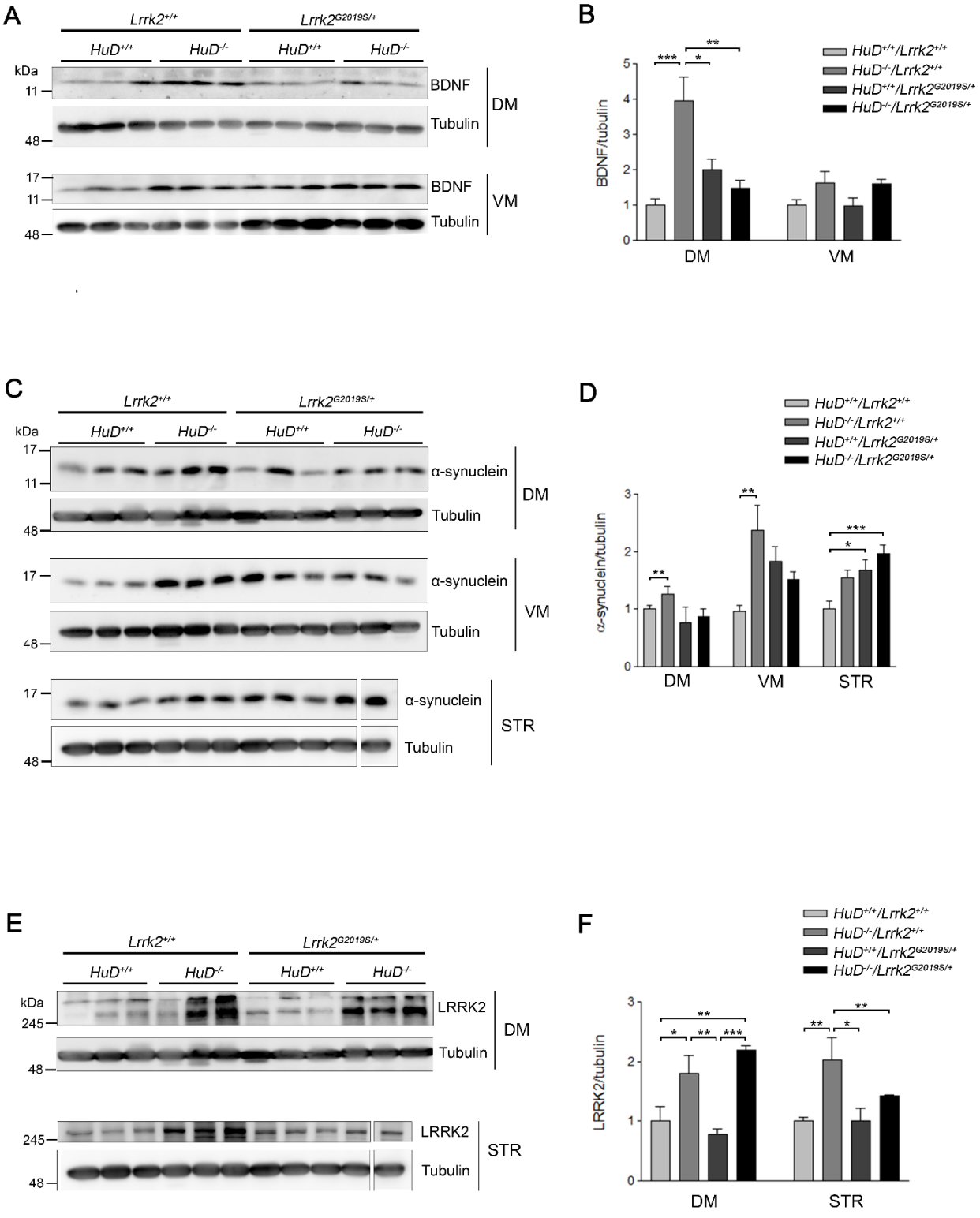
A
Lrrk2+/+
Lrrk2G2019S/+
HuD+/+
HuD-/-
HuD+/+
HuD-/-
kDa
11
48
BDNF
Tubulin
DM
17
11
48
BDNF
Tubulin
VM
B
HuD+/+/Lrrk2+/+
HuD-/-/Lrrk2+/+
HuD+/+/LrrkG2019S/+
HuD-/-/LrrkG2019S/+
BDNF/tubulin
DM
VM
C
Lrrk2+/+
Lrrk2G2019S/+
HuD+/+
HuD-/-
HuD+/+
HuD-/-
kDa
17
11
48
α-synuclein
Tubulin
DM
17
48
α-synuclein
Tubulin
VM
17
48
α-synuclein
Tubulin
STR
D
HuD+/+/Lrrk2+/+
HuD-/-/Lrrk2+/+
HuD+/+/LrrkG2019S/+
HuD-/-/LrrkG2019S/+
α-synuclein/tubulin
DM
VM
STR
E
Lrrk2+/+
Lrrk2G2019S/+
HuD+/+
HuD-/-
HuD+/+
HuD-/-
kDa
245
48
LRRK2
Tubulin
DM
245
48
LRRK2
Tubulin
STR
F
HuD+/+/Lrrk2+/+
HuD-/-/Lrrk2+/+
HuD+/+/LrrkG2019S/+
HuD-/-/LrrkG2019S/+
LRRK2/tubulin
DM
STR

Figure 16: LRRK2 G2019S modifies effects of HuD on target protein expression. Dorsal midbrain (DM), ventral midbrain (VM) and striatum (STR) tissues were isolated from 4 week old wild type mice (*HuD*$^{+/+}$*/Lrrk2*$^{+/+}$), HuD knockout mice (*HuD*$^{-/-}$*/Lrrk2*$^{+/+}$), LRRK2 G2019S mice (*HuD*$^{+/+}$*/Lrrk2*$^{G2019S/+}$), and HuD knockout/LRRK2 G2019S mice (*HuD*$^{-/-}$*/Lrrk2*$^{G2019S/+}$). Tissues were lysed in homogenization buffer and assessed for protein expression of mRNAs bound by HuD using western blot. Representative blots show 2-3 mice per genotype and were probed using primary antibodies specific for (A) BDNF, (C) α-synuclein and (E) LRRK2. (B, D, F) Expression of proteins in (A, C & E) was quantified with the addition of 2-3 mice per genotype (not shown) using tubulin as a loading control. Expression was averaged between mice of the same genotype and is shown relative to wild type mice (*HuD*$^{+/+}$*/Lrrk2*$^{+/+}$). Data are means (n=5-6) +/- SEM. Statistical significance was determined by one-way analysis of variance (ANOVA). Asterisks indicate statistical significance between individual conditions as determined by Tukey's post-hoc tests; *p<0.05, **p<0.01, ***p<0.001.

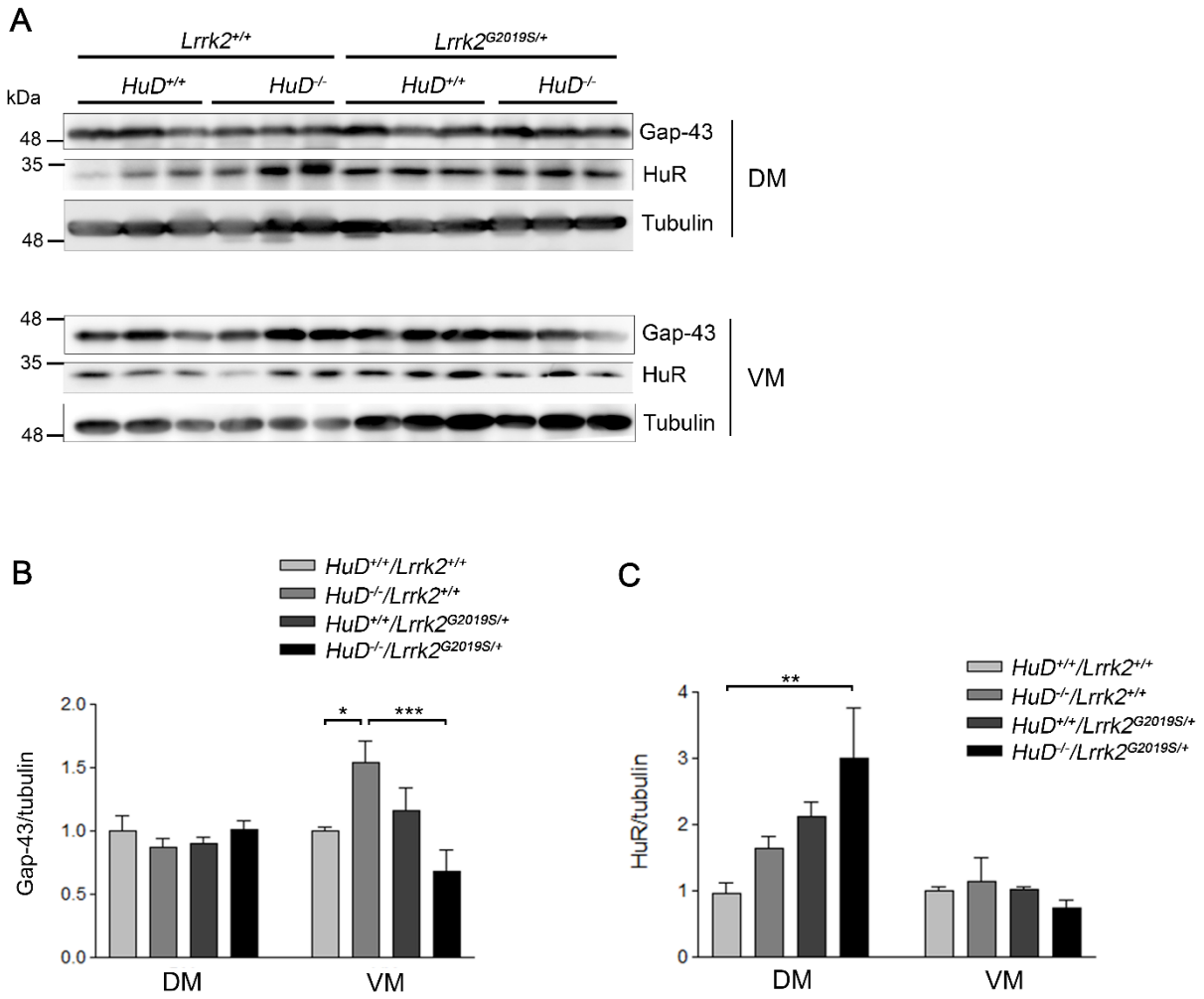

Figure 17: Gap-43 and HuR are affected by HuD knockout and LRRK2 G2019S in the midbrain. Dorsal midbrain (DM) and ventral midbrain (VM) tissues were isolated and homogenized from 4 week old wild type mice (*HuD*$^{+/+}$*/Lrrk2*$^{+/+}$), HuD knockout mice (*HuD*$^{-/-}$*/LrrkK2*$^{+/+}$), LRRK2 G2019S mice (*HuD*$^{+/+}$*/Lrrk2*$^{G2019S/+}$), and HuD knockout/LRRK2 G2019S mice (*HuD*$^{-/-}$*/Lrrk2*$^{G2019S/+}$). (A) Tissue lysates were assessed for Gap-43 and HuR protein expression by western blot. Representative blots show 3 mice per genotype. (B) Gap-43 and (C) HuR expression was quantified in western blots using tubulin as a normalization control. Expression was averaged between mice of the same genotype and is shown relative to wild type mice (*HuD*$^{+/+}$*/Lrrk2*$^{+/+}$). Data are means (n=3) +/- SEM. Statistical significance was determined by one-way analysis of variance (ANOVA). Asterisks indicate statistical significance between individual conditions as determined by Tukey's post-hoc tests; *p<0.05, **p<0.01, ***p<0.001.

Discussion

Part 1: LRRK2 kinase activity affects mRNA binding by HuD *in vitro* and *in vivo*

LRRK2 phosphorylates HuD, but an interaction is not detectable

In this study, we demonstrated that LRRK2 phosphorylates HuD *in vitro*. Not only this, but we observed a 3.0-fold increase in HuD phosphorylation by the LRRK2 G2019S over-active kinase mutant when compared with phosphorylation by wild type LRRK2. These findings are consistent with previous studies that have shown that the G2019S mutation causes a 2.0-4.0 fold increase in LRRK2-mediated phosphorylation of other known substrates including several Rab GTPases (Rab8a, Rab3a, Rab5b and Rab10), Moesin, Snapin, and members of the MAPKKK family (MKK3/6 and MKK4/7) (West et al., 2005; MacLeod et al., 2006; Jaleel et al., 2007; Gloeckner et al., 2009; Yun et al., 2013; Steger et al., 2016; Lis et al., 2018). Though further experiments should be performed to confirm HuD as a physiological substrate of LRRK2, these findings propose a possible mechanism in which LRRK2 could act on HuD.

Though most known LRRK2 substrates to date have been shown to interact with LRRK2 through its N-terminal protein-protein interaction domains or ROC domain, we were not able to detect any evidence of an association between LRRK2 and HuD by co-immunoprecipitation (Shin et al., 2008; Hsu et al., 2010; Ohta et al., 2011; Yun et al., 2013). It is possible that our immunoprecipitation methods were too stringent to capture an interaction, especially if it is a weak, transient interaction only lasting long enough for the phosphorylation reaction to occur. In a similar assay that used co-immunoprecipitation to detect an interaction between LRRK2 and its kinase substrates in the MKK family (MKK3/6 and 4/7), an association between LRRK2 and MKK4 was undetectable despite robust phosphorylation of the substrate (Hsu et al., 2010).

It should additionally be noted that in the majority of studies reporting an interaction between LRRK2 and one of its phosphorylation substrates, LRRK2 was either over-expressed, or an *in vitro* pull-down assay combining pure LRRK2 with the substrate of interest was used (Shin et al., 2008; Hsu et al., 2010; Ohta et al., 2011; Yun et al., 2013). In fact, one of these studies reported that while the interaction between Snapin and LRRK2 in SH-SY5Y cells over-expressing Flag-tagged LRRK2 was quite clear, an

interaction between endogenous LRRK2 and Snapin was weak (Yun et al., 2013). Since we did not over-express LRRK2 in our cell line prior to co-immunoprecipitation, it is possible that if an interaction between endogenous LRRK2 and FLAG-HuD exists, it may be weak and undetectable by our methods.

HuD binds mRNA encoding LRRK2 and α-synuclein in cells of human lineage

We used SH-SY5Y cells transfected with FLAG-tagged HuD as our model for the majority of our *in vitro* studies on the effects of LRRK2 on the post-transcriptional regulation of HuD mRNA targets. The SH-SY5Y cell line is derived from the catecholaminergic SK-N-SH cell line and is one of the most common *in vitro* models used to study the cellular and molecular mechanisms underlying PD (Lopes et al., 2010; Kovalevich and Langford, 2013; Xicoy et al., 2017). Though our SH-SY5Y cell line lacked endogenous HuD expression, it showed high levels of LRRK2 expression which was otherwise difficult to introduce into other cell lines by plasmid transfection or lentiviral transduction due the large plasmid size of ~14kb. Thus, we decided that SH-SY5Y cells were a favourable compromise between mouse embryonic fibroblasts that are not of neuronal lineage, and neural crest-derived PC12 cells or neuroblastic N2A cells that express HuD but do not express detectable levels of LRRK2. Though certain differentiation protocols can drive the SH-SY5Y cell line towards a dopaminergic phenotype, we used undifferentiated cells for our studies as they possess advantages over differentiated cells such as rapid proliferation and greater efficiency of siRNA and plasmid DNA uptake (Lopes et al., 2010; Xicoy et al., 2017). The limitations of using undifferentiated cells for our assays will be discussed in subsequent sections.

To determine the effects of LRRK2-mediated phosphorylation on the post-transcriptional regulatory activity of HuD, we chose to assess the binding of mRNAs that showed the most significant and consistent enrichment in FLAG-tagged HuD immunoprecipitations. Of the mRNAs chosen, those encoding BDNF and p21 are well-known targets of HuD while mRNAs encoding LRRK2 and α-synuclein are novel targets explored in our study. The binding of these transcripts by Hu proteins is supported by a recent study by Scheckel et al., (2016), who performed CLIP on human brain samples

using an antibody against all three neuronal Hu proteins. Their results showed that *LRRK2* and *SNCA* (α-synuclein) mRNA were enriched in IP samples to a greater degree than *GAP43* and *CDKN1A* (p21) mRNA, indicating that the neuronal Hu proteins may bind and regulate the expression of these mRNAs (Scheckel et al., 2016). A second study by Marchese et al., (2017) supported these findings by showing that HuR binds the 3'UTR of *SNCA* mRNA with high affinity.

LRRK2 modifies HuD-mRNA binding in cells and mice

We found that LRRK2 kinase inhibition and knockdown by siRNA in SH-SY5Y cells caused a significant reduction in binding of *LRRK2, BDNF* and *SNCA* mRNA by HuD, while expression of the over-active LRRK2 G2019S mutant in mice gave a significant elevation of *Bdnf* mRNA binding by HuD. While binding of *Lrrk2* mRNA was not evaluated in mice expressing the G2019S mutation, *Snca* mRNA binding also showed a trend towards elevated binding, but was not significant due to variability in our small population of mice (n=4). Additional mice should be evaluated for *Snca* mRNA binding in an attempt to decrease variation and determine whether this trend is significant. As previously mentioned, protein kinase C (PKC) is one of the only proteins referenced in the literature that mediates the phosphorylation of HuD. In correlation with our findings, two research groups showed that HuD phosphorylation mediated by the activation of protein kinase C (PKC) promoted the binding and stabilization of *BDNF* mRNA by HuD (Lim and Alkon, 2012, Vanevski et al., 2015). Vanevski et al. (2015) additionally showed that preventing the phosphorylation of HuD, caused a significant reduction in binding of *BDNF* mRNA by HuD. Though several studies have shown that the activation of PKC isoforms α and ε induced the phosphorylation of HuD, it remains unclear if HuD is a direct substrate of PKC (Pascale et al., 2005, Lim and Alkon, 2012, Bronick and Jasmin, 2013, Vanevski et al., 2015). Since LRRK2 is known to be phosphorylated by at least one PKC isoform (ζ), it is possible that the effects on HuD observed in response to PKC activation by Lim and Alkon, (2012) and Vanevski et al., (2105) are in fact mediated by LRRK2 (Zach et al., 2010). Additional experiments should be performed to determine whether HuD is in fact a physiological substrate of PKC, or if PKC is farther upstream and exerts its

effects on mRNA binding through LRRK2. This could be tested using *in vitro* phosphorylation assays by combining different PKC isoforms with LRRK2 to confirm that PKC α and ε also phosphorylate LRRK2 in addition to the ζ isoform. To evaluate whether LRRK2 is required for PKC to affect mRNA binding by HuD through LRRK2, the binding of mRNAs such as *BDNF* and *SNCA* by HuD could be tested upon PKC activation in wild type and LRRK2 knockout cells. This would give insight as to whether LRRK2 is required for PKC-mediated effects on HuD.

Effects of LRRK2 on mRNA binding by HuD may be transcript- or species-specific

Interestingly, not all of the mRNAs tested in LRRK2 G2019S mice and knockdown/kinase inhibition in cells followed the same pattern. As previously discussed, we observed a slight trend towards an increase of *Snca* mRNA binding by HuD in LRRK2 G2019S mice, but this trend was not significant. Though we saw that human *SNCA* mRNA binding to HuD was significantly decreased in LRRK2 knockdown and kinase inhibition conditions, these experiments were performed in cell lysates rather than a complex *in vivo* system. Also, the model cell line (SH-SY5Y) was of human origin while the *in vivo* studies were completed in mice. It is possible that HuD binds and regulates the expression of this transcript differently in humans and mice. In fact, our assessment of the 3'UTR sequence of this transcript showed very little sequence similarity between human and mouse, with the human 3'UTR sequence being close to 5X longer than the mouse 3'UTR. Though both human and mouse transcripts possessed several potential Hu-binding motifs interspersed throughout the 3'UTR, it is enticing to propose that the elevated length of the human 3'UTR may provide more opportunities for the binding of HuD than the mouse transcript. However, this is only speculative, and would need to be confirmed in future experiments (for example by RNA-electrophoretic mobility shift assay using each 3'UTR sequence). It is also possible that there are differences in the effects of LRRK2 G2019S phosphorylation on HuD between mice and humans. The existence of species-specific effects is supported by the fact that LRRK2 G2019S mice do not show the typical PD-related locomotor impairments and dopaminergic neuron loss that is observed in

human patients possessing the same mutation (Li et al., 2010; Ramonet et al., 2011; Daher et al., 2012; Longo et al., 2014).

Though we saw a slight trend towards reduced binding of well-characterized HuD mRNA target *CDKN1A* encoding p21 in LRRK2 kinase inhibition and knockdown conditions, this difference was not significant. There are a few possible reasons for this, firstly being that there was a considerable amount of variability between biological replicates. Since p21 is a cell cycle control factor and mediates stress responses, it is possible that p21 expression and mRNA binding by HuD was influenced by cell confluence, growth rate and stress conditions upon collection for immunoprecipitation and thus more variable than other mRNAs in binding to HuD (Chang et al., 2000). It is also possible that phosphorylation of HuD is necessary for the binding and regulation of certain mRNAs, but not others. This proposal is supported by several studies that have assessed the effects of phosphorylation on mRNA binding by HuR. One particular study performed with HuR suggested that checkpoint kinase 2 (Chk2)-mediated phosphorylation of HuR promoted the binding of mRNAs encoding prothymosin-α (*PTMA*) and p21, but reduced the binding of other mRNAs like those encoding like sirtuin-1 (*SIRT1*) (Abdelmohsen et al., 2007). It has also been suggested that positive and negative regulation of mRNA binding is affected by certain external stressors such as UV radiation (Wang et al., 2000; Lal et al., 2004; Lal et al., 2005). Together, these observations support the hypothesis that changes in the association of HuR with a given mRNA due to a certain stimulus are partly dependent on the transcript.

Phosphorylation of RRM2 sites is necessary for mRNA binding by HuD

In addition to being transcript-dependent, our findings showed that HuD-mRNA binding is affected by the specific residue being phosphorylated. We identified candidate sites in HuD for phosphorylation by the LRRK2 G2019S using *in vitro* kinase assays. We chose to use the over-active LRRK2 mutant in our assays in order to maximize the probability of detecting phosphorylation. The sites detected in our assays that were of particular interest were T149, T174 and S233 in the mouse HuD sequence (conserved as T144, T169 and S228 respectively in the human sequence). These sites exhibited high phosphorylation

intensities compared to LRRK2 kinase-dead and HuD only control conditions, and were consistently phosphorylated by LRRK2 G2019S in multiple samples compared to control samples. In support of our results, Vanevski et al.(2015) also identified T149 as a candidate for PKC-mediated phosphorylation using *in silico* methods, while S228/S233 in the mouse/human sequence has been reported as a site of phosphorylation in a number of high-throughput studies that have globally identified and characterized protein phosphorylation (Lundby et al., 2012; Luerman 2014; Sacco et al., 2016; Mertins et al., 2016). T174 is a novel phosphorylation site and has not been reported to date in any global phosphoproteomics studies. Since our assays were performed with LRRK2 G2019S protein, it is possible that T174 is phosphorylated by LRRK2 G2019S but not by wild type LRRK2. This offers insight into a possible mechanism for the characteristic gain-of-function phenotype commonly associated with the G2019S mutation that is not observed when LRRK2 wild type is overexpressed. In order to confirm this, additional *in vitro* phosphorylation assays and mass spectrometry experiments should be performed to compare the sites phosphorylated by wild type LRRK2 against those phosphorylated by LRRK2 G2019S. These findings could also be supported by *in vivo* detection of HuD phosphorylation by LRRK2 (WT and G2019S) using tissues from our mice.

HuD residues T149 and T174 are located in RRM2, while S233 is located in the linker region. Since RRM2 has been shown to be critical for mRNA binding by HuD, we were particularly interested in sites T149 and T174 and whether their phosphorylation by LRRK2 mediated the effects on mRNA binding that we observed in LRRK2 kinase inhibition and knockdown conditions. Non-conservative mutation of these two threonine sites to alanine to prevent phosphorylation gave a significant reduction in binding of *LRRK2, SNCA* and *CDKN1A* mRNAs. These findings were evident for both of the individual mutations and the double mutation, suggesting that phosphorylation of both sites is important for the binding of these mRNAs by HuD. Binding of *BDNF* mRNA by HuD was significantly reduced by only the double mutation, suggesting the possibility that the two threonine sites may act in a combinatorial mechanism to mediate binding of certain mRNAs. The activating effect of T149 phosphorylation is supported by Vanevski et al., (2015) in the context of HuD localization and translation. This group discovered that the

prevention of PKC-mediated phosphorylation of murine HuD at T149 along with a second threonine site (T165) by site-directed mutagenesis to alanine affected the dendritic localization of HuD (Vanevski et al., 2015). PKC activation was additionally found to be necessary for dendritic translation of HuD-bound *BDNF* mRNA (Vanevski et al., 2015). The mechanism in which this occurs however is still uncertain, as Vanevski et al. (2015) failed to show that PKC directly mediates the phosphorylation of residue T149. As previously mentioned, LRRK2 has been shown to be phosphorylated by PKC isoform zeta, therefore it is possible that LRRK2 could be mediating PKC-induced effects on HuD observed in this study (Zach et al., 2010). The study by Vanevski et al. (2015) was additionally confounded by the fact that they mutated site T165 alongside T149 and did not perform any experiments with single mutants, making it unclear whether one or both of the threonine to alanine mutations were necessary to disrupt regulation of HuD function (Vanevski et al., 2015). Fortunately, we can gain additional insight from phosphoproteomics studies on HuR. T149 in the mouse HuD sequence is conserved as T118 in the human HuR sequence and is a target of phosphorylation by checkpoint kinase Chk2 and p38 mitogen-activated protein kinase (MAPK) (Abdelmohsen et al., 2007; Lafarga et al., 2009). Consistent with our results in the context of mRNA binding, prevention of Chk2-mediated phosphorylation of T118 caused a decrease in the binding of several mRNAs by HuR including *CDKN1A* (Abdelmohsen et al., 2007). A second study supported that p38 MAPK-mediated phosphorylation of T118 enhanced the binding of HuR to *CDKN1A* mRNA and induced its cytoplasmic localization (Lafarga et al., 2009). These results together clearly demonstrate the importance of the phosphorylation of T118 in HuR and T149 in HuD for mRNA binding, and propose a novel site (T174) in HuD involved in mRNA binding.

The effect of phosphorylation on the tertiary protein structure of HuD and RNA binding was studied by Wang et al. (2001), who determined the crystal structure of RRM1 and RRM2 in complex with short RNA sequences containing clustered AREs (the c-fos ARE and TNFα11 ARE). This group identified the amino acids making direct contact with the RNA and suggested that phosphorylation of any of these residues or those adjacent to the RNA-binding surface would affect the ability of HuD to bind RNA (Wang et al., 2001). When we mapped sites T149 and T174 to the crystal structure described by Wang et

al., (2001), neither site is predicted to make contact with RNA. These predictions may be limited however, as this study used very short RNA sequences with clustered AREs in order to maximize HuD binding recognition and affinity. It is possible that longer RNAs like *LRRK2*, *CDKN1A* or others used in our study may make contact with a different profile of amino acids. Also, phosphorylation of some proteins regulates their function by inducing long-distance changes in conformation and creating or obstructing docking sites for binding partners (Salazar et al., 2009). Since T149 and T174 are located close to the mRNA binding site, it is possible that their phosphorylation is necessary to maintain proper protein conformation to allow the mRNA access to the binding site.

In order to definitely link the importance of LRRK2-mediated phosphorylation of these sites to mRNA binding, a few key experiments should be completed. Firstly, *in vitro* kinase assays should be repeated with LRRK2 using the non-phosphorylatable threonine to alanine HuD mutants to confirm that T144/T149 and T169/T174 are sites of LRRK2 phosphorylation in the mouse/human HuD sequence. These experiments are currently in progress in our lab. Next, we should assess whether LRRK2-mediated phosphorylation of these sites is critical for the ability of HuD to bind *LRRK2, BDNF* and *SNCA* mRNA. To do this, RNA-electrophoretic mobility shift assays (REMSA) could be used by combining these mRNAs with wild type HuD and each HuD mutant in the presence of wild type LRRK2. These assays could be repeated with kinase-dead LRRK2 to determine if there are additional sites of phosphorylation in HuD that modify mRNA binding. Finally, we did not pursue the candidate phosphorylation site S233 in our assays, but the location of this site in the nuclear localization signal (NLS) of the hinge region of HuD suggests that it may have implications on protein trafficking. In fact, phosphorylation of the conserved site in HuR (S202) by Cdk1 has been shown to be critical for its nucleocytoplasmic shuttling (Fan and Steitz, 1998; Kasashima et al., 1999; Kim et al., 2008; Kim and Gorospe, 2008). To determine the effect of S233 phosphorylation on the localization of HuD, we could use a HuD plasmid with a fluorescent tag (GFP or RFP) to create a non-phosphorylatable mutation to alanine at S233. We could then transfect this HuD mutant into our model cell line and visualize its effects on protein localization using fluorescence microscopy methods.

Part 2: Expression of HuD-bound mRNAs in cells is LRRK2-dependent

No effect of LRRK2 or HuD on mRNA stability in SH-SY5Y cells

So far, we have shown compelling evidence to suggest that LRRK2-mediated phosphorylation of HuD is required for the binding of mRNAs including *BDNF, SNCA* and *LRRK2* itself. As previously described, the dominant model in current literature assumes that Hu proteins exert a stabilizing effect on most bound mRNAs to promote their expression (Deschênes-Furry et al., 2006; Bolognani et al., 2009). Following this model, we hypothesized that LRRK2 knockdown would lead to a reduction in stability and total cellular levels of *BDNF* and *SNCA* mRNA, and a subsequent reduction in their translation (Mobarak et al., 2000; Anderson et al., 2000; Fujiwara et al., 2006; Bronicki and Jasmin, 2013). Similarly, we anticipated that the absence of endogenous HuD in SH-SY5Y cells would give decreased stabilization of its mRNA targets and reduced translation of these mRNAs in comparison to conditions in which FLAG-HuD was introduced by transfection. However, our results consistently disagreed with the dominant Hu-mRNA stabilization model. The manipulation of LRRK2 and HuD in our experiments gave no significant changes in the total levels of mRNAs that are bound by HuD including *GAP43, CDKN1A, ELAVL1* (encoding HuR)*, BDNF* or *SNCA*. Similarly, we observed no significant differences in Gap-43, p21 or HuR protein expression in any of our conditions. There are several possible explanations for these findings.

As previously described, SH-SY5Y cells were the most favourable cell line to use for *in vitro* experiments, however a few limitations still existed in using these cells as our model. Firstly, the fact that endogenous HuD expression was undetectable under standard conditions indicated that it may not be critical in mediating mRNA stability in this cell line. Even though introducing FLAG-HuD by transfection showed that it bound strongly to several mRNAs known to be bound by HuD and was affected by the kinase activity of LRRK2, it is possible that other critical components are lacking that would allow it to become engaged in mediating the stability of these mRNAs. This may have confounded any effects that LRRK2 and HuD would otherwise have on mediating cellular mRNA levels. Due to the close sequence homology between the RNA-binding domains of the four Hu proteins and the overlap in

mRNAs which they bind, it is likely that HuB, HuC or HuR may have bound many of the mRNAs examined in our study and obscured the effect of HuD (Okano and Darnell, 1997; Hinman and Lou, 2008; Bronicki and Jasmin, 2013; Colombrita et al., 2013). Compensation of the other Hu proteins for HuD was suggested by Akamatsu et al. (2005), as an explanation for the lack of severe neurological and motor phenotypes in HuD knockout mice (Okano and Darnell, 1997; Deschênes-Furry et al., 2006). While HuC knockout mice exhibit fairly normal neuronal development and motor phenotypes, HuC/HuD double knockout mice die shortly after birth demonstrating the strong compensatory actions exhibited between HuC and HuD (Ince-Dunn et al., 2012; Colombrita et al., 2013). Though not significant, we observed a trend towards elevation in HuR protein levels upon LRRK2 knockdown, suggesting a possible scenario where increased HuR was able to compensate for the loss of mRNA target binding by HuD induced by LRRK2 knockdown. In order to confirm this, further research should be completed by knocking down HuR to determine whether it is necessary for the stabilization of our mRNAs of interest.

Though SH-SY5Y cells are said to be locked in an early stage of neuronal differentiation, our cells showed poor expression of typical neuronal markers like Gap-43 by both RT-qPCR and western blot, indicated by high cycle number (>35 cycles) and weak bands respectively. This suggested that its regulation by HuD was not essential to the cells at this point in their growth. Three phenotypic variations of undifferentiated SH-SY5Y cells have been described and represent different lineages of the neural crest that express diverse profiles of cellular protein markers (Ross and Spengler, 2007; Lopes et al., 2010). These lineages have been defined as epithelial-like 'S-type' that express no neuronal markers, neuroblastic 'N-type' that grow small neurites and possess moderate expression of early neuronal markers including HuD, and 'I-type' with intermediate growth characteristics between N- and S-type cells and low neuronal marker expression (Lazarova et al., 1999; Ross and Spengler, 2007; Kovelavich and Langford, 2013; Shipley et al., 2017). In comparing these characteristics with our observations, it is likely that our cells are either S-type or I-type where HuD-mediated regulation of mRNA targets is not required (Lazarova et al., 1999; Ross and Spengler, 2007). In order to obtain a clearer understanding of LRRK2-mediated effects on the stability of HuD mRNA targets, it may be necessary to repeat our experiments in N-type cells.

LRRK2 knockout promotes the expression of BDNF and α-synuclein

Our findings at the protein level indicated that the loss of LRRK2 in cells transfected with FLAG-HuD promoted the expression of certain mRNAs bound by HuD. In particular, we observed a significant elevation in BDNF and α-synuclein protein levels and a trend towards elevation in p21 and HuR upon LRRK2 knockdown. Our results showed that HuD overexpression did not modify levels of these proteins on its own, suggesting that the effects LRRK2-dependent. We did however observe that HuD can act as a modifier of these effects, as protein levels were rescued in cells lacking both HuD and LRRK2. In searching for a possible mechanism to explain these findings, we must consider that both LRRK2 and HuD have been shown to affect translation by acting on different external factors and pathways. LRRK2 enhances translation by phosphorylating ribosomal subunit s15 and translation inhibitor 4E-BP1, while HuD interacts with eIF4A to promote cap-dependent translation (Imai et al., 2008; Fukao et al., 2009; Martin et al., 2014). While it is possible that these factors were partially responsible in mediating the increased expression of BDNF and α-synuclein in LRRK2 knockdown conditions, it is unlikely that they were solely responsible for these effects. Based on current literature, phosphorylation of 4E-BP1 or ribosomal subunit s15 by LRRK2 would likely affect global mRNA translation rather than only a subset of mRNAs bound by HuD (Imai et al., 2008; Tain et al., 2009; Martin et al., 2014). Similarly, the mechanism by which HuD enhances cap-dependent translation by acting on eIF4A has yet to be linked to only HuD-bound mRNAs (Fukao et al., 2009; Chen and Shyu, 2009). It is likely that there are LRRK2-mediated pathways involved in regulating the expression of HuD-bound mRNAs that have yet to be uncovered in the literature. These pathways may involve factors that regulate translation, or post-translational activities like protein sequestration or degradation. Nonetheless, our findings suggest that LRRK2 is necessary for mRNA binding by HuD while also repressing the expression of certain HuD-bound mRNAs. Since the effects of LRRK2 loss on the protein expression of mRNAs bound by HuD are rescued when HuD is also absent, this indicates that HuD is required for LRRK2-mediated effects on protein expression and may be indirectly involved in this mechanism.

It is unclear as to why the protein expression of certain mRNAs bound by HuD (BDNF and α-synuclein) was affected by the manipulation of HuD and LRRK2, while others such as Gap-43 showed no change. To reiterate our previous hypothesis, it is possible that because our cells were not differentiated and would not have required the neurite-inducing activity of Gap-43, the regulation of its expression was not required by HuD or LRRK2. The complexity of our findings demonstrates the need for continued studies in this field to uncover novel LRRK2-mediated pathways and factors that affect the expression of HuD-bound mRNAs.

Part 3: Complex but interconnected regulation of HuD-bound mRNAs by LRRK2 and HuD in mice

HuD does not stabilize all bound transcripts

Some of our most prominent findings surrounding the expression of HuD-bound mRNAs at the protein level opposed the current dominant Hu-mRNA stabilization model in the literature. This was evident in HuD KO/LRRK2 WT mice we observed a significant increase in BDNF, α-synuclein and LRRK2 protein levels in the dorsal midbrain, and in some cases in the ventral midbrain (α-synuclein and Gap-43) . This suggests that HuD may repress the expression of some of its mRNA targets at the protein level. This could occur through HuD-mediated repression of translation, or through the direct destabilization of certain mRNA targets bound by HuD. While the model that Hu proteins stabilize bound mRNAs has dominated discussion around these RNA-binding proteins, numerous studies have discovered cases where the Hu proteins appear to destabilize mRNAs that they bind. These results are often ignored or excluded since they do not agree with the dominant Hu-mRNA stabilization model in the literature. An obvious example of exclusion is in a 2009 study by Bolognani et al. who used transgenic mice overexpressing HuD to assess the frequency of HuD binding sequences in misregulated transcripts, but only considered those mRNAs that were significantly upregulated. By not including the analysis of downregulated transcripts, this study perpetuated the one-way bias of the Hu-mRNA stabilization model in the literature. A second high-throughput study performed in 2012 by Ince-Dunn et al. compared total mRNA levels in the cortical tissue of wild type and HuC/HuD knockout mice. They reported that 27% of

the transcripts that were significantly downregulated in KO mice had Hu binding sites in the 3'UTR, but failed to mention that 40% of the significantly upregulated transcripts contained Hu binding sites as well (Ince-Dunn et al., 2012). This result would in fact suggest that more mRNA transcripts bound by HuD are destabilized, not stabilized as the dominant model suggests. A more recent study by Scheckel et al. in 2016 evaluated global changes in the transcriptome in response to HuB, HuC and HuD (nHu) knockdown in human IMR-32 neuroblastoma cells. They identified >700 genes that were significantly misregulated upon nHu knockdown (Scheckel et al., 2016). While 16% of the downregulated transcripts were among the top 1000 nHu 3'UTR targets (defined through CLIP experiments), 7% of upregulated transcripts were in the top 1000 nHu 3'UTR targets (Scheckel et al., 2016). These studies suggest that the expression of some HuD-bound transcripts may in fact be downregulated by the neuronal Hu proteins. This would allow their levels to rise when HuD is absent, supporting our findings at the protein level in HuD KO mice.

HuD-dependent and independent mechanisms regulating the expression of mRNA targets

The absence of knowledge in the literature surrounding the proposed destabilization and translational repression of certain mRNAs bound by HuD makes it difficult to propose just one hypothetical mechanism responsible for these effects. The effects may be directly or indirectly dependent on HuD, and may involve a combination of multiple pathways and mechanisms. One possibility of a HuD-dependent mechanism is by the interference of HuD with microRNA (miRNA)-mediated silencing of mRNAs; a process that has been shown to be influenced by RBP activity (George and Tenenbaum, 2006; Kedde and Agami, 2008; Fabian and Sonenberg, 2012). There are several instances in the literature demonstrating competition between HuR and different miRNAs for control of gene expression. For example, HuR can relieve miR-122-mediated silencing of *CAT-1* mRNA encoding cationic amino acid transporter-1 under conditions of amino acid starvation (Bhattacharyya et al., 2006; Fabian and Sonenberg, 2012). In contrast, there have been several cases demonstrated in the literature where HuR cooperates with miRNAs to repress gene expression. HuR associates with the *c-myc* transcript close to the

let-7 miRNA binding site and recruits let-7 to the 3'UTR of the mRNA to inhibit its expression (Kim et al., 2009). It has been shown that both HuR and let-7 are required for c-myc repression, indicating that they work synergistically (Kim et al., 2009). Similarly, the regulation of antiapoptotic Ras homolog B (RhoB) expression by miR-19 has been shown to require the binding of HuR to the 3'UTR of the *RhoB* mRNA (Glorian et al., 2011). These cases of cooperation between HuR and miRNAs are some of the most well-defined examples to date of Hu proteins destabilizing or inhibiting the translation of mRNAs, and it has been suggested that many more instances of synergistic regulation involving the other Hu proteins including HuD have yet to be uncovered (Filipowicz et al., 2008; Srikantan et al., 2012). This provides a potential mechanism to explain why the absence of HuD in mice could promote the stability and translation of certain mRNAs like *Bdnf*, *Snca* and *Lrrk2* in the dorsal midbrain.

A HuD-independent mechanism that offers an explanation to the complexity of our findings at the protein level in HuD KO mice is that the stability and translation of many transcripts bound by HuD is likely regulated by HuB, HuC, HuR, and other RNA-binding proteins in the absence of HuD. Many neuronal RBPs that bind ARE elements in 3'UTRs including AUF1, TTP, KSRP, nucleolin and CUG-binding protein 2 (CUG-BP2) have been shown to compete with HuD or the other Hu proteins to exert effects on their target mRNAs. Consistent with competitive binding assays in the literature, it is likely that in the absence of HuD, other ARE-binding proteins may have more control over the regulation of mRNA targets of HuD (Bird et al., 2013; Bronicki and Jasmin, 2013). For example, KSRP has been shown to compete with HuD for the binding of *GAP43* mRNA, and binds with higher affinity when the ratio of KSRP to HuD is shifted in its favour (Bird et al., 2013). Finally, it should be mentioned that perhaps the most well-known pathway in which HuD affects translation is through its interaction with eIF4A to promote cap-dependent translation (Chen and Shyu, 2009). However, our data suggest that binding of mRNAs to HuD repressed protein expression instead since we observed an increase in certain protein levels in HuD knockout mice. The effect of this interaction on translation was discovered by Fukao et al., (2009) in HeLa cells and has not been confirmed to date *in vivo* or in species other than humans (Fukao et

al., 2009; Chen and Shyu, 2009). Therefore, it is possible that HuD may have alternative effects on eIF4a including repressing translation in complex *in vivo* systems or in other species like mice.

Significance to Parkinson's disease

Based on evidence in human PD patients in the literature, we anticipated that mice expressing the LRRK2 G2019S mutation may show a decrease in BDNF in the midbrain region in correlation with the reduction observed in the SNc of human brains (Howells et al., 2000; Baquet et al., 2005; Costa et al., 2015). However, the brain regions examined in LRRK2 G2019S mice showed no significant changes in BDNF, or other proteins encoded by mRNA targets of HuD such as Gap-43 or HuR. This could be due in part to the young age of our mice (4 weeks old) in the scope of PD, as well as the fact that many studies have shown that LRRK2 G2019S mouse models poorly represent the neuropathology and motor symptoms associated with PD in human patients (Lin et al., 2009; Li et al., 2010; Ramonet et al., 2011; Longo et al., 2014). The only brain region in LRRK2 G2019S mice where we observed any significant effects on protein expression was in the striatum, where we saw a significant increase in α-synuclein protein levels in both the presence and absence of HuD. In agreement with these findings, a few other studies have reported an increase and aggregation of α-synuclein inclusions in the PD-relevant brain regions of LRRK2 G2019S mice (Lin et al., 2009; Valpolicelli-Daley et al., 2016). This may suggest the beginnings of α-synuclein aggregation in Lewy bodies in this brain region, though this would need to be confirmed by staining fixed tissue sections for α-synuclein.

Rescue effect of HuD KO/LRRK2 G2019S

Interestingly, the elevation in BDNF and α-synuclein protein levels that was observed in HuD KO/LRRK2 WT mice was rescued in HuD KO mice expressing the LRRK2 G2019S mutation. This ultimately suggests that LRRK2 G2019S can recover aberrant expression of HuD mRNA targets caused by the loss of HuD. These findings are reminiscent of the unpublished data that formed the basis of our project, where the deletion of HuD homolog RBP9 in Drosophila rescued the PD-like phenotype caused

by the over-active LRRK2 kinase mutant I2020T (recall fly eye phenotypes from Figure 3). Though it is difficult to propose a possible mechanism to explain these findings due to the vast complexity of the unknown pathways and factors involved, it is evident that both HuD KO and LRRK2 G2019S are required for the misregulation of many HuD mRNA targets.

Conclusions and Future directions

The findings presented herein establish a strong foundation of evidence to suggest that LRRK2 acts on HuD to regulate the expression of HuD-bound PD-relevant transcripts. We showed that LRRK2 phosphorylates HuD *in vitro,* and that LRRK2 kinase activity is critical for regulating HuD-mRNA binding. The manipulation of HuD and LRRK2 expression in cells and in mice affects the protein levels of mRNAs bound by HuD in a complex mechanism that likely involves a number of other factors in addition to LRRK2 and HuD. Future research in our lab aims to explore this mechanism and to definitively establish the downstream effects of LRRK2 G2019S on HuD in the context of PD pathology.

In this study, we identified several candidate HuD residues for hyperphosphorylation by LRRK2 G2019S by mass spectrometry. Current studies in our lab aim to validate the LRRK2-mediated phosphorylation of these sites using phosphorylation assays that combine HuD mutants (containing non-conservative substitutions at candidate phosphorylated residues) with LRRK2 G2019S and wild type LRRK2. This experiment is key in elucidating the mechanism in which LRRK2 G2019S acts on HuD to affect mRNA binding and stability. It will give insight into whether LRRK2 G2019S simply hyperphosphorylates one or a combination of HuD residues, or if LRRK2 G2019S phosphorylates an additional HuD residue that is not phosphorylated by wild type LRRK2 in a gain-of-function mechanism. Additionally, the phosphorylation of these residues should be validated *in vivo* to confirm that HuD is a physiological substrate of LRRK2.

Preliminary behavioural studies in 10 week old mice from our lab have shown HuD-dependent motor deficits that correlate with previous studies in the literature (Akamatsu et al., 2005; DeBoer et al., 2014), but we have not observed any LRRK2-dependent effects or rescue of HuD-dependent

abnormalities in locomotor activity of mice to date. However, this is not unexpected, as very few studies have shown evidence of PD-related locomotor deficits or dopaminergic neuron death in LRRK2 G2019S mice as old as 21 months of age (Lin et al., 2009, Li et al., 2010; Ramonet et al., 2011; Longo et al., 2014). It may be favourable to use a different *in vivo* model rather than continuing to age our mice past 4 weeks of age in an attempt to mimic the disease. Several studies have presented transgenic flies as an encouraging model for studying PD pathology (Liu et al., 2007; Imai et al., 2008; Ng et al., 2009; Cording et al., 2017). Flies overexpressing PD-associated human LRRK2 mutations have shown key neuropathological traits and phenotypes associated with the disease including age-dependent dopaminergic neuron loss and dendrite degeneration and motor deficits that are reminiscent of human patients (Liu et al., 2007; Imai et al., 2008; Ng et al., 2009; Cording et al., 2017). In order to obtain a better understanding of the effects of LRRK2 G2019S on HuD-mRNA binding in the context of Parkinson's disease, there may be value in manipulating the *rbp9* gene in flies expressing the LRRK2 G2019S mutation.

Finally, though slightly overlooked in our study, the effects of *LRRK2* mRNA binding by HuD on LRRK2 expression and downstream signalling pathways should be explored in future studies. The potential of an inter-regulatory mechanism between LRRK2 and HuD has complex implications on PD pathology. It is possible that LRRK2 G2019S-mediated hyperphosphorylation of HuD may promote *LRRK2* mRNA binding (similar to our observations of *BDNF* mRNA binding by HuD in LRRK2 G2019S mice), and in turn could modify the expression or localization of the mutant LRRK2 G2019S protein. The hypothetical HuD-dependent regulation of LRRK2 G2019S expression provides further evidence to support that HuD is a favourable candidate for continued research into PD therapeutic options.

References

Abbas, T. & Dutta, A. (2009). p21 in cancer: intricate networks and multiple activities. Nature Review Cancer, 9(6): 400–414. doi:10.1038/nrc2657.

Abeliovich, A., Schmitz, Y., Farinas, I., Choi-Lundberg, D., Ho, W. H., Castillo, P. E., … Rosenthal, A. (2000). Mice lacking alpha-synuclein display functional deficits in the nigrostriatal dopamine system. Neuron, 25(1), 239–252. https://doi.org/10.1016/S0896-6273(00)80886-7

Adams, S. J., Crook, R. J. P., DeTure, M., Randle, S. J., Innes, A. E., Yu, X. Z., … McGowan, E. (2009). Overexpression of wild-type murine tau results in progressive tauopathy and neurodegeneration. American Journal of Pathology, 175(4), 1598–1609. https://doi.org/10.2353/ajpath.2009.090462

Aigner, L., Arber, S., Kapfhammer, J. P., Laux, T., Schneider, C., Botteri, F., … Caroni, P. (1995). Overexpression of the neural growth-associated protein GAP-43 induces nerve sprouting in the adult nervous system of transgenic mice. Cell, 83(2), 269–278. https://doi.org/10.1016/0092-8674(95)90168-X

Akamatsu, W., Okano, H. J., Osumi, N., Inoue, T., Nakamura, S., Sakakibara, S.-I., … Okano, H. (1999). Mammalian ELAV-like neuronal RNA-binding proteins HuB and HuC promote neuronal development in both the central and the peripheral nervous systems. Proceedings of the National Academy of Sciences, 96(17), 9885–9890. https://doi.org/10.1073/pnas.96.17.9885

Akamatsu, W., Fujihara, H., Mitsuhashi, T., Yano, M., Shibata, S., Hayakawa, Y., … Okano, H. (2005). The RNA-binding protein HuD regulates neuronal cell identity and maturation. Proceedings of the National Academy of Sciences of the United States of America, 102(12), 4625–4630. https://doi.org/10.1073/pnas.0407523102

Akten, B., Kye, M. J., Hao, L. T., Wertz, M. H., Singh, S., Nie, D., … Sahin, M. (2011). Interaction of survival of motor neuron (SMN) and HuD proteins with mRNA cpg15 rescues motor neuron axonal deficits. Proceedings of the National Academy of Sciences, 108(25), 10337–10342. https://doi.org/10.1073/pnas.1104928108

Alegre-Abarrategui, J., Christian, H., Lufino, M. M. P., Mutihac, R., Venda, L. L., Ansorge, O., & Wade-Martins, R. (2009). LRRK2 regulates autophagic activity and localizes to specific membrane microdomains in a novel human genomic reporter cellular model. Human Molecular Genetics, 18(21), 4022–4034. https://doi.org/10.1093/hmg/ddp346

Alipanahi, B., Delong, A., Weirauch, M. T., & Frey, B. J. (2015). Predicting the sequence specificities of DNA- and RNA-binding proteins by deep learning. Nature Biotechnology, 33(8), 831–838. https://doi.org/10.1038/nbt.3300

Allen, M., Bird, C., Feng, W., Liu, G., Li, W., Perrone-Bizzozero, N. I., & Feng, Y. (2013). HuD Promotes BDNF Expression in Brain Neurons via Selective Stabilization of the BDNF Long 3′UTR mRNA. PLoS ONE, 8(1). https://doi.org/10.1371/journal.pone.0055718

Anand, V. S., Reichling, L. J., Lipinski, K., Stochaj, W., Duan, W., Kelleher, K., … Braithwaite, S. P. (2009). Investigation of leucine-rich repeat kinase 2: Enzymological properties and novel assays. FEBS Journal, 276(2), 466–478. https://doi.org/10.1111/j.1742-4658.2008.06789.x

Anderson, K. D., Sengupta, J., Morin, M., Neve, R. L., Valenzuela, C. F., & Perrone-Bizzozero, N. I. (2001). Overexpression of HuD accelerates neurite outgrowth and increases GAP-43 mRNA expression in cortical neurons and retinoic acid-induced embryonic stem cells in vitro. Experimental Neurology, 168(2), 250–258. https://doi.org/10.1006/exnr.2000.7599

Anderson, K. D., Morin, M. A., Beckel-Mitchener, A., Mobarak, C. D., Neve, R. L., Furneaux, H. M., … Perrone-Bizzozero, N. I. (2000). Overexpression of HuD, but not of its truncated form HuD I+II, promotes GAP-43 gene expression and neurite outgrowth in PC12 cells in the absence of nerve growth factor. Journal of Neurochemistry, 75(3), 1103–1114. https://doi.org/10.1046/j.1471-4159.2000.0751103.x

Andres-Mateos, E., Mejias, R., Sasaki, M., Li, X., Lin, B. M., Biskup, S., … Dawson, V. L. (2009). Unexpected Lack of Hypersensitivity in LRRK2 Knock-Out Mice to MPTP (1-Methyl-4-Phenyl-1,2,3,6-Tetrahydropyridine). Journal of Neuroscience, 29(50), 15846–15850. https://doi.org/10.1523/JNEUROSCI.4357-09.2009

Aranda-Abreu, G. E., Behar, L., Chung, S., Furneaux, H., & Ginzburg, I. (1999). Embryonic lethal abnormal vision-like RNA-binding proteins regulate neurite outgrowth and tau expression in PC12 cells. The Journal of Neuroscience : The Official Journal of the Society for Neuroscience, 19(16), 6907–6917.

Arenas, E. (2014). Wnt signaling in midbrain dopaminergic neuron development and regenerative medicine for Parkinson's disease. Journal of Molecular Cell Biology, 6(1), 42–53. https://doi.org/10.1093/jmcb/mju001

Bakheet, T. (2006). ARED 3.0: the large and diverse AU-rich transcriptome. Nucleic Acids Research, 34(90001), D111–D114. https://doi.org/10.1093/nar/gkj052

Bakheet, T., Frevel, M., Williams, B. R., Greer, W., & Khabar, K. S. (2001). ARED: human AU-rich element-containing mRNA database reveals an unexpectedly diverse functional repertoire of encoded proteins. Nucleic Acids Research, 29(1), 246–254. https://doi.org/10.1093/nar/29.1.246

Baquet, Z. C. (2005). Brain-Derived Neurotrophic Factor Is Required for the Establishment of the Proper Number of Dopaminergic Neurons in the Substantia Nigra Pars Compacta. Journal of Neuroscience, 25(26), 6251–6259. https://doi.org/10.1523/JNEUROSCI.4601-04.2005

Barrett, J. C., Hansoul, S., Nicolae, D. L., Cho, J. H., Duerr, R. H., Rioux, J. D., … Daly, M. J. (2008). Genome-wide association defines more than 30 distinct susceptibility loci for Crohn's disease. Nature Genetics, 40(8), 955–962. https://doi.org/10.1038/ng.175

Beckel-Mitchener, A. C., Miera, A., Keller, R., & Perrone-Bizzozero, N. I. (2002). Poly(A) tail length-dependent stabilization of GAP-43 mRNA by the RNA-binding protein HuD. Journal of Biological Chemistry, 277(31), 27996–28002. https://doi.org/10.1074/jbc.M201982200

Bellavia, D., Mecarozzi, M., Campese, A. F., Grazioli, P., Talora, C., Frati, L., … Screpanti, I. (2007). Notch3 and the Notch3-upregulated RNA-binding protein HuD regulate Ikaros alternative splicing. The EMBO Journal, 26(6), 1670–1680. http://doi.org/10.1038/sj.emboj.7601626

Berwick, D. C., & Harvey, K. (2014). The regulation and deregulation of Wnt signaling by PARK genes in health and disease. Journal of Molecular Cell Biology, 6(1), 3–12. https://doi.org/10.1093/jmcb/mjt037

Bhattacharyya, S. N., Habermacher, R., Martine, U., Closs, E. I., & Filipowicz, W. (2006). Relief of microRNA-Mediated Translational Repression in Human Cells Subjected to Stress. Cell, 125(6), 1111–1124. https://doi.org/10.1016/j.cell.2006.04.031

Bird, C. W., Gardiner, A. S., Bolognani, F., Tanner, D. C., Chen, C. Y., Lin, W. J., … Perrone-Bizzozero, N. (2013). KSRP modulation of GAP-43 mRNA stability restricts axonal outgrowth in embryonic hippocampal neurons. PLoS ONE, 8(11), 1–12. https://doi.org/10.1371/journal.pone.0079255

Biskup, S., Moore, D. J., Rea, A., Lorenz-Deperieux, B., Coombes, C. E., Dawson, V. L., … West, A. B. (2007). Dynamic and redundant regulation of LRRK2 and LRRK1 expression. BMC Neuroscience, 8, 1–11. https://doi.org/10.1186/1471-2202-8-102

Blake, J. A., Christie, K. R., Dolan, M. E., Drabkin, H. J., Hill, D. P., Ni, L., … Westerfeld, M. (2015). Gene ontology consortium: Going forward. Nucleic Acids Research, 43(D1), D1049–D1056. https://doi.org/10.1093/nar/gku1179

Bolognani, F., Qiu, S., Tanner, D.C., Paik, J., Perrone-Bizzozero, N.I., Weeber, E.J. (2007). Associative and spatial learning and memory deficits in transgenic mice overexpressing the RNA-binding protein HuD. Neurobiology of Learning and Memory. 87(4), 635-643. https://doi.org/10.1016/j.nlm.2006.11.004.

Bolognani, F., Contente-Cuomo, T., & Perrone-Bizzozero, N. I. (2009). Novel recognition motifs and biological functions of the RNA-binding protein HuD revealed by genome-wide identification of its targets. Nucleic Acids Research, 38(1), 117–130. https://doi.org/10.1093/nar/gkp863

Bonifati, V. (2007). LRRK2 low-penetrance mutations (Gly2019Ser) and risk alleles (Gly2385Arg) - Linking familial and sporadic Parkinson's disease. Neurochemical Research, 32(10), 1700–1708. https://doi.org/10.1007/s11064-007-9324-y

Bouhouche, A., Tibar, H., Haj, R. B. El, El Bayad, K., Razine, R., Tazrout, S., … Regragui, W. (2017). LRRK2 G2019S Mutation: Prevalence and Clinical Features in Moroccans with Parkinson's Disease. Parkinson's Disease. 2017. https://doi.org/10.1155/2017/2412486

Bräuer, U., Zaharieva, E., & Soller, M. (2014). Regulation of ELAV/Hu RNA-binding proteins by phosphorylation: Figure 1. Biochemical Society Transactions, 42(4), 1147–1151. https://doi.org/10.1042/BST20140103

Brennan, C. M., & Steitz, J. A. (2001). HuR and mRNA stability. Cellular and Molecular Life Sciences, 58(2), 266–277. https://doi.org/10.1007/PL00000854

Bronicki, L. M., & Jasmin, B. J. (2013). Emerging complexity of the HuD/ELAVl4 gene ; implications for neuronal development, function, and dysfunction. RNA, 19, 1019–1037. https://doi.org/10.1261/rna.039164.113.1

Bubunenko, M., Korepanov, A., Court, D. L., Jagannathan, I., Dickinson, D., Chaudhuri, B. R. O. Y., … Culver, G. M. (2006). 30S ribosomal subunits can be assembled in vivo without primary binding ribosomal protein S15. RNA Biology, 1229–1239. https://doi.org/10.1261/rna.2262106.

Chang, B. D., Watanabe, K., Broude, E. V, Fang, J., Poole, J. C., Kalinichenko, T. V, & Roninson, I. B. (2000). Effects of p21Waf1/Cip1/Sdi1 on cellular gene expression: implications for carcinogenesis, senescence, and age-related diseases. Proc Natl Acad Sci U S A, 97(8), 4291–4296. https://doi.org/10.1073/pnas.97.8.4291

Chen, C. Y., Weng, Y. H., Chien, K. Y., Lin, K. J., Yeh, T. H., Cheng, Y. P., … Wang, H. L. (2012). (G2019S) LRRK2 activates MKK4-JNK pathway and causes degeneration of SN dopaminergic neurons in a transgenic mouse model of PD. Cell Death and Differentiation, 19(10), 1623–1633. https://doi.org/10.1038/cdd.2012.42

Chen, C. Y. A., & Shyu, A. Bin. (2009). HuD Stimulates Translation via eIF4A. Molecular Cell, 36(6), 920–921. https://doi.org/10.1016/j.molcel.2009.12.013

Chen, H-H., Xu, J., Safarpour, F., Stewart, A. F. R. (2007). LMO4 mRNA stability is regulated by extracellular ATP in F11 cells. Biochemical and Biophysical Research Communications, 357(1), 56-61. https://doi.org/10.1016/j.bbrc.2007.03.113

Chen, J., Martindale, J. L., Cramer, C., Gorospe, M., Atasoy, U., Drew, P. D., & Yu, S. (2017). The RNA-binding protein HuR contributes to neuroinflammation by promoting C-C chemokine receptor 6 (CCR6) expression on Th17 cells. Journal of Biological Chemistry, 292(35), 14532–14543. https://doi.org/10.1074/jbc.M117.782771

Chia, R., Haddock, S., Beilina, A., Rudenko, I. N., Mamais, A., Kaganovich, A., … Cookson, M. R. (2014). Phosphorylation of LRRK2 by casein kinase 1α regulates trans-Golgi clustering via differential interaction with ARHGEF7. Nature Communications, 5, 1–11. https://doi.org/10.1038/ncomms6827

Chuang, C. L., Lu, Y. N., Wang, H. C., & Chang, H. Y. (2014). Genetic dissection reveals that Akt is the critical kinase downstream of LRRK2 to phosphorylate and inhibit FOXO1, and promotes neuron survival. Human Molecular Genetics, 23(21), 5649–5658. https://doi.org/10.1093/hmg/ddu281

Chung, S., Eckrich, M., Perrone-Bizzozero, N., Kohn, D. T., & Furneaux, H. (1997). The Elav-like proteins bind to a conserved regulatory element in the 3'- untranslated region of GAP-43 mRNA. Journal of Biological Chemistry, 272(10), 6593–6598. https://doi.org/10.1074/jbc.272.10.6593

Chung, S., Jiang, L., Cheng, S., & Furneaux, H. (1996). Purification and properties of HuD, a neuronal RNA-binding protein. Journal of Biological Chemistry, 271(19), 11518–11524. https://doi.org/10.1074/jbc.271.19.11518

Cohen-Cory, S., Kidane, A. H., Shirkey, N. J., & Marshak, S. (2011). Brain-Derived Neurotrophic Factor and the Development of Structural Neuronal Connectivity. Neurobiology, 70(5), 271–288. https://doi.org/10.1002/dneu.20774.

Cooper, A., Gitler, A.D., Cashikar, A., Haynes, C.M., Hill, K.J., Bhullar, B., … Lindquist, S. (2006). a-Synuclein Blocks ER-Golgi Traffic and Rab1 Rescues Neuron Loss in Parkinson's Models. Science, 313, 324–329.

Colombrita, C., Silani, V., & Ratti, A. (2013). ELAV proteins along evolution: Back to the nucleus? Molecular and Cellular Neuroscience, 56, 447–455. https://doi.org/10.1016/j.mcn.2013.02.003

Cording, A. C., Shiaelis, N., Petridi, S., Middleton, C. A., Wilson, L. G., & Elliott, C. J. H. (2017). Targeted kinase inhibition relieves slowness and tremor in a Drosophila model of LRRK2 Parkinson's disease. Npj Parkinson's Disease. 34, 1-8. https://doi.org/10.1038/s41531-017-0036-y

Costa, A., Peppe, A., Carlesimo, G. A., Zabberoni, S., Scalici, F., Caltagirone, C., & Angelucci, F. (2015). Brain-derived neurotrophic factor serum levels correlate with cognitive performance in Parkinson's disease patients with mild cognitive impairment. Frontiers in Behavioral Neuroscience, 9(253), 1–8. https://doi.org/10.3389/fnbeh.2015.00253

Cuadrado, A., Navarro-Yubero, C., Furneaux, H., Kinter, J., Sonderegger, P., Muñoz, A. (2002). HuD binds to three AU-rich sequences in the 3'-UTR of neuroserpin mRNA and promotes the accumulation of neuroserpin mRNA and protein. Nucleic Acids Research. 30(10), 2202-11.

Dae-Lee, D. B., Dawson, V. L. & Dawson, T. M. (2012). Leucine rich repeat kinase 2 (LRRK2) as a potential therapeutic target for Parkinson's disease. Trends in Pharmacological Sciences. 33(7): 365–373. doi:10.1016/j.tips.2012.04.001.

Daher, J. P. L., Pletnikova, O., Biskup, S., Musso, A., Gellhaar, S., Galter, D., … Moore, D. J. (2012). Neurodegenerative phenotypes in an A53T α-synuclein transgenic mouse model are independent of LRRK2. Human Molecular Genetics, 21(11), 2420–2431. https://doi.org/10.1093/hmg/dds057

Dauer, W., & Przedborski, S. (2003). Parkinson's disease: Mechanisms and models. Neuron, 39(6), 889–909. https://doi.org/10.1016/S0896-6273(03)00568-3

David, P. S., Tanveer, R., & Port, J. D. (2007). FRET-detectable interactions between the ARE binding proteins, HuR and p37AUF1. Rna, 13(9), 1453–1468. https://doi.org/10.1261/rna.501707

DeBoer, E. M., Azevedo, R., Vega, T. A., Brodkin, J., Akamatsu, W., Okano, H., … Rasin, M.-R. (2014). Prenatal Deletion of the RNA-Binding Protein HuD Disrupts Postnatal Cortical Circuit Maturation and Behavior. Journal of Neuroscience, 34(10), 3674–3686. https://doi.org/10.1523/JNEUROSCI.3703-13.2014

Deschênes-Furry, J., Perrone-Bizzozero, N., & Jasmin, B. J. (2006). The RNA-binding protein HuD: A regulator of neuronal differentiation, maintenance and plasticity. BioEssays, 28(8), 822–833. https://doi.org/10.1002/bies.20449

Deschênes-Furry, J., Belanger, G., Mwanjewe, J., Lunde, J. A., Parks, R. J., Perrone-Bizzozero, N., Jasmin, B. J. (2005). The RNA-binding Protein HuR Binds to Acetylcholinesterase Transcripts and Regulates Their Expression in Differentiating Skeletal Muscle Cells. Journal of Biological Chemistry, 280(27), 25361-8.

Destefano, A. L., Lew, M. F., & Klein, C. (2009). Replication of association between ELAVL4 and Parkinson disease: the *Gene*PD study, 124(1), 95–99. https://doi.org/10.1007/s00439-008-0526-4.

Doller, A., Akool, E.-S., Huwiler, A., Muller, R., Radeke, H. H., Pfeilschifter, J., & Eberhardt, W. (2008). Posttranslational Modification of the AU-Rich Element Binding Protein HuR by Protein Kinase C Elicits Angiotensin II-Induced Stabilization and Nuclear Export of Cyclooxygenase 2 mRNA. Molecular and Cellular Biology, 28(8), 2608–2625. https://doi.org/10.1128/MCB.01530-07

Doller, A., Schlepckow, K., Schwalbe, H., Pfeilschifter, J., & Eberhardt, W. (2010). Tandem Phosphorylation of Serines 221 and 318 by Protein Kinase C Coordinates mRNA Binding and Nucleocytoplasmic Shuttling of HuR. Molecular and Cellular Biology, 30(6), 1397–1410. https://doi.org/10.1128/MCB.01373-09

Dorval, V., & Hébert, S. S. (2012). LRRK2 in transcription and translation regulation: Relevance for Parkinson's disease. Frontiers in Neurology, FEBS, 3(12), 2–7. https://doi.org/10.3389/fneur.2012.00012

Dorval, V., Mandemakers, W., Jolivette, F., Coudert, L., Mazroui, R., De Strooper, B., & Hébert, S. S. (2014). Gene and microRNA transcriptome analysis of Parkinson's related LRRK2 mouse models. PLoS ONE, 9(1), 1–10. https://doi.org/10.1371/journal.pone.0085510

Dzamko, N., Inesta-Vaquera, F., Zhang, J., Xie, C., Cai, H., Arthur, S., … Alessi, D. R. (2012). The IkappaB kinase family phosphorylates the Parkinson's disease kinase LRRK2 at Ser935 and Ser910 during Toll-Like Receptor signaling. PLoS ONE, 7(6). https://doi.org/10.1371/journal.pone.0039132

Fabian, M. R., & Sonenberg, N. (2012). The mechanics of miRNA-mediated gene silencing: A look under the hood of miRISC. Nature Structural and Molecular Biology, 19(6), 586–593. https://doi.org/10.1038/nsmb.2296

Fallini, C., Bassell, G. J., & Rossoll, W. (2012). The ALS disease protein TDP-43 is actively transported in motor neuron axons and regulates axon outgrowth. Human Molecular Genetics, 21(16), 3703–3718. https://doi.org/10.1093/hmg/dds205

Fan, X. C., & Steitz, J. A. (1998). HNS, a nuclear-cytoplasmic shuttling sequence in HuR (nuclear localization RNA degradation nuclear export). Biochemistry, 95, 15293–15298. https://doi.org/10.1073/pnas.95.26.15293

Farrer, M., Stone, J., Mata, I.F., Lincoln, S., Kachergus, J., Hulihan, M., Strain, K.J., & Maraganore, D.M. (2005). LRRK2 mutations in Parkinson disease. Neurology. 65(5):738-40. 10.1212/01.wnl.0000169023.51764.b0

Fialcowitz-White, E. J., Brewer, B. Y., Ballin, J. D., Willis, C. D., Toth, E. A., & Wilson, G. M. (2007). Specific protein domains mediate cooperative assembly of HuR oligomers on AU-rich mRNA-destabilizing sequences. Journal of Biological Chemistry, 282(29), 20948–20959. https://doi.org/10.1074/jbc.M701751200

Filipowicz, W., Bhattacharyya, S. N., & Sonenberg, N. (2008). Mechanisms of post-transcriptional regulation by microRNAs: Are the answers in sight? Nature Reviews Genetics, 9(2), 102–114. https://doi.org/10.1038/nrg2290

Filippova, N., Yang, X., King, P., & Nabors, L. B. (2012). Phosphoregulation of the RNA-binding protein Hu antigen R (HuR) by Cdk5 affects centrosome function. Journal of Biological Chemistry, 287(38), 32277–32287. https://doi.org/10.1074/jbc.M112.353912

Fujiwara, T., Mori, Y., Chu, D. L., Miyata, S., Tanaka, H., Yachi, K., … Tohyama, M. (2006). CARM1 Regulates Proliferation of PC12 Cells by Methylating HuD CARM1 Regulates Proliferation of PC12 Cells by Methylating HuD. Molecular and Cellular Biology, 26(6), 2273–2285. https://doi.org/10.1128/MCB.26.6.2273

Fujiwara, T., Fukao, A., Sasano, Y., Matsuzaki, H., Kikkawa, U., Imataka, H., … Sakamoto, H. (2012). Functional and direct interaction between the RNA binding protein HuD and active Akt1. Nucleic Acids Research, 40(5), 1944–1953. https://doi.org/10.1093/nar/gkr979

Fukao, A., Sasano, Y., Imataka, H., Inoue, K., Sakamoto, H., Sonenberg, N., … Fujiwara, T. (2009). The ELAV Protein HuD Stimulates Cap-Dependent Translation in a Poly(A)- and eIF4A-Dependent Manner. Molecular Cell, 36(6), 1007–1017. https://doi.org/10.1016/j.molcel.2009.11.013

Gaig, C., Martí, M. J., Ezquerra, M., Rey, M. J., Cardozo, A., & Tolosa, E. (2007). G2019S LRRK2 mutation causing Parkinson's disease without Lewy bodies. Journal of Neurology, Neurosurgery and Psychiatry, 78(6), 626–628. https://doi.org/10.1136/jnnp.2006.107904

Gartel, A. L., & Tyner, A. L. (1999). Transcriptional Regulation of the p21(WAF1/CIP1)Gene. Experimental Cell Research, 246(2), 280–289. https://doi.org/10.1006/excr.1998.4319

Gasser, T. (2009). Mendelian forms of Parkinson's disease. Biochimica et Biophysica Acta - Molecular Basis of Disease. 1792(7):587-96. https://doi.org/10.1016/j.bbadis.2008.12.007

Gehrke, S., Imai, Y., Sokol, N. & Lu, B. (2010). Pathogenic LRRK2 negatively regulates microRNA-mediated translational repression. Nature, 466(7306): 637–641. doi:10.1038/nature09191.

George, A. D., & Tenenbaum, S. A. (2006). MicroRNA modulation of RNA-binding protein regulatory elements. RNA Biology, 3(2), 57–59. https://doi.org/10.4161/rna.3.2.3250

Gerfen, C. R. & Surmeier, J. D. (2011). Modulation of striatal projection systems by dopamine. Annual Review of Neuroscience. 34: 441–466. doi:10.1146/annurev-neuro-061010-113641.

Giaime, E., Tong, Y., Wagner, L. K., Yuan, Y., Huang, G., & Shen, J. (2017). Age-Dependent Dopaminergic Neurodegeneration and Impairment of the Autophagy-Lysosomal Pathway in LRRK-Deficient Mice. Neuron, 96(4), 796–807.e6. https://doi.org/10.1016/j.neuron.2017.09.036

Gitler, A. D., Bevis, B. J., Shorter, J., Strathearn, K. E., Hamamichi, S., Su, L. J., … Lindquist, S. (2008). The Parkinson's disease protein alpha-synuclein disrupts cellular Rab homeostasis. Proceedings of the National Academy of Sciences of the United States of America, 105(1), 145–150. https://doi.org/10.1073/pnas.0710685105

Glisovic, T., Bachorik, J. L., Yong, J., & Dreyfuss, G. (2008). RNA-binding proteins and post-transcriptional gene regulation. FEBS Letters, 582(14), 1977–1986. https://doi.org/10.1016/j.febslet.2008.03.004

Gloeckner, C. J., Schumacher, A., Boldt, K., & Ueffing, M. (2009). The Parkinson disease-associated protein kinase LRRK2 exhibits MAPKKK activity and phosphorylates MKK3/6 and MKK4/7, in vitro. Journal of Neurochemistry, 109(4), 959–968. https://doi.org/10.1111/j.1471-4159.2009.06024.x

Glorian, V., Maillot, G., Polès, S., Iacovoni, J. S., Favre, G., & Vagner, S. (2011). HuR-dependent loading of miRNA RISC to the mRNA encoding the Ras-related small GTPase RhoB controls its translation during UV-induced apoptosis. Cell Death and Differentiation, 18(11), 1692–1701. https://doi.org/10.1038/cdd.2011.35

Goris, A., Williams-Gray, C. H., Clark, G. R., Foltynie, T., Lewis, S. J. G., Brown, J., … Sawcer, S. J. (2007). Tau and α-synuclein in susceptibility to, and dementia in, Parkinson's disease. Annals of Neurology, 62(2), 145–153. https://doi.org/10.1002/ana.21192

Greggio, E. (2012). Role of LRRK2 kinase activity in the pathogenesis of Parkinson's disease. Biochemical Society Transactions, 40(5), 1058–1062. https://doi.org/10.1042/BST20120054

Greggio, E., & Cookson, M. R. (2009). Leucine-Rich Repeat Kinase 2 Mutations and Parkinson's Disease: Three Questions. ASN Neuro, 1(1), AN20090007. https://doi.org/10.1042/AN20090007

Greggio, E., Jain, S., Kingsbury, A., Bandopadhyay, R., Lewis, P., Kaganovich, A., … Cookson, M. R. (2006). Kinase activity is required for the toxic effects of mutant LRRK2/dardarin. Neurobiology of Disease, 23(2), 329–341. https://doi.org/10.1016/j.nbd.2006.04.001

Greggio, E., Zambrano, I., Kaganovich, A., Beilina, A., Taymans, J. M., Daniëls, V., … Cookson, M. R. (2008). The Parkinson disease-associated leucine-rich repeat kinase 2 (LRRK2) is a dimer that undergoes intramolecular autophosphorylation. Journal of Biological Chemistry, 283(24), 16906–16914. https://doi.org/10.1074/jbc.M708718200

Groban, E. S., Narayanan, A., & Jacobson, M. P. (2006). Conformational changes in protein loops and helices induced by post-translational phosphorylation. PLoS Computational Biology, 2(4), 238–250. https://doi.org/10.1371/journal.pcbi.0020032

Häbig, K., Walter, M., Poths, S., Riess, O., & Bonin, M. (2008). RNA interference of LRRK2-microarray expression analysis of a Parkinson's disease key player. Neurogenetics, 9(2), 83–94. https://doi.org/10.1007/s10048-007-0114-0

Hardy, J. (2010). Genetic analysis of pathways to parkinson disease. Neuron, 68(2), 201–206. https://doi.org/10.1016/j.neuron.2010.10.014

Haugarvoll, K., Toft, M., Ross, O. A., Stone, J. T., Heckman, M. G., White, L. R., … Farrer, M. J. (2007). ELAVL4, PARK10, and the celts. Movement Disorders, 22(4), 585–587. https://doi.org/10.1002/mds.21336

Hayashi, S., Yano, M., Igarashi, M., Okano, H. J., & Okano, H. (2015). Alternative role of HuD splicing variants in neuronal differentiation. Journal of Neuroscience Research, 93(3), 399–409. https://doi.org/10.1002/jnr.23496

Hemsley, A., Arnheim, N., Toney, M. D., Cortopassi, G., & Galas, D. J. (1989). A simple method for site-directed mutagenesis using the polymerase chain reaction. Nucleic Acids Research, 17(21), 8915. https://doi.org/10.1093/nar/17.21.8915

Herzig, M. C., Kolly, C., Persohn, E., Theil, D., Schweizer, T., Hafner, T., … Shimshek, D. R. (2011). LRRK2 protein levels are determined by kinase function and are crucial for kidney and lung homeostasis in mice. Human Molecular Genetics, 20(21), 4209–4223. https://doi.org/10.1093/hmg/ddr348

Hinkle, K. M., Yue, M., Behrouz, B., Dächsel, J. C., Lincoln, S. J., Bowles, E. E., … Melrose, H. L. (2012). LRRK2 knockout mice have an intact dopaminergic system but display alterations in exploratory and motor co-ordination behaviors. Molecular Neurodegeneration, 7(1), 1–17. https://doi.org/10.1186/1750-1326-7-25

Hinman, M. N., & Lou, H. (2008). Diverse molecular functions of Hu proteins. Cellular and Molecular Life Sciences, 65(20), 3168–3181. https://doi.org/10.1007/s00018-008-8252-6

Ho, S. N., Hunt, H. D., Horton, R. M., Pullen, J. K., & Pease, L. R. (1989). Site-directed mutagenesis by overlap extension using the polymerase chain reaction. Gene, 77(1), 51–59. https://doi.org/10.1016/0378-1119(89)90358-2

Howells, D. W., Porritt, M. J., Wong, J. Y. F., Batchelor, P. E., Kalnins, R., Hughes, A. J., & Donnan, G. A. (2000). Reduced BDNF mRNA expression in the Parkinson's disease substantia nigra. Experimental Neurology, 166(1), 127–135. https://doi.org/10.1006/exnr.2000.7483

Hsu, C. H., Chan, D., Greggio, E., Saha, S., Guillily, M. D., Ferree, A., ... Wolozin, B. (2010). MKK6 binds and regulates expression of Parkinson's disease- related protein LRRK2. Journal of Neurochemistry. 112(6): 1593–1604. doi:10.1111/j.1471-4159.2010.06568.x.

Hubers, L., Valderrama-Carvajal, H., Laframboise, J., Timbers, J., Sanchez, G., & Côté, J. (2011). HuD interacts with survival motor neuron protein and can rescue spinal muscular atrophy-like neuronal defects. Human Molecular Genetics, 20(3), 553–579. https://doi.org/10.1093/hmg/ddq500

Huot, P., Lévesque, M., & Parent, A. (2007). The fate of striatal dopaminergic neurons in Parkinson's disease and Huntington's chorea. Brain, 130(1), 222–232. https://doi.org/10.1093/brain/awl332

Hyeon, H. K., & Gorospe, M. (2008). Phosphorylated HuR shuttles in cycles. Cell Cycle, 7(20), 3124–3126. https://doi.org/10.4161/cc.7.20.6884

Imai, Y., Gehrke, S., Wang, H. Q., Takahashi, R., Hasegawa, K., Oota, E., & Lu, B. (2008). Phosphorylation of 4E-BP by LRRK2 affects the maintenance of dopaminergic neurons in Drosophila. EMBO Journal, 27(18), 2432–2443. https://doi.org/10.1038/emboj.2008.163

Ince-Dunn, G., Okano, H. J., Jensen, K., Park, W-Y., Ru, Z., Ule, J., ... Darnell, R. B. (2012). Neuronal Elav-like (Hu) proteins regulate RNA splicing and abundance to control glutamate levels and neuronal excitability. Neuron, 75(6): 1067–1080. doi:10.1016/j.neuron.2012.07.009.

Inestrosa, N. C., & Arenas, E. (2010). Emerging roles of Wnts in the adult nervous system. Nature Reviews Neuroscience, 11(2), 77–86. https://doi.org/10.1038/nrn2755

Ito, G., Okai, T., Fujino, G., Takeda, K., Ichijo, H., Katada, T., & Iwatsubo, T. (2007). GTP binding is essential to the protein kinase activity of LRRK2, a causative gene product for familial Parkinson's disease. Biochemistry, 46(5), 1380–1388. https://doi.org/10.1021/bi061960m

Jaleel, M., Nichols, R. J., Deak, M., Campbell, D. G., Gillardon, F., Knebel, A., & Alessi, D. R. (2007). LRRK2 phosphorylates moesin at threonine-558: characterization of how Parkinson's disease mutants affect kinase activity. Biochemical Journal, 405(2), 307–317. https://doi.org/10.1042/BJ20070209

Jankovic, J. (2008). Parkinson's disease: Clinical features and diagnosis. Journal of Neurology, Neurosurgery and Psychiatry, 79(4), 368–376. https://doi.org/10.1136/jnnp.2007.131045

Jin, T. (2008). The WNT signalling pathway and diabetes mellitus. Diabetologia, 51(10), 1771–1780. https://doi.org/10.1007/s00125-008-1084-y

Joseph, B., Orlian, M., & Furneaux, H. (1998). p21(waf1) mRNA contains a conserved element in its 3'-untranslated region that is bound by the Elav-like mRNA-stabilizing proteins. Journal of Biological Chemistry, 273(32), 20511–20516. https://doi.org/10.1074/jbc.273.32.20511

Kalia, L. V., Lang, A. E., Hazrati, L. N., Fujioka, S., Wszolek, Z. K., Dickson, D. W., … Marras, C. (2015). Clinical correlations with lewy body pathology in LRRK2-related Parkinson disease. JAMA Neurology, 72(1), 100–105. https://doi.org/10.1001/jamaneurol.2014.2704

Kasashima, K., Sakashita, E., Saito, K., & Sakamoto, H. (2002). Complex formation of the neuron-specific ELAV-like Hu RNA-binding proteins, 30(20), 4519–4526.

Kasashima, K., Terashima, K., Yamamoto, K., Sakashita, E., & Sakamoto, H. (1999). Cytoplasmic localization is required for the mammalian ELAV-like protein HuD to induce neuronal differentiation. Genes to Cells, 4(11), 667–683. https://doi.org/10.1046/j.1365-2443.1999.00292.x

Katsanou, V., Papadaki, O., Milatos, S., Blackshear, P. J., Anderson, P., Kollias, G., & Kontoyiannis, D. L. (2005). HuR as a negative posttranscriptional modulator in inflammation. Molecular Cell, 19(6), 777–789. https://doi.org/10.1016/j.molcel.2005.08.007

Kawakami, F., Yabata, T., Ohta, E., Maekawa, T., Shimada, N., Suzuki, M., … Obata, F. (2012). LRRK2 phosphorylates tubulin-associated tau but not the free molecule: LRRK2-mediated regulation of the tau-tubulin association and neurite outgrowth. PLoS ONE, 7(1), 1–9. https://doi.org/10.1371/journal.pone.0030834

Kedde, M., & Agami, R. (2008). Interplay between microRNAs and RNA-binding proteins determines developmental processes. Cell Cycle, 7(7), 899–903. https://doi.org/10.4161/cc.7.7.5644

Keene, J. D. (2007). RNA regulons: Coordination of post-transcriptional events. Nature Reviews Genetics, 8(7), 533–543. https://doi.org/10.1038/nrg2111

Kim, H. H., Abdelmohsen, K., & Gorospe, M. (2010). Regulation of HuR by DNA damage response Kinases. Journal of Nucleic Acids, 2010. https://doi.org/10.4061/2010/981487

Kim, H. H., Abdelmohsen, K., Lal, A., Pullmann, R., Yang, X., Srikantan, R. S., … Francisco, S. (2008). Nuclear Retention of HuR Through Phosphorylation by Cdk1. Genes & Development, 1–30. https://doi.org/10.1101/gad.1645808.that

Kim, H. H., Kuwano, Y., Srikantan, S., Dev, G., Lee, E. K., Martindale, J. L., & Gorospe, M. (2009). HuR recruits let-7 / RISC to repress c-Myc expression. Genes & Development, 23, 1743–1748. https://doi.org/10.1101/gad.1812509

Kim, H. H. & Gorospe, M. (2008). Phosphorylated HuR shuttles in cycles. Cell Cycle. 7(20): 3124–3126. https://doi.org/10.4161/cc.7.20.6884.

Kim, Y. J., & Baker, B. S. (1993). The Drosophila gene rbp9 encodes a protein that is a member of a conserved group of putative RNA binding proteins that are nervous system-specific in both flies and humans. The Journal of Neuroscience, 13(3), 1045–1056.

King, P. H. (2000). RNA-binding analyses of HuC and HuD with the *VEGF* and c-*myc* 3′-untranslated regions using a novel ELISA-based assay. Nucleic Acids Research, 28(7), e20.

Kish, S. J., Shannak, K. & Hornykiewicz, O. (1988). Uneven pattern of dopamine loss in patients with idiopathic Parkinson's disease. The New England Journal of Medicine. 318(14), 876-880.

Kovalevich, J., & Langford, D. (2013). Considerations for the Use of SH-SY5Y Neuroblastoma Cells in Neurobiology. Neuronal Cell Culture, 1078, 9–21. https://doi.org/10.1007/978-1-62703-640-5.

Krüger, R., Kuhn, W., Müller, T., Woitalla, D., Graeber, M., Kösel, S., … Riess, O. (1998). Ala30Pro mutation in the gene encoding alpha-synuclein in Parkinson's disease. Nature Genetics, 18(2), 106–108. https://doi.org/10.1038/ng0298-106

Kullmann, M., Göpfert, U., Siewe, B., & Hengst, L. (2002). ELAV/Hu proteins inhibit p27 translation via an IRES element in the p27 5′UTR. Genes & Development, 16(23), 3087–3099. http://doi.org/10.1101/gad.248902/.

Kumar, A., Greggio, E., Beilina, A., Kaganovich, A., Chan, D., Taymans, J. M., … Cookson, M. R. (2010). The Parkinson's disease associated LRRK2 exhibits weaker in vitro phosphorylation of 4E-BP compared to autophosphorylation. PLoS ONE, 5(1). https://doi.org/10.1371/journal.pone.0008730

Lafarga, V., Cuadrado, A., Lopez de Silanes, I., Bengoechea, R., Fernandez-Capetillo, O., & Nebreda, A. R. (2009). p38 Mitogen-Activated Protein Kinase- and HuR-Dependent Stabilization of p21Cip1 mRNA Mediates the G1/S Checkpoint. Molecular and Cellular Biology, 29(16), 4341–4351. https://doi.org/10.1128/MCB.00210-09

Lal, A., Kawai, T., Yang, X., Mazan-Mamczarz, K., & Gorospe, M. (2005). Antiapoptotic function of RNA-binding protein HuR effected through prothymosin α. EMBO Journal, 24(10), 1852–1862. https://doi.org/10.1038/sj.emboj.7600661

Lal, A., Mazan-Mamczarz, K., Kawai, T., Yang, X., Martindale, J. L., & Gorospe, M. (2004). Concurrent versus individual binding of HuR and AUF1 to common labile target mRNAs. EMBO Journal, 23(15), 3092–3102. https://doi.org/10.1038/sj.emboj.7600305

Lazarova, D. L., Spengler, B. A., Biedler, J. L., & Ross, R. A. (1999). HuD, a neuronal-specific RNA-binding protein, is a putative regulator of N-myc pre-mRNA processing/stability in malignant human neuroblasts. Oncogene, 18(17), 2703–2710. https://doi.org/10.1038/sj.onc.1202621

Lebedeva, S., Jens, M., Theil, K., Schwanhäusser, B., Selbach, M., Landthaler, M., & Rajewsky, N. (2011). Transcriptome-wide Analysis of Regulatory Interactions of the RNA-Binding Protein HuR. Molecular Cell, 43(3), 340–352. https://doi.org/10.1016/j.molcel.2011.06.008

Lee, E. K., Kim, W., Tominaga, K., Martindale, J. L., Yang, X., Subaran, S. S., … Gorospe, M. (2012). HuD, RNA-binding Protein Controls Insulin Translation. Molecular Cell, 45(6), 1–10. https://doi.org/10.1016/j.molcel.2012.01.016

Lei, P., Ayton, S., Finkelstein, D. I., Adlard, P. A., Masters, C. L., & Bush, A. I. (2010). Tau protein: Relevance to Parkinson's disease. International Journal of Biochemistry and Cell Biology, 42(11), 1775–1778. https://doi.org/10.1016/j.biocel.2010.07.016

Li, X., Patel, J. C., Wang, J., Avshalumov, M. V., Nicholson, C., Buxbaum, J. D., … Yue, Z. (2010). Enhanced Striatal Dopamine Transmission and Motor Performance with LRRK2 Overexpression in Mice Is Eliminated by Familial Parkinson's Disease Mutation G2019S. Journal of Neuroscience, 30(5), 1788–1797. https://doi.org/10.1523/JNEUROSCI.5604-09.2010

Lim, C. S., & Alkon, D. L. (2012). Protein kinase C stimulates HuD-mediated mRNA stability and protein expression of neurotrophic factors and enhances dendritic maturation of hippocampal neurons in culture. Hippocampus, 22(12), 2303–2319. https://doi.org/10.1002/hipo.22048

Lin, C.-H., Tsai, P.-I., Wu, R.-M., & Chien, C.-T. (2010). LRRK2 G2019S Mutation Induces Dendrite Degeneration through Mislocalization and Phosphorylation of Tau by Recruiting Autoactivated GSK3 . Journal of Neuroscience, 30(39), 13138–13149. https://doi.org/10.1523/JNEUROSCI.1737-10.2010

Lin, X., Parisiadou, L., Gu, X. L., Wang, L., Shim, H., Sun, L., … Cai, H. (2009). Leucine-Rich Repeat Kinase 2 Regulates the Progression of Neuropathology Induced by Parkinson's-Disease-Related Mutant α-synuclein. Neuron, 64(6), 807–827. https://doi.org/10.1016/j.neuron.2009.11.006

Lis, P., Burel, S., Steger, M., Mann, M., Brown, F., Diez, F., … Alessi, D. R. (2017). Development of phospho-specific Rab protein antibodies to monitor in vivo activity of the LRRK2 Parkinson's disease kinase. Biochemical Journal, 475, 1-22. https://doi.org/10.1042/BCJ20170802

Liu, Z., Wang, X., Yu, Y., Li, X., Wang, T., Jiang, H., … Smith, W. W. (2008). A Drosophila model for LRRK2-linked parkinsonism. Proceedings of the National Academy of Sciences of the United States of America, 105(7), 2693–2698. https://doi.org/10.1073/pnas.0708452105

Lo Bianco, C., Ridet, J.-L., Schneider, B. L., Deglon, N., & Aebischer, P. (2002). α-Synucleinopathy and selective dopaminergic neuron loss in a rat lentiviral-based model of Parkinson's disease. Proceedings of the National Academy of Sciences, 99(16), 10813–10818. https://doi.org/10.1073/pnas.152339799

Longo, F., Russo, I., Shimshek, D. R., Greggio, E., & Morari, M. (2014). Genetic and pharmacological evidence that G2019S LRRK2 confers a hyperkinetic phenotype, resistant to motor decline

associated with aging. Neurobiology of Disease, 71, 62–73. https://doi.org/10.1016/j.nbd.2014.07.013

Lopes, F. M., Schröder, R., Júnior, M. L. C. da F., Zanotto-Filho, A., Müller, C. B., Pires, A. S., … Klamt, F. (2010). Comparison between proliferative and neuron-like SH-SY5Y cells as an in vitro model for Parkinson disease studies. Brain Research, 1337, 85–94. https://doi.org/10.1016/j.brainres.2010.03.102

Luerman, G.C., Nguyen, C., Samaroo, H., Loos, P., Xi, H., Hurtado-Lorenzo, A., ... Hirst, W.D. (2014). Phosphoproteomic evaluation of pharmacological inhibition of leucine-rich repeat kinase 2 reveals significant off-target effects of LRRK-2-IN-1. 128(4):561-76. doi: 10.1111/jnc.12483.

Luk, K. C., Kehm, V., Carroll, J., Zhang, B., Brien, P. O., Trojanowski, J. Q., & Lee, V. M. (2012). Pathological *a*-Synuclein Transmission Initiates Parkinson-like Neurodegeneration in Nontransgenic Mice. Science, 338(6109), 949–954. https://doi.org/10.1126/science.1227157

Lundby, A., Secher, A., Lage, K., Nordsborg, N. B., Dmytriyev, A., Lundby, C., & Olsen, J. V. (2012). Quantitative maps of protein phosphorylation sites across 14 different rat organs and tissues. Nature Communications, 3, 810–876. https://doi.org/10.1038/ncomms1871

Luzón-Toro, B., de la Torre, E. R., Delgado, A., Pérez-Tur, J., & Hilfiker, S. (2007). Mechanistic insight into the dominant mode of the Parkinson's disease-associated G2019S LRRK2 mutation. Human Molecular Genetics, 16(17), 2031–2039. https://doi.org/10.1093/hmg/ddm151

Ma, W. J., Chung, S., & Furneaux, H. (1997). The Elav-like proteins bind to AU-rich elements and to the poly(A) tail of mRNA. Nucleic Acids Research, 25(18), 3564–3569. https://doi.org/10.1093/nar/25.18.3564

Ma, W., Cheng, S., Campbell, C., Wright, A., & Furneaux, H. (1996). Cloning and Characterization of HuR, a Ubiquitously Expressed Elav-like Protein. The Journal of Biological Chemistry. 271(14), 8144–8151. https://doi.org/10.1074/jbc.271.14.8144

MacLeod, D. A., Rhinn, H., Kuwahara, T., Zolin, A., Di Paolo, G., MacCabe, B. D., … Abeliovich, A. (2013). RAB7L1 Interacts with LRRK2 to Modify Intraneuronal Protein Sorting and Parkinson's Disease Risk. Neuron, 77(3), 425–439. https://doi.org/10.1016/j.neuron.2012.11.033

MacLeod, D., Dowman, J., Hammond, R., Leete, T., Inoue, K., & Abeliovich, A. (2006). The Familial Parkinsonism Gene LRRK2 Regulates Neurite Process Morphology. Neuron, 52(4), 587–593. https://doi.org/10.1016/j.neuron.2006.10.008

Majumder, M., House, R., Palanisamy, N., Qie, S., Day, T. A., Neskey, D., … Palanisamy, V. (2016). RNA-Binding Protein FXR1 Regulates p21 and TERC RNA to Bypass p53-Mediated Cellular Senescence in OSCC. PLoS Genetics, 12(9), 1–27. https://doi.org/10.1371/journal.pgen.1006306

Mansfield, K. D., & Keene, J. D. (2012). Neuron-specific ELAV/Hu proteins suppress HuR mRNA during neuronal differentiation by alternative polyadenylation. Nucleic Acids Research, 40(6), 2734–2746. https://doi.org/10.1093/nar/gkr1114

Marchese, D., Botta-Orfila, T., Cirillo, D., Rodriguez, J. A., Livi, C. M., Fernández-Santiago, R., … Tartaglia, G. G. (2017). Discovering the 3'UTR-mediated regulation of alpha-synuclein. Nucleic Acids Research, 45(22), 12888–12903. https://doi.org/10.1093/nar/gkx1048

Marcogliese, P. C., Abuaish, S., Kabbach, G., Abdel-Messih, E., Seang, S., Li, G., … Park, D. S. (2017). LRRK2(I2020T) functional genetic interactors that modify eye degeneration and dopaminergic cell loss in Drosophila. Human Molecular Genetics, 26(7), 1247–1257. https://doi.org/10.1093/hmg/ddx030

Martin, I., Kim, J. W., Lee, B. D., Kang, H. C., Xu, J. C., Jia, H., … Dawson, V. L. (2014). Ribosomal protein s15 phosphorylation mediates LRRK2 neurodegeneration in Parkinson's disease. Cell, 157(2), 472–485. https://doi.org/10.1016/j.cell.2014.01.064

Masliah, E., Rockenstein, E., Veinbergs, I., Mallory, M., Hashimoto, M., Takeda, a, … Mucke, L. (2000). Dopaminergic loss and inclusion body formation in alpha-synuclein mice: implications for neurodegenerative disorders. Science. 287(2000), 1265–1269. https://doi.org/10.1126/science.287.5456.1265

Mata, I. F., Wedemeyer, W. J., Farrer, M. J., Taylor, J. P., & Gallo, K. A. (2006). LRRK2 in Parkinson's disease: protein domains and functional insights. Trends in Neurosciences, 29(5), 286–293. https://doi.org/10.1016/j.tins.2006.03.006

McCarthy, M. M., Moore-Kochlacs, C., Gu, X., Boyden, E. S., Han, X., & Kopell, N. (2011). Striatal origin of the pathologic beta oscillations in Parkinson's disease. Proceedings of the National Academy of Sciences, 108(28), 11620–11625. https://doi.org/10.1073/pnas.1107748108

Mertins, P., Mani, D. R., Ruggles, K. V., Gillette, M. A., Clauser, K. R., Wang, P., … Carr, S. A. (2016). Proteogenomics connects somatic mutations to signalling in breast cancer. Nature, 534(7605), 55–62. https://doi.org/10.1038/nature18003

Mobarak, C. D., Anderson, K. D., Morin, M., Beckel-Mitchener, A., Rogers, S. L., Furneaux, H., … Perrone-Bizzozero, N. I. (2000). The RNA-binding Protein HuD Is Required for GAP-43 mRNA Stability, GAP-43 Gene Expression, and PKC-dependent Neurite Outgrowth in PC12 Cells. Molecular Biology of the Cell, 11(9), 3191–3203. https://doi.org/10.1091/mbc.11.9.3191

Moehle, M. S., Webber, P. J., Tse, T., Sukar, N., Standaert, D. G., DeSilva, T. M., … West, A. B. (2012). LRRK2 Inhibition Attenuates Microglial Inflammatory Responses. Journal of Neuroscience, 32(5), 1602–1611. https://doi.org/10.1523/JNEUROSCI.5601-11.2012

Mokretar, K., Pease, D., Taanman, J.-W., Soenmez, A., Ejaz, A., Lashley, T., … Proukakis, C. (2018). Somatic copy number gains of α-synuclein (SNCA) in Parkinson's disease and multiple system atrophy brains. Brain, (2018), 1–13. https://doi.org/10.1093/brain/awy157

Moussaud, S., Jones, D. R., Moussaud-Lamodière, E. L., Delenclos, M., Ross, O. A., & McLean, P. J. (2014). Alpha-synuclein and tau: teammates in neurodegeneration? Molecular Neurodegeneration, 9(43), 1-14. https://doi.org/10.1186/1750-1326-9-43

Muda, K., Bertinetti, D., Gesellchen, F., Hermann, J. S., von Zweydorf, F., Geerlof, A., … Herberg, F. W. (2014). Parkinson-related LRRK2 mutation R1441C/G/H impairs PKA phosphorylation of LRRK2 and disrupts its interaction with 14-3-3. Proceedings of the National Academy of Sciences, 111(1), E34–E43. https://doi.org/10.1073/pnas.1312701111

Mukherjee, N., Corcoran, D. L., Nusbaum, J. D., Reid, D. W., Georgiev, S., Hafner, M., … Keene, J. D. (2011). Integrative regulatory mapping indiciates that the RNA-binding protein HuR (ELAVL1) couples pre-mRNA processing and mRNA stability. Mol Cell, 43(3), 327–339. https://doi.org/10.1016/j.molcel.2011.06.007

Ng, C., Mok, S. Z. S., Koh, C., Ouyang, X., Fivaz, M. L., Dawson, V. L., … Lim, K. (2010). Parkin Protects Against LRRK2 G2019S Mutant-induced Dopaminergic Neurodegeneration in Drosophila. J Neurosci., 29(36), 11257–11262. https://doi.org/10.1523/JNEUROSCI.2375-09.2009.Parkin

Nikonova, E. V., Xiong, Y., Tanis, K. Q., Dawson, V. L., Vogel, R. L., Finney, E. M., … Dawson, T. M. (2012). Transcriptional responses to loss or gain of function of the leucine-rich repeat kinase 2 (LRRK2) gene uncover biological processes modulated by LRRK2 activity. Human Molecular Genetics, 21(1), 163–174. https://doi.org/10.1093/hmg/ddr451

Noureddine, M. A., Qin, X. J., Oliveira, S. A., Skelly, T. J., van der Walt, J., Hauser, M. A., … Li, Y. J. (2005). Association between the neuron-specific RNA-binding protein ELAVL4 and Parkinson disease. Human Genetics, 117(1), 27–33. https://doi.org/10.1007/s00439-005-1259-2

Ohta, E., Kawakami, F., Kubo, M., & Obata, F. (2011). LRRK2 directly phosphorylates Akt1 as a possible physiological substrate: Impairment of the kinase activity by Parkinson's disease-associated mutations. FEBS Letters, 585(14), 2165–2170. https://doi.org/10.1016/j.febslet.2011.05.044

Okano, H. J., & Darnell, R. B. (1997). A hierarchy of Hu RNA binding proteins in developing and adult neurons. The Journal of Neuroscience : The Official Journal of the Society for Neuroscience, 17(9), 3024–3037. https://doi.org/10.1523/JNEUROSCI.17-09-03024.1997

Olgiati, S., Thomas, A., Quadri, M., Breedveld, G. J., Graafland, J., Eussen, H., … Bonifati, V. (2015). Early-onset parkinsonism caused by alpha-synuclein gene triplication: Clinical and genetic findings in a novel family. Parkinsonism and Related Disorders, 21(8), 981–986. https://doi.org/10.1016/j.parkreldis.2015.06.005

O'Neill, T., Giarratani, L., Chen, P., Iyer, L., Lee, C. H., Bobiak, M., … Rathbun, G. A. (2002). Determination of substrate motifs for human Chk1 and hCds1/Chk2 by the oriented peptide library approach. Journal of Biological Chemistry, 277(18), 16102–16115. https://doi.org/10.1074/jbc.M111705200

Osgerby, L., Lai, Y-C., Thornton, P.J., Amalfitano, J., Le Duff, C., Jabeen, I., ... Mehellou, Y. (2017). Kinetin Riboside and Its ProTides Activate the Parkinson's Disease Associated PTEN-Induced Putative Kinase 1 (PINK1) Independent of Mitochondrial Depolarization. Journal of Medicinal Chemistry. 60(8): 3518–3524. 10.1021/acs.jmedchem.6b01897

Paisán-Ruíz, C., Jain, S., Evans, E. W., Gilks, W. P., Simón, J., Van Der Brug, M., … Singleton, A. B. (2004). Cloning of the gene containing mutations that cause PARK8-linked Parkinson's disease. Neuron, 44(4), 595–600. https://doi.org/10.1016/j.neuron.2004.10.023

Papkovskaia, T. D., Chau, K. Y., Inesta-vaquera, F., Papkovsky, D. B., Healy, D. G., Nishio, K., … Cooper, J. M. (2012). G2019S leucine-rich repeat kinase 2 causes uncoupling protein-mediated mitochondrial depolarization. Human Molecular Genetics, 21(19), 4201–4213. https://doi.org/10.1093/hmg/dds244

Parisiadou, L., Xie, C., Cho, H. J., Lin, X., Gu, X.-L., Long, C.-X., … Cai, H. (2009). Phosphorylation of Ezrin/Radixin/Moesin Proteins by LRRK2 Promotes the Rearrangement of Actin Cytoskeleton in Neuronal Morphogenesis. Journal of Neuroscience, 29(44), 13971–13980. https://doi.org/10.1523/JNEUROSCI.3799-09.2009

Park, S., Myszka, D. G., Yu, M., Littler, S. J., & Laird-Offringa, I. a. (2000). HuD RNA recognition motifs play distinct roles in the formation of a stable complex with AU-rich RNA. Molecular and Cellular Biology, 20(13), 4765–4772. https://doi.org/10.1128/MCB.24.15.6888.2004

Park-Lee, S., Kim, S., & Laird-Offringa, I. A. (2003). Characterization of the interaction between neuronal RNA-binding protein HuD and AU-rich RNA. Journal of Biological Chemistry, 278(41), 39801–39808. https://doi.org/10.1074/jbc.M307105200

Pascale, A., Amadio, M., Scapagnini, G., Lanni, C., Racchi, M., Provenzani, A., … Quattrone, A. (2005). Neuronal ELAV proteins enhance mRNA stability by a PKCalpha-dependent pathway. Proceedings of the National Academy of Sciences of the United States of America, 102(34), 12065–12070. https://doi.org/10.1073/pnas.0504702102

Patterson, S. L., Abel, T., Deuel, T. A. S., Martin, K. C., Rose, J. C., & Kandel, E. R. (1996). Recombinant BDNF rescues deficits in basal synaptic transmission and hippocampal LTP in BDNF knockout mice. Neuron, 16(6), 1137–1145. https://doi.org/10.1016/S0896-6273(00)80140-3

Pechnick, R. N., Zonis, S., Wawrowsky, K., Pourmorady, J., & Chesnokova, V. (2008). p21Cip1 restricts neuronal proliferation in the subgranular zone of the dentate gyrus of the hippocampus. Proceedings of the National Academy of Sciences, 105(4), 1358–1363. https://doi.org/10.1073/pnas.0711030105

Perera, G., Ranola, M., Rowe, D. B., Halliday, G. M., & Dzamko, N. (2016). Inhibitor treatment of peripheral mononuclear cells from Parkinson's disease patients further validates LRRK2 dephosphorylation as a pharmacodynamic biomarker. Scientific Reports, 6(31391), 1–8. https://doi.org/10.1038/srep31391

Perrone-Bizzozero, N., & Bird, C. W. (2013). Role of HuD in nervous system function and pathology. Frontiers in Bioscience (Scholar Edition), 5, 554–563. https://doi.org/10.2741/S389

Perrone-Bizzozero, N., & Bolognani, F. (2002). Role of HuD and other RNA-Binding proteins in neural development and plasticity. Journal of Neuroscience Research, 68(2), 121–126. https://doi.org/10.1002/jnr.10175

Plowey, E. D., Cherra, S. J., Liu, Y. J., & Chu, C. T. (2008). Role of autophagy in G2019S-LRRK2-associated neurite shortening in differentiated SH-SY5Y cells. Journal of Neurochemistry, 105(3), 1048–1056. https://doi.org/10.1111/j.1471-4159.2008.05217.x

Polacchini, A., Metelli, G., Francavilla, R., Baj, G., Florean, M., Mascaretti, L. G., & Tongiorgi, E. (2015). A method for reproducible measurements of serum BDNF: Comparison of the performance of six commercial assays. Scientific Reports, 5(17989), 1–10. https://doi.org/10.1038/srep17989

Polymeropoulos, M. H., Lavedan, C., Leroy, E., Ide, S. E., Dehejia, A., Dutra, A., … Nussbaum, R. L. (1997). Mutation in the α-Synuclein Gene Identified in Families with Parkinson's Disease. Science, 276, 2045–2047. https://doi.org/10.1126/science.276.5321.2045

Porritt, M., Stanic, D., Finkelstein, D., Batchelor, P., Lockhart, S., Hughes, A., … Howells, D. (2005). Dopaminergic innervation of the human striatum in Parkinson's disease. Movement Disorders, 20(7), 810–818. https://doi.org/10.1002/mds.20399

Qin, Q., Zhi, L. T., Li, X. T., Yue, Z. Y., Li, G. Z., & Zhang, H. (2017). Effects of LRRK2 Inhibitors on Nigrostriatal Dopaminergic Neurotransmission. CNS Neuroscience and Therapeutics, 23(2), 162–173. https://doi.org/10.1111/cns.12660

Ramonet, D., Daher, J. P. L., Lin, B. M., Stafa, K., Kim, J., Banerjee, R., … Moore, D. J. (2011). Dopaminergic Neuronal loss, Reduced Neurite Complexity and Autophagic Abnormalities in Transgenic Mice Expressing G2019S Mutant LRRK2. PLoS ONE, 6(4), 13–19. https://doi.org/10.1371/journal.pone.0018568

Recasens, A., Dehay, B., Bové, J., Carballo-Carbajal, I., Dovero, S., Pérez-Villalba, A., … Vila, M. (2014). Lewy body extracts from Parkinson disease brains trigger α-synuclein pathology and neurodegeneration in mice and monkeys. Annals of Neurology, 75(3), 351–362. https://doi.org/10.1002/ana.24066

Reimand, J., Arak, T., Adler, P., Kolberg, L., Reisberg, S., Peterson, H., & Vilo, J. (2016). g:Profiler-a web server for functional interpretation of gene lists (2016 update). Nucleic Acids Research, 44(W1), W83–W89. https://doi.org/10.1093/nar/gkw199

Reith, A. D., Bamborough, P., Jandu, K., Andreotti, D., Mensah, L., Dossang, P., … Gray, N. S. (2012). GSK2578215A; A potent and highly selective 2-arylmethyloxy-5-substitutent- N-arylbenzamide LRRK2 kinase inhibitor. Bioorganic and Medicinal Chemistry Letters, 22(17), 5625–5629. https://doi.org/10.1016/j.bmcl.2012.06.104

Ross, R. A., & Spengler, B. A. (2007). Human neuroblastoma stem cells. Seminars in Cancer Biology, 17(3), 241–247. https://doi.org/10.1016/j.semcancer.2006.04.006

Ross, R. A., Lazarova, D. L., Manley, G.T., Smitt, P. S., Spengler, B. A., Posner, J. B., Biedler, J. L. (1997). HuD, a neuronal-specific RNA-binding protein, is a potential regulator of MYCN expression in human neuroblastoma cells. European Journal of Cancer (Oxford, England), 33(12), 2071-2074. DOI: 10.1016/S0959-8049(97)00331-6

Rüdel, S., Wang, Y., Lenobel, R., Körner, R., Hsiao, H. H., Urlaub, H., … Meister, G. (2011). Phosphorylation of human Argonaute proteins affects small RNA binding. Nucleic Acids Research, 39(6), 2330–2343. https://doi.org/10.1093/nar/gkq1032

Russo, I., Bubacco, L., & Greggio, E. (2014). LRRK2 and neuroinflammation: Partners in crime in Parkinson's disease? Journal of Neuroinflammation, 11(1), 1–9. https://doi.org/10.1186/1742-2094-11-52

Sacco, F., Humphrey, S. J., Cox, J., Mischnik, M., Schulte, A., Klabunde, T., … Mann, M. (2016). Glucose-regulated and drug-perturbed phosphoproteome reveals molecular mechanisms controlling insulin secretion. Nature Communications, 7(13250). https://doi.org/10.1038/ncomms13250

Salazar, C., & Höfer, T. (2009). Multisite protein phosphorylation - From molecular mechanisms to kinetic models. FEBS Journal, 276(12), 3177–3198. https://doi.org/10.1111/j.1742-4658.2009.07027.x

Samson, M. L. (2008). Rapid functional diversification in the structurally conserved ELAV family of neuronal RNA binding proteins. BMC Genomics, 9, 1–11. https://doi.org/10.1186/1471-2164-9-392

Samson, M. L., & Chalvet, F. (2003). Found in neurons, a third member of the Drosophila elav gene family, encodes a neuronal protein and interacts with elav. Mechanisms of Development, 120(3), 373–383. https://doi.org/10.1016/S0925-4773(02)00444-6

Scheckel, C., Drapeau, E., Frias, M. A., Park, C. Y., Fak, J., Zucker-Scharff, I., … Darnell, R. B. (2016). Regulatory consequences of neuronal ELAV-like protein binding to coding and non-coding RNAs in human brain. eLife, 5(e10421), 1–35. https://doi.org/10.7554/eLife.10421

Schulz, C., Paus, M., Frey, K., Schmid, R., Kohl, Z., Mennerich, D., … Gillardon, F. (2011). Leucine-rich repeat kinase 2 modulates retinoic acid-induced neuronal differentiation of murine embryonic stem cells. PLoS ONE, 6(6). https://doi.org/10.1371/journal.pone.0020820

Scoumanne, A., Cho, S. J., Zhang, J., & Chen, X. (2011). The cyclin-dependent kinase inhibitor p21 is regulated by RNA-binding protein PCBP4 via mRNA stability. Nucleic Acids Research, 39(1), 213–224. https://doi.org/10.1093/nar/gkq778

Shang, J., & Zhao, Z. (2017). Emerging role of HuR in inflammatory response in kidney diseases. Acta Biochimica et Biophysica Sinica, 49(9), 753–763. https://doi.org/10.1093/abbs/gmx071

Shanley, M. R., Hawley, D., Leung, S., Zaidi, N. F., Dave, R., Schlosser, K. A., … Liu, M. (2015). LRRK2 Facilitates tau Phosphorylation through Strong Interaction with tau and cdk5. Biochemistry, 54(33), 5198–5208. https://doi.org/10.1021/acs.biochem.5b00326

Shevchenko, A., Tomas, H., Havlis, J., Olsen, J. V., Mann, M. (2007). In-gel digestion for mass spectrometric characterization of proteins and proteomes. Nature Protocols, 1(6), 2856-2860

Shin, N., Jeong, H., Kwon, J., Heo, H. Y., Kwon, J. J., Yun, H. J., … Seol, W. (2008). LRRK2 regulates synaptic vesicle endocytosis. Experimental Cell Research, 314(10), 2055–2065. https://doi.org/10.1016/j.yexcr.2008.02.015

Shipley, M. M., Mangold, C. A., & Szpara, M. L. (2017). 94. Differentiation of the SH-SY5Y human neuroblastoma cell line. J Vis Exp, 108(108), 53193. https://doi.org/10.3791/53193.

Smith, W. W., Pei, Z., Jiang, H., Moore, D. J., Liang, Y., West, A. B., … Ross, C. A. (2005). Leucine-rich repeat kinase 2 (LRRK2) interacts with parkin, and mutant LRRK2 induces neuronal degeneration. Proceedings of the National Academy of Sciences, 102(51), 18676–18681. https://doi.org/10.1073/pnas.0508052102

Smith, W. W., Pei, Z., Jiang, H., Dawson, V. L., Dawson, T. M., & Ross, C. A. (2006). Kinase activity of mutant LRRK2 mediates neuronal toxicity. Nature Neuroscience, 9(10), 1231–1233. https://doi.org/10.1038/nn1776

Spillantini, M. G., Schmidt, M. L., Lee, V. M.-Y., Trojanowski, J. Q., Jakes, R., & Goedert, M. (1997). alpha-Synuclein in Lewy bodies. Nature, 388(6645), 839–840. https://doi.org/10.1038/42166

Srikantan, S., Tominaga, K., & Gorospe, M. (2012). Functional Interplay between RNA-Binding Protein HuR and microRNAs. Current Protein and Peptide Science, 13(4), 372–379. https://doi.org/10.2174/138920312801619394

Stefl, R., Skrisovska, L., & Allain, F. H. T. (2005). RNA sequence- and shape-dependent recognition by proteins in the ribonucleoprotein particle. EMBO Reports, 6(1), 33–38. https://doi.org/10.1038/sj.embor.7400325

Steger, M., Tonelli, F., Ito, G., Davies, P., Trost, M., Vetter, M., … Mann, M. (2016). Phosphoproteomics reveals that Parkinson's disease kinase LRRK2 regulates a subset of Rab GTPases. eLife, 5(e12813), 1–28. https://doi.org/10.7554/eLife.12813.001

Suzuki, E., Tsutsumi, A., Sugihara, M., Mamura, M., Goto, D., Matsumoto, I., … Sumida, T. (2006). Expression of TNF-α, tristetraprolin, T-cell intracellular antigen-1 and Hu antigen R genes in synovium of patients with rheumatoid arthritis. International Journal of Molecular Medicine, 18(2), 273–278.

Szabo, A., Dalmau, J., Manley, G., Rosenfeld, M., Wong, E., Henson, J., Posner, J.B., Furneaux, H.M. (1991). HuD, a paraneoplastic encephalomyelitis antigen, contains RNA-binding domains and is homologous to Elav and Sex-lethal. Cell. 67(2):325-33.

Tain, L. S., Mortiboys, H., Tao, R. N., Ziviani, E., Bandmann, O., & Whitworth, A. J. (2009). Rapamycin activation of 4E-BP prevents parkinsonian dopaminergic neuron loss. Nature Neuroscience, 12(9), 1129–1135. https://doi.org/10.1038/nn.2372

Taliaz, D., Stall, N., Dar, D. E., & Zangen, A. (2010). Knockdown of brain-derived neurotrophic factor in specific brain sites precipitates behaviors associated with depression and reduces neurogenesis. Molecular Psychiatry, 15(1), 80–92. https://doi.org/10.1038/mp.2009.67

Tiruchinapalli, D. M., Ehlers, M. D., & Keene, J. D. (2008). Activity-dependent expression of RNA binding protein HuD and its association with mRNAs in neurons. RNA Biology, 5(3), 157-168.

Tong, Y., Yamaguchi, H., Giaime, E., Boyle, S., Kopan, R., Kelleher, R. J., & Shen, J. (2010). Loss of leucine-rich repeat kinase 2 causes impairment of protein degradation pathways, accumulation of α-synuclein, and apoptotic cell death in aged mice. Proceedings of the National Academy of Sciences, 107(21), 9879–9884. https://doi.org/10.1073/pnas.1004676107

Umeno J, Asano K, Matsushita T, Matsumoto T, Kiyohara Y, Iida M, Nakamura Y, Kamatani N, Kubo M. (2011). Meta-analysis of published studies identified eight additional common susceptibility loci for Crohn's disease and ulcerative colitis. Inflammatory Bowel Disease. 17(12):2407-15. doi: 10.1002/ibd.21651.

Vanevski, F., & Xu, B. (2015). HuD interacts with Bdnf mRNA and is essential for activity-induced Bdnf synthesis in dendrites. PLoS ONE, 10(2), 1–20. https://doi.org/10.1371/journal.pone.0117264

Venderova, K., Kabbach, G., Abdel-Messih, E., Zhang, Y., Parks, R. J., Imai, Y., … Park, D. S. (2009). Leucine-rich repeat kinase 2 interacts with Parkin, DJ-1 and PINK-1 in a Drosophila melanogaster model of Parkinson's disease. Human Molecular Genetics, 18(22), 4390–4404. https://doi.org/10.1093/hmg/ddp394

Volpicelli-Daley, L. A., Abdelmotilib, H., Liu, Z., Stoyka, L., Daher, J. P. L., Milnerwood, A. J., … West, A. B. (2016). G2019S-LRRK2 Expression Augments α-Synuclein Sequestration into Inclusions in Neurons. Journal of Neuroscience, 36(28), 7415–7427. https://doi.org/10.1523/JNEUROSCI.3642-15.2016

Wakamatsu, Y., & Weston, J. A. (1997). Sequential expression and role of Hu RNA-binding proteins during neurogenesis. Development, 124(17), 3449–3460. http://www.ncbi.nlm.nih.gov/pubmed/9310339

Wallings, R., Manzoni, C., & Bandopadhyay, R. (2015). Cellular processes associated with LRRK2 function and dysfunction. FEBS Journal, 282(15), 2806–2826. https://doi.org/10.1111/febs.13305

Wang, D., Tang, B., Zhao, G., Pan, Q., Xia, K., Bodmer, R., & Zhang, Z. (2008). Dispensable role of Drosophila ortholog of LRRK2 kinase activity in survival of dopaminergic neurons. Molecular Neurodegeneration, 3(1), 1–7. https://doi.org/10.1186/1750-1326-3-3

Wang, H., Zeng, F., Liu, Q., Liu, H., Liu, Z., Niu, L., … Li, X. (2013). The structure of the ARE-binding domains of Hu antigen R (HuR) undergoes conformational changes during RNA binding. Acta Crystallographica Section D: Biological Crystallography, 69(3), 373–380. https://doi.org/10.1107/S0907444912047828

Wang, H., Molfenter, J., Zhu, H., & Lou, H. (2010). Promotion of exon 6 inclusion in HuD pre-mRNA by Hu protein family members. Nucleic Acids Research, 38(11), 3760–3770. https://doi.org/10.1093/nar/gkq028

Wang, W., Furneaux, H., Cheng, H., Caldwell, M. C., Hutter, D., Liu, Y., … Gorospe, M. (2000). HuR Regulates p21 mRNA Stabilization by UV Light. Molecular and Cellular Biology, 20(3), 760–769. https://doi.org/10.1128/MCB.20.3.760-769.2000

Wang, X., & Hall, T. M. (2001). Structural basis for recognition of AU-rich element RNA by the HuD protein. Nature Structural Biology, 8(2), 141–145. https://doi.org/10.1038/84131

Wang, X., Yan, M. H., Fujioka, H., Liu, J., Wilson-delfosse, A., Chen, S. G., … Zhu, X. (2012). LRRK2 regulates mitochondrial dynamics and function through direct interaction with DLP1. Human Molecular Genetics, 21(9), 1931–1944. https://doi.org/10.1093/hmg/dds003

Wein, G., Rossler, M., Klug, R., Herget, T. (2003). The 3′-UTR of the mRNA coding for the major protein kinase C substrate MARCKS contains a novel CU-rich element interacting with the mRNA stabilizing factors HuD and HuR. Eur J Biochem, 270(2), 350-65. https://doi.org/10.1046/j.1432-1033.2003.03396.x

West, A. B., Moore, D. J., Biskup, S., Bugayenko, A., Smith, W. W., Ross, C. A., … Dawson, T. M. (2005). From The Cover: Parkinson's disease-associated mutations in leucine-rich repeat kinase 2 augment kinase activity. Proceedings of the National Academy of Sciences, 102(46), 16842–16847. https://doi.org/10.1073/pnas.0507360102

West, A. B. (2015). Ten years and counting: Moving leucine-rich repeat kinase 2 inhibitors to the clinic. Movement Disorders, 30(2), 180–189. https://doi.org/10.1002/mds.26075

West, A. B., Moore, D. J., Choi, C., Andrabi, S. A., Li, X., Dikeman, D., … Dawson, T. M. (2007). Parkinson's disease-associated mutations in LRRK2 link enhanced GTP-binding and kinase activities to neuronal toxicity. Human Molecular Genetics, 16(2), 223–232. https://doi.org/10.1093/hmg/ddl471

Westerlund, M., Belin, A. C., Anvret, A., Bickford, P., Olson, L., & Galter, D. (2008). Developmental regulation of leucine-rich repeat kinase 1 and 2 expression in the brain and other rodent and human organs: Implications for Parkinson's disease. Neuroscience, 152(2), 429–436. https://doi.org/10.1016/j.neuroscience.2007.10.062

Winner, B., Kohl, Z., Gage, F.H. (2011). Neurodegenerative disease and adult neurogenesis. European Journal of Neuroscience. 33(6):1139-51. https://doi.org/10.1111/j.1460-9568.2011.07613.x

Winzen, R., Gowrishankar, G., Bollig, F., Redich, N., Resch, K., & Holtmann, H. (2004). Distinct domains of AU-rich elements exert different functions in mRNA destabilization and stabilization by p38 mitogen-activated protein kinase or HuR. Molecular and Cellular Biology, 24(11), 4835–4847. https://doi.org/10.1128/MCB.24.11.4835-4847.2004

Xicoy, H., Wieringa, B., & Martens, G. J. M. (2017). The SH-SY5Y cell line in Parkinson's disease research: a systematic review. Molecular Neurodegeneration, 12(1), 1–11. https://doi.org/10.1186/s13024-017-0149-0

Xiong, Y., & Yu, J. (2018). Modeling Parkinson's disease in Drosophila: What have we learned for dominant traits? Frontiers in Neurology, 9(228). https://doi.org/10.3389/fneur.2018.00228

Yannoni, Y. M., & White, K. (1999). Domain necessary for Drosophila ELAV nuclear localization: function requires nuclear ELAV. Journal of Cell Science, 112, 4501–4512.

Yu, T. X., Wang, P. Y., Rao, J. N., Zou, T., Liu, L., Xiao, L., … Wang, J. Y. (2011). Chk2-dependent HuR phosphorylation regulates occludin mRNA translation and epithelial barrier function. Nucleic Acids Research, 39(19), 8472–8487. https://doi.org/10.1093/nar/gkr567

Yun, H. J., Park, J., Ho, D. H., Kim, H., Kim, C. H., Oh, H., … Seol, W. (2013). LRRK2 phosphorylates Snapin and inhibits interaction of Snapin with SNAP-25. Experimental and Molecular Medicine, 45(8), e36-11. https://doi.org/10.1038/emm.2013.68

Zabetian, C.P., Samii, A., Mosley, A.D., Roberts, J.W., Leis, B.C., Yearout, D., Raskind, W.H., Griffith, A. (2005). A clinic-based study of the LRRK2 gene in Parkinson disease yields new mutations. Neurology. 65(5):741-4. 10.1212/01.wnl.0000172630.22804.73.

Zach, S., Felk, S., & Gillardon, F. (2010). Signal transduction protein array analysis links LRRK2 to Ste20 kinases and PKC zeta that modulate neuronal plasticity. PLoS ONE, 5(10). https://doi.org/10.1371/journal.pone.0013191

Zaharieva, E., Haussmann, I. U., Bräuer, U., & Soller, M. (2015). Concentration and localization of co-expressed ELAV/Hu proteins control specificity of mRNA processing. Molecular and Cellular Biology, 35(18), MCB.00473-15. https://doi.org/10.1128/MCB.00473-15

Zhang, F.-R., Huang, W., Chen, S.-M., Sun, L.-D., Liu, H., Li, Y., … Liu, J.-J. (2009). Genomewide Association Study of Leprosy. New England Journal of Medicine, 361(27), 2609–2618. https://doi.org/10.1056/NEJMoa0903753

Zhao, H. T., John, N., Delic, V., Ikeda-Lee, K., Kim, A., Weihofen, A., … Volpicelli-Daley, L. A. (2017). LRRK2 Antisense Oligonucleotides Ameliorate α-Synuclein Inclusion Formation in a Parkinson's Disease Mouse Model. Nucleic Acids, 8, 508–519. https://doi.org/10.1016/j.omtn.2017.08.002

Zhao, J., Molitor, T. P., Langston, J. W., & Nichols, R. J. (2015). LRRK2 dephosphorylation increases its ubiquitination. Biochemical Journal, 469(1), 107–120. https://doi.org/10.1042/BJ20141305

Zhou, H.-L., Hinman, M. N., Barron, V. A., Geng, C., Zhou, G., Luo, G., … Lou, H. (2011). Hu proteins regulate alternative splicing by inducing localized histone hyperacetylation in an RNA-dependent manner. Proceedings of the National Academy of Sciences, 108(36), E627–E635. https://doi.org/10.1073/pnas.1103344108

Zhu, H., Hasman, A., Barron, V.A., Luo, G., & Lou, H. (2006). A Nuclear Function of Hu Proteins as Neuron-specific Alternative RNA Processing Regulators. 17, 5105–5114. 10.1091/mbc.E06-02-0099.

Zhu, H., Hinman, M. N., Hasman, R. A., Mehta, P., & Lou, H. (2008). Regulation of Neuron-Specific Alternative Splicing of Neurofibromatosis Type 1 Pre-mRNA. Molecular and Cellular Biology, 28(4), 1240–1251. https://doi.org/10.1128/MCB.01509-07

Zimprich, A., Biskup, S., Leitner, P., Lichtner, P., Farrer, M., Lincoln, S., … Gasser, T. (2004). Mutations in LRRK2 cause autosomal-dominant parkinsonism with pleomorphic pathology. Neuron, 44(4), 601–607. https://doi.org/10.1016/j.neuron.2004.11.005

Appendix

Supplementary Tables and Figures

Supplementary Tables

Table 1: Antisense siRNA sequences of Thermo Fisher Scientific Silencer® Select siRNAs used in this study.

Target gene	siRNA ID	Catalog #	Antisense sequence (5'-3')
Elavl4 (mouse)	s67974	4390771	AAAUUGUCCAGCCUGAAUCuu
LRRK2 (human)	s42413 s42415	4392420 4392420	UUCGGUUAUAAGGCACAGCct AGUUGUAAUAAUCGUUUCCgg
Negative control	N/A	4390847	N/A

Table 2: Mice used in this study.

Genotype		Litter	Sex	Age	Application
HuD	***Lrrk2***				
+/+	+/+	A	933 - F	4w+3d	WB (Figure 15-17)
		A	934 - M	4w+3d	WB (Figure 15-17)
		B	1645 - M	3w+6d	HuD-RNA IP (Figure 11); WB ((Figure 15-17)
		B	1662 - F	3w+6d	HuD-RNA IP (Figure 11); WB (Figure 15-17)
		B	1663 - F	3w+6d	HuD-RNA IP (Figure 11); WB (Figure 15-17); LC-MS/MS (Table 3)
		C	1996 - M	3w+6d	HuD-RNA IP (Figure 11); WB (Figure 15-17); LC-MS/MS (Table 3)
		D	2011 - F	3w+2d	WB (Figure 15-17)
		D	2012 - F	3w+2d	WB (Figure 15-17)
		D	2013 - F	3w+2d	WB (Figure 15-17)
-/-	+/+	A	932 F	4w+3d	WB (Figure 15-17)
		E	938 F	4w+2d	WB (Figure 15-17)
		E	939 F	4w+2d	WB (Figure 15-17)
-/-	+/+	E	940 F	4w+2d	WB (Figure 15-17)

		F	947 F	3w+3d	WB (Figure 15-17)
		F	948 F	3w+3d	WB (Figure 15-17)
+/+	G2019S/+	G	975 F	3w+6d	WB (Figure 15-17)
		G	976 F	3w+6d	HuD-RNA IP (Figure 11); WB (Figure 15-17)
		G	978 M	3w+6d	WB (Figure 15-17)
		G	979 M	3w+6d	WB (Figure 15-17)
		G	981 M	3w+6d	WB (Figure 15-17)
		H	985 M	4w+0d	HuD-RNA IP (Figure 11);
		I	1766 M	4w+2d	WB (Figure 15-17)
		I	1767 M	4w+2d	WB (Figure 15-17); LC-MS/MS (Table 3)
		I	1768 M	4w+2d	WB (Figure 15-17); LC-MS/MS (Table 3)
		J	1985 F	4w+2d	HuD-RNA IP (Figure 11); WB (Figure 7&8);
		J	1986 F	4w+2d	WB (Figure 15-17)
		J	1987 F	4w+2d	WB (Figure 15-17)
-/-	G2019S/+	K	1760	3w+5d	WB (Figure 15-17)
		K	1761	3w+5d	WB (Figure 15-17)
		K	1769	3w+5d	WB (Figure 15-17)
		L	1587	4w+1d	WB (Figure 15-17)
		M	1892	4w+4d	WB (Figure 15-17)
+/+	-/-	N	1785 F	3w+6d	LC-MS/MS (Table 3)

Table 3: Antibodies used in this study for immunoblotting (unless otherwise indicated).

Antibody	Dilution	Supplier	Catalogue #
Primary			
α-synuclein	1:5000	Cell Signalling Technology	2628
α-Tubulin	1:20,000	Thermo Fisher Scientific	PA5-22060
β-Actin	1:10,000	Sigma	A5441-.2ML
BDNF	1:3000	Abcam	Ab205067
eIF4A (C32B4)	1:10,000	Cell Signalling Technology	2013S
FLAG (M2)	1:5000	Sigma	F1804-IMG
Gap-43	1:10,000	Millipore	Ab5220
HuD (H-9)	1:5000	Santa Cruz	sc48421
HuD	1:3000	Abcam	Ab96474
HuR (3A2)	1:5000	Santa Cruz	sc5261
LRRK2 (MJFF2[c41-2])	1:1000	Abcam	Ab133474
LRRK2 PSer935 (UDD2-10(12))	1:1000	Abcam	Ab13340
P-Thr (H2)	1:1000	Santa Cruz	sc5267
p21 (EPR362)	1:3000	Abcam	Ab109520
HRP-secondary			
Goat anti-mouse	1:5000	Jackson ImmunoResearch	115-035-174
Goat anti-rabbit	1:5000	Jackson ImmunoResearch	111-035-144
Isotype control (for immunoprecipitation)			
Mouse IgG1 K immunoglobulin	N/A	eBioscience	14-4714-82

Table 4: Primer sets used in this study.

Target gene	Species	Sequence (5' – 3')		Application
Actb	Mouse	Fwd	AGATCAAGATCATTGCTCCTCCT	RT-qPCR
		Rev	ACGCAGCTCAGTAACAGTCC	
BDNF	Human	Fwd	GGCGGCAGACAAAAAGACTG	
		Rev	CACTGGGAGTTCCAATGCCT	
Bdnf	Mouse	Fwd	TGCGGATATTGCGAAGGGTT	
		Rev	ACCTGGTGGAACATTGTGGC	
CDKN1A	Human	Fwd	CCAGCATGACAGATTTCTACCAC	
		Rev	AGAAGATGTAGAGCGGGCCT	
ELAVL4	Human	Fwd	GCGTAAAGAGACTGATGTCTGGA	
		Rev	CACTCTCATCGGAATCGGGG	
Elavl4	Mouse	Fwd	GCTTGTATGTGTAGCGGTGC	
		Rev	TGGTGCTAATTATCATCTTCAAGCC	
ELAVL1	Human	Fwd	GGCGCAGAGATTCAGGTTCT	
		Rev	CCAAACGGCCCAAACATCTG	
GAP43	Human	Fwd	CAAACAGAATTAAAAGGGAACCTGG	
		Rev	TTAAGCAAGGGCTGAGGTGT	
GAPDH	Human	Fwd	ATCACCATCTTCCAGGAGCGA	
		Rev	TCTCCATGGTGGTGAAGACG	
Gapdh	Mouse	Fwd	CCCTTAAGAGGGATGCTGCC	
		Rev	TACGGCCAAATCCGTTCACA	
LRRK2	Human	Fwd	GCACAGCTAGGAAGCCTTAAA	
		Rev	GGAAGATTGATGTCCCAAACGG	
Lrrk2	Mouse	Fwd	CTCACCCCCACTTCATGACC	

		Rev	GAAGAGGCACGAGCCTTGAT	
MAPT	Human	Fwd	TGACCCAAGAGCCTGAAAGT	
		Rev	TGTGTCCTCAGGTCCTGTCC	
SNCA	Human	Fwd	GCAACAGTGGCTGAGAAGAC	
		Rev	AATTCCTTCCTGTGGGGCTC	
Snca	Mouse	Fwd	ACCAGATGGGCAAGGGTGAG	
		Rev	GAACTGAGCACTTGTACGCC	
TBP	Human	Fwd	AGTGACCCAGCATCACTGTTT	
		Rev	CGCTGGAACTCGTCTCACTA	
HuD-T144A		Fwd	GCCCAGAAGGAACTGGAGCAACTTTTCTCGCA	Site-directed mutagenesis
		Rev	CATGGTTTTGGGAAGGCCGCTAACATAGAGGT	
HuD-T169A		Fwd	GCAGGAGTGTCCAGAGGGGTGGGATTCAT	
		Rev	GACTTGATCAACCAGGATTCGTGAGGTGATG	
ELAVL4 - Sequence 1			GGAGTCTCTTCGGGAGCATTGG	DNA sequencing
ELAVL4 - Sequence 2			GTTAGCGGCCTTCCCAAAAC	

Table 5: Potential HuD-binding sites in the 3'UTR of transcripts encoding human and mouse LRRK2 and alpha-synuclein. Binding sites were predicted using the RBPmap database (http://rbpmap.technion.ac.il/) using representative query HuD-binding motifs listed in Table 1 (see introduction); HUUUUK; UUKRUUU; $(AUUUA)_2$; KUUUKUUUKK; UUUUUHUUUW. All underlined sequences represent statistically significant matches below a user-defined threshold ($p<0.005$). Sequences in red represent cases where two motifs overlap, while highlighted sequences represent at least three overlapping motifs.

Transcript	3'UTR sequence (5' to 3')
Human *LRRK2*	gaaaauuauucucuccucuuguaaauauuuauuuuaaaaauguucacauggaaaggguacucacauu uuuugaaauagcucguguguaugaaggaauguuauuauuuuuaauuuaaauauguaaaaauacuu accaguaaaugugguauuuuaaagaacuauuuaaaacacaauguuauauuucuuauaaauaccaguua cuuucguucauuaauuaaugaaaauaaaucugugaaguaccuaauuuaaguacucauacuaaaauuu auaaggccgauaauuuuuuguuuucuugucugguaauggaggguaaacuuuauuuuaauucugugcuu aagacaggacuauugcuugucgauuuuucuagaaaucugcacgguauaaugaaaauauuaagacagu uucccauguaauguauuccuucuagauugcaucgaaaugcacuaucauauaugcuuguaaauauuc aaaugaauuugcacuaauaaaguccuuuguuggguaugugaauucucuuuguugcuguugcaaacagu gcaucuuacacaacuucacucaauucaaaagaaaacuccauuaaaaguacuaaugaaaaaacaugac auacugucaaaguccucauaucuaggaaagacacagaaacucucuuugucacagaaacucucugugu cuuuccuagacauaauagaguuguuuuuucaacucuauguuugaauguggauacccugaauuuuguau aauuaguguaaauacaguguucaguccuucaagugauauuuuuauuuuuuuauucauaccacuagcu acuuguuuucuaaucugcuucauucuaaugcuuauauucaucuuuucccuaaauuugugaugcugca gauccuacaucauucagauagaaaccuuuuuuuuuuuucagaauuauagaauuccacagcuccuacca agaccaugaggauaaauaucuaacacuuuucaguugcugaaggagaaaggagcuuuaguuaugaugg auaaaaauaucugccacccuaggcuuccaaauuauacuuaaauuguuuacauagcuuaccacaauag gaguaucagggccaaauaccuauguaauaauuugaggucauuucugcuuuaggaaaaguacuuucgg uaaauucuuuggcccugaccaguauucauuauuucagauaauucccugugauaggacaacuaguaca uuuaauauucucagaacuuauggcauuuuacuaugugaaaacuuuaaauuuauuuauauuaagggua aucaauucuuaaagaugaaagauuuucuguauuuuaaaggaagcuaugcuuuaacuuguuauguaa uuaacaaaaaaaucauauauaauagagcucuuuguuccaguguuaucucuuucauuguuacuuugua uuugcaauuuuuuuuaccaaagacaaauuaaaaaaaugaauaccauauuuaaauggaauaauaaagg uuuuuuaaaaacuu
Mouse *Lrrk2*	aaagacaucaggcagucucgauguuauauugaauaagacaucagacauccucgucacuauauugaaa aggacaucagacauccucgccaauauguuagaaaauguacucuucuuuuuaaaauauauuuuuaaaa uguuuuacauugaaaagaguaugccuauucuuuacaaaguucauauguauauugaaggaauguguaugu cuuauguuuaauuuaauauauguaaaaauauuuaucaguaaauauguuuuaaaaaacuauuuaauuu agcauuauauuuucuauacuccuuaacuaauuugaagggauaaacaaaagaaaucuacaaagcauuu aauuucaguauuuauacuaaaauuaauaaaaauaucauguuuguuuugcuauguauugugaugauaa agccuauuuuaaauuguugauuaagacacagauguugcuugauuaucuauggacucagcggaguaga auaaaauaucuggucaauuuccaaguaagagacucuuucauaucuuguuuucaagugaauuaucauc auuaauguaaacugucauauuuucacuaauaaagauuuuuguuagcucaggaa
Human *SNCA*	gaaauaucuuugcucccaguuucuugagaucugcugacagauguuccauccuguacaagugcucagu uccaaugugcccagucaugacauuuucucaaaguuuuuacaguguaucucgaagucuuccaucagcag ugauugaaguaucuguaccugccccacucagcauuucggugcuucccuuucacugaagugaauaca ugguagcagggucuuugugugcuguggauuuugugguucaaucuacgauguuaaaacaaauuaaaa acaccuaagugacuaccacuuauuucuaaauccucacuauuuuuuuguugcuguuguucagaaguug uuagugauuugcuaucauauauuauaagauuuuuaggugucuuuuaaugauacugucuaagaauaau gacguauugugaaauuuguuaauauauauaauacuuaaaaauaugugagcaugaaacuaugcaccua uaaauacuaaauaugaaauuuuaccauuuugcgauguguuuuauucacuuguguuuguauauaaaug gugagaauuaaaauaaaacguuaucucauugcaaaaauauuuuauuuuuaucccaucucacuuuaau aauaaaaaucaugcuuauaagcaacaugaauuaagaacugacacaaaggacaaaaauauaaaguuau uaauagccauuugaagaaggaggaauuuuagaagagguagagaaaauggaacauuaacccuacacuc

	ggaauucccugaagcaacacugccagaagugugguuuugguaugcacugguuccuuaaguggcuguga uuaauuauugaaaguggggguguugaagaccccaacuacuauuguagaguggucuauuucucccuuca auccuguca**auguuugcuuua**cguauuuuggggaacuguuguuugaugugua**uguguuuauaaauugu** **uauacauuuuuuaauugagccuuuuauuaa**acauauauuguuauuuuuugucucgaa**auaauuuuuuuagu** **uaaaaucuauuuuugucuga**uauuggugugaaugcuguaccuuucugacaauaaauaauauucgacca ugaauaaaaaaaaaaaaaaaguggguucccgggaacuaagcaguguagaagaugauuuugacuacac ccuccuuagagagccauaagacacauuagcacauauuagcacauucaaggcucugagagaauguggu ua**acuuuguuuaacucag**ca**uuccucacuuuuuuuuuuuuaaucauca**gaaauucucucucucucucu cucuuuuucucucgcu**cucuuuuuuuuuuuuuuuuuua**cagg**aaaugccuuuaaacaucguuggaacu** accagagucaccuuaaaggagaucaauucucuagacugauaaaaauuucauggccucccuuuaaaaguu ugccaaauauaugaauucuag**gauuuuuccuuag**gaaa**gguuuuucucuuuc**agggaagaucuauua acucccccaugggugcugaaaauaaacuugauggugaaaaacucuguauaaa**uuaauuu**aaaa**auuau** **uugguuucucuuuuuaauuauuc**uggggcauagucauuucuaaaagucacuaguagaaaguauaaauu ucaagacagaauauucuagacaugcuagcaguuuauauguauucaugaguaaugugauauauauuugg gcgcuggugaggaaggaaggaggaaugagugacuauaaggaugguuaccauagaa**acuuccuuuuuu** **accu**aauugaagagagacuacuacagagugcuaagcugcaugugucaucuuacacuagagagaaaug gua**aguuucuuguuuuauuuaaguuauguuua**agcaaggaaaggauuuguuauugaacaguauauuu caggaagguuagaaaguggcgguuaggau**auauuuuaa**aucuaccuaaagcagc**auauuuuaa**aaaau uuaaaaguauuugguauuaaauuaagaaauagaggacagaacuagacugauagcagugaccuagaaca auuugagauuaggaaaguugugaccaugaauuuaaggauuuauguggauacaaauucuccuuuaaag uguuucuucccu**uaauauuuauc**ugac**gguaauuuuug**agcaguga**auuacuuu**auauaucuu**aaua** **guuuauuuggg**accaaacacuuaaacaaaaguucuuuaagucauauaagccuuuucaggaagcuug ucucauauucacucccgagacauucaccugccaaguggccugaggaucaauccaguccuaggguuuau uuugcagacuuacauucucccaaguuauucagccucauaugacuccacggucggcuuuaccaaaaca guucagagugcacuuuggcacacaauugggaacagaacaaucuaaug**ugugguuuug**guauucccaagu ggggucuuuuucagaaucucugcacuagugugagaugcaaacauguuuccucaucuuucuggcuuau ccaguauguagcuauuugugacauaauaaauauauacauauaugaaaaua
Mouse *Snca*	gaaugucauugcacccaaucuccuaagaucugccggcugcucuuccauggcguacaagugcucaguu ccaaugugcccagucaugaccuuuucucaaagcuguacaguguguuucaaagucuuccaucagcagu gaucggcguccuguaccugccccucagcaucccggugcucccccucucacuacagugaaaaccuggua gcagggucuuguguguguggauauuguuguggcuucacacuuaaauuguuagaagaaacuuaaaac accuaagugacuacc**acuuauuucuaaa**uc**uucaucguuuucuuuuuguug**cuguucuuaa**gaa**guu **gugauuu**gcuccaagaguuuuaggugucc**ugaaugacucuuucugucuaagaaugauguguugugaa auuuguuaa**uauauauuuu**aaaauuaugugagcaugagacuaugcaccuauaaa**uauua**auuua**uga** **a**uuuuacaguuu**ugug**auguguuuuauua**ac**uuguguuuguaua**uaaaugguggaaaauaaaauaaa** auauuauccauugcaaaauc

Supplementary Figures:

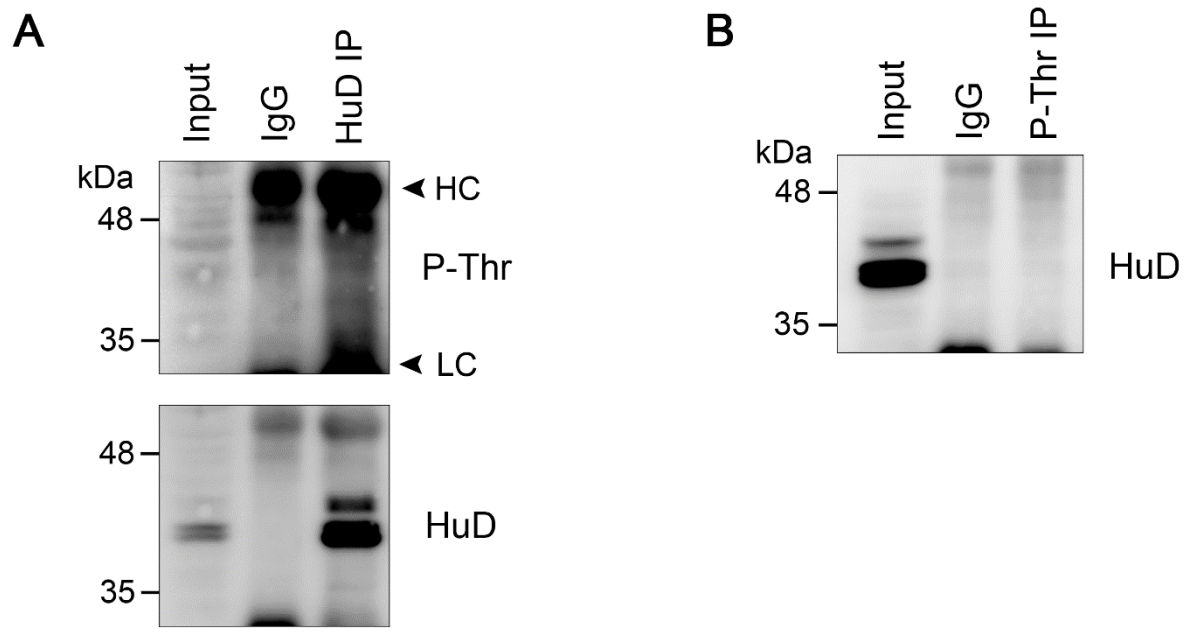

Figure 1: No evidence of HuD phosphorylation *in vivo* in Neuro2A cells. (A) Neuro 2A cell lysates were subjected to immunoprecipitation with a HuD antibody and IgG isotype control antibody. Total lysate (input) and immunoprecipitates were analyzed by western blot using antibodies against phosphothreonine (P-Thr) and HuD. Migration of antibody immunoglobulin heavy chain (*HC*) and light chain (*LC*) is indicated. (B) Cell lysates were subjected to immunoprecipitation with a P-Thr antibody and IgG isotype control antibody. Total lysate (input) and immunoprecipitates were analyzed by western blot using a HuD antibody.

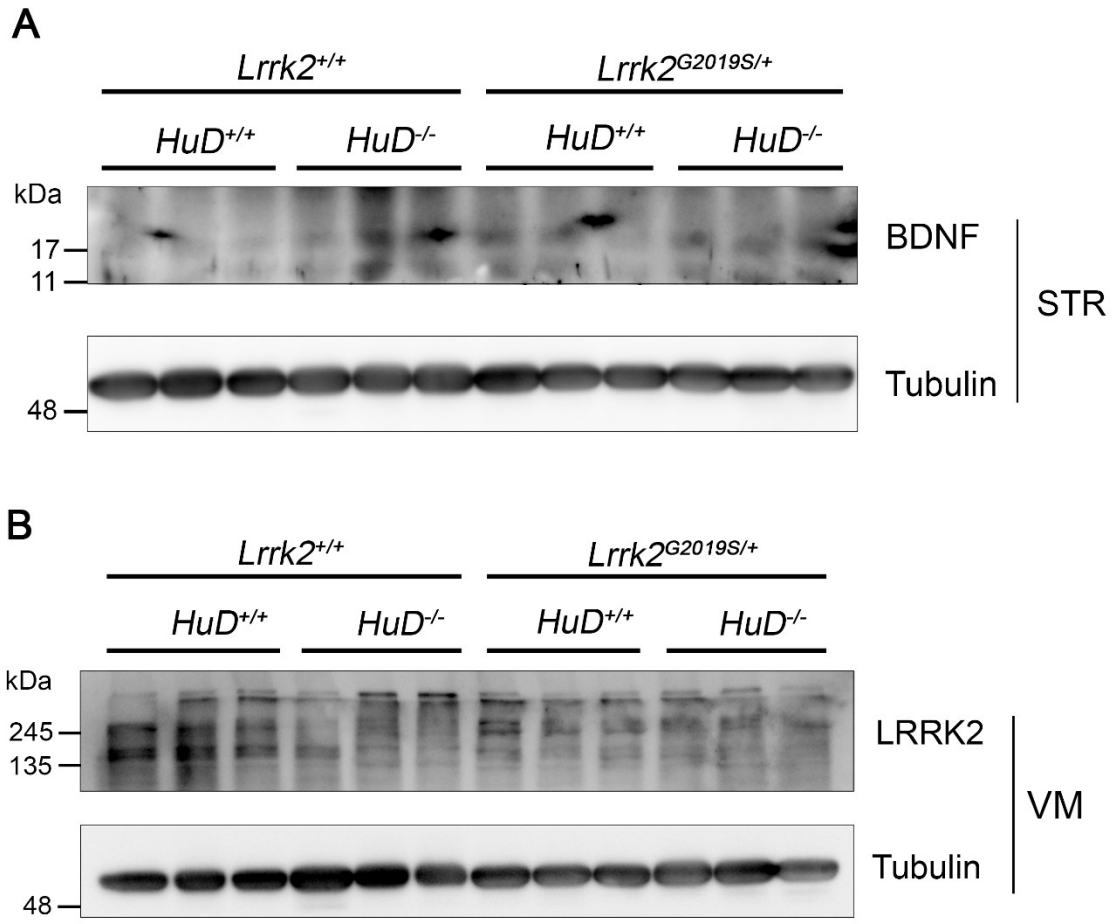

Figure 2: Weak expression of BDNF in the striatum and LRRK2 in the ventral midbrain. Striatum (STR) and ventral midbrain (VM) tissues were isolated from 4 week old wild type mice (*HuD*$^{+/+}$*/Lrrk2*$^{+/+}$), HuD knockout mice (*HuD*$^{-/-}$*/Lrrk2*$^{+/+}$), LRRK2 G2019S mice (*HuD*$^{+/+}$*/Lrrk2*$^{G2019S/+}$), and HuD knockout/LRRK2 G2019S mice (*HuD*$^{-/-}$*/Lrrk2*$^{G2019S/+}$). Tissues were assessed for (A) BDNF expression in the striatum and (B) LRRK2 expression in the ventral midbrain using western blot and appropriate antibodies. Representative blots show 2-3 mice per genotype.